541.182.642.085:541.64

MEDEDELINGEN LANDBOUWHOGESCHOOL
WAGENINGEN • NEDERLAND • 71-20 (1971)

POLYMER ADSORPTION AND ITS EFFECT ON COLLOIDAL STABILITY

A THEORETICAL AND EXPERIMENTAL STUDY ON THE POLYVINYL ALCOHOL-SILVER IODIDE SYSTEM

G. J. FLEER

Laboratory for Physical and Colloid Chemistry, Agricultural University, Wageningen, The Netherlands

(Received 2-IX-1971)

H. VEENMAN & ZONEN N.V.–WAGENINGEN–1971

Mededelingen Landbouwhogeschool
Wageningen 71–20 (1971)
(Communications Agricultural University)
is also published as a thesis

CONTENTS

1. INTRODUCTION

1.1. GENERAL

In recent years much attention has been paid to the behaviour of polymers at interfaces. Because of the large number of repeating units in each molecule polymers adsorb onto nearly any surface. Even if the gain in free energy due to adsorption of one unit is small, the decrease in free energy per adsorbed molecule can become very high.

When polymer is adsorbed on the surface of the particles of a colloidal dispersion the stability of the dispersion is usually affected, sometimes drastically. The classical factors determining the colloidal stability are the electrostatic repulsion and the VAN DER WAALS attraction. A quantitative description has been given in the well-known DLVO theory (DERYAGIN and LANDAU 1941, VERWEY and OVERBEEK 1948). In the presence of adsorbed polymers, not only are these factors influenced directly, but also important additional contributions to the particle interaction free energy play a role. Under different conditions a dispersion can be stabilised or destabilised by a polymer. Often these two effects may occur in the same system : at low concentrations of polymer the dispersion may flocculate, whereas at high concentrations the system may be strongly stabilised.

This effect on the stability of dispersions is one of the main causes of interest in the adsorption of polymers. There are many applications in very different areas of the present day technology. Some of them will be mentioned here.

Polymers are frequently used as *stabilisers for emulsions*. The practical applications are most widespread in food technology and the pharmaceutical industry. The stabilisation of emulsions by polymers and the factors determining it have been described by KITCHENER and MUSSELWHITE (1968) and LANKVELD (1970).

Dispersions of solids in liquids are often stabilised by polymers. Examples are : pigment dispersions, fillers and lacquers. Further examples, especially in non-aqueous systems, can be found in the review by LYKLEMA (1968).

A very important practical application is the *destabilisation of suspensions*. In the industrial production of metals the problem always arises of the dewatering of suspensions, i.e. the separation of solid and liquid phases. This separation is usually attained in two steps, the first being thickening of the slurry. After thickening, the water content is normally about 50%, and further dewatering is achieved by filtration. The use of polymers can accelerate both processes considerably. The usual basis of thickening is sedimentation. The rate of sedimentation depends primarily on the size of the suspended particles, according

to STOKES' law. By flocculating the slurry with polymer additives, large flocs are formed, which settle rapidly. The sediment is filtrated more easily if polymers are used because of the very loose structure of the flocs.

A very extensive review of the application of flocculants for industrial uses has been given by KUZ'KIN and NEBERA (1963). An illustrative example is the production of aluminium from bauxite. After milling and grinding of the mineral, the alumina is selectively dissolved as aluminate under basic conditions. The remaining dispersion, mainly red mud, is flocculated with a polymeric flocculant and separated from the solution. After addition of acid to the solution the precipitated aluminium oxide is flocculated, again by use of a flocculant, and the thus concentrated Al_2O_3 sediment can be further treated for the production of aluminium.

In lead, copper and nickel plants flocculants are used to concentrate the overflow after the flotation process. Many other examples have been given (KUZ'KIN and NEBERA 1963, BASF-brochure 1967).

Another field of application of polymeric flocculants is in *water purification.* Industrial waste water is often clarified in this way. But also in the purification of natural waters polymers are used, e.g. in clarifying muddy river water (TAJOMA 1957). In general the solid content of natural waters is very low, and flocculation can be made more effective by adding, prior to the polymer, other solids, such as quartz sand (GALGÓCZI 1964), and ferric- or aluminium oxides, as formed by hydrolysis of the metal ions (LIPS 1968).

A quite different, but in future perhaps an equally important, application of polymers is in the *improvement of the soil structure* (RUEHRWEIN and WARD 1952, MICHAELS and LAMBE 1953, WILLIAMS et al. 1968). A soil should contain relatively large, loose and stable aggregates to maintain ready circulation of air and water. A poor soil is characterised by a high bulk density, low permeability and the possibility of caking and cracking on drying. By treatment with a solution of a suitable polymer at low concentration the water stability and water retention capacity of the soil both increase, the bulk density decreases and the resistance to erosion is improved. The small particles in the soil are flocculated and already existing aggregates are stabilised (MICHAELS and LAMBE 1953).

Soil stabilisation by polymers is relevant also in improving the mechanical properties of soils destined for highways, airports etc. (FUNGAROLI et al. 1969). Until now the main reason for the limited application of soil stabilisers has been the high cost.

The kinds of polymers that have been used have varied considerably. Originally use was made of natural products like glue, starches, gluten, proteins (e.g. casein) and gums (e.g. extracts of seaweed, alginates). At the present time,

mainly synthetic products are employed most of which are based on polyacryl amide (KUZ'KIN and NEBERA 1963). Polyvinyl alcohol has sometimes been used as a flocculant or as a soil stabiliser (WILLIAMS et al. 1968, KIJNE 1967).

1.2. THE MECHANISM OF POLYMER ADSORPTION AND FLOCCULATION BY POLYMERS

Adsorption

A general feature of the adsorption of polymers at interfaces is the fact that much more material can be adsorbed than the amount necessary to form a monolayer on the surface, although no steps occur in the adsorption isotherm, so formation of discrete monolayers may be precluded. JENKEL and RUMBACH (1951) were the first to propose the loop model for polymer adsorption: only part of the segments is attached to the surface and the remainder parts stick out into the solution. At present this idea is generally accepted and an adsorbed homopolymer molecule is supposed to exist of trains and loops. A *train* is a sequence of segments all lying in the surface and a *loop* is a sequence of which no one segment is in contact with the surface. As a consequence, the polymer layer can be rather thick. A great deal of an adsorbed polymer is in contact with the solvent; small variations in solvent power affect the configuration of an adsorbed molecule substantially. (See reviews of polymer adsorption, e.g. SILBERBERG 1962b, PATAT et al. 1964 and STROMBERG 1967).

Measurements to obtain the fraction of segments that is adsorbed have been reported (e.g. FONTANA and THOMAS 1961, THIES et al. 1964). This fraction is usually between 0.2 and 0.5, thus corroborating the loop model.

Because of the large number of attached segments it is statistically very unlikely that desorption can take place, so, as a rule, the adsorption of polymers is irreversible. This is in fact what is found in practice. In most cases the adsorption obeys a 'high affinity' type adsorption isotherm, i.e. at low concentrations the polymer is adsorbed nearly completely.

The mechanism of attachment of segments to the surface can be very different in different cases. Some possibilities are: electrostatic interaction (sometimes very local as in ion exchange) and chemical bonding (e.g. the formation of an insoluble salt) for polyelectrolytes; hydrogen bonding; and the VAN DER WAALS type of interaction for all types of polymer. Hydrophobic bonding is also possible.

Several workers have tried to formulate a theory for polymer adsorption (FRISCH and SIMHA 1954, 1955, 1957; SILBERBERG 1962, 1967, 1968; HOEVE 1965, 1966). The main effects are, in general, rather well described by these theories, although an exact quantitative comparison with experiment is difficult because of the variety of parameters involved in these theories.

Flocculation

The flocculation of dispersions by oppositely charged polymers can be explained by *charge neutralisation.* The polymer will adsorb strongly, lowering the STERN potential of the particles so that the electrostatic repulsion is reduced, and, due to the VAN DER WAALS attraction, flocculation occurs. It has been shown (GREGORY 1969) that at optimal flocculation the electrophoretic mobility of the particles is zero, when particles and flocculant are oppositely charged. At high polymer dosage charge reversal and subsequent restabilisation can take place.

However, it appears that negatively charged suspensions can also be flocculated by negative polyelectrolytes (MICHAELS 1954, LINKE and BOOTH 1960, HEALY and LA MER (1962). Some nonionic polymers are powerful flocculants, even if the suspended particles possess a considerable charge. These effects imply that in these cases another mechanism must be operative.

RUEHRWEIN and WARD (1952) introduced the *bridging* concept: long loops, extruding from one particle can reach another particle and adsorb thereon. Thus an extended network of particles interconnected by polymer bridges is formed. Other investigations supported this view (MICHAELS 1954, LINKE and BOOTH 1960, LA MER and HEALY 1963, SLATER and KITCHENER 1966) and this model is accepted now by most workers in this field. Reviews concerning flocculation by polymers have been given by LA MER and HEALY (1963) and by AUDSLEY (1965).

Bridging can occur only at low coverage because only then is free surface available on which adsorption of a molecule attached to another particle can take place.

The loops should be longer than the thickness of the double layer for flocculation to be effective. From this it is clear firstly, that the flexibility, configuration and length of the chain are important. MICHAELS (1954) found that polyacryl amide was most effective if a certain charge on the polymer was present to elongate the macromolecule. Secondly, the thickness of the double layer depends on the salt concentration and the efficacy of flocculation is influenced very much by small amounts of salt. In addition, small concentrations of divalent cations are sometimes needed to accomplish adsorption of negatively charged polymers on particles of like charge (SOMMERAUER et al. 1968).

At high polymer coverage a dispersion is stabilised and even protected against large amounts of salt. This is caused by an increase in free energy when two particles approach; this increase can be brought about by *volume restriction* of the adsorbed chains or by *osmotic effects* due to polymer-solvent interaction. Theories concerning the volume restriction effect have been given by CLAYFIELD and LUMB (1966, 1968), MEIER (1967) and HESSELINK (1971); the osmotic effect has been considered by FISCHER (1958), MEIER (1967) and HESSELINK (1971).

1.3. Terminology

In the literature some confusion exists concerning the terms coagulation and flocculation. La Mer (1966) proposed a distinction between the two. We agree more or less with this proposal. So we will use the term *coagulation* for the destabilisation of a suspension solely by electrolytes. When a polymer causes destabilisation the phenomenon will be referred to as *flocculation*. Depending on the flocculation mechanism a distinction can be made between:

(i) *Adsorption flocculation*, i.e. flocculation by polymer only

(ii) *Sensitisation*, i.e. flocculation by a polymer with the help of small amounts of salt.

1.4. Outline of this study

As mentioned before, the practical applications of flocculation are numerous and widespread. Many researches have been carried out, often however, with rather ill-defined systems. In many cases the amount of salt present was not specified. Until now no case has been reported in the literature in which an attempt has been made to compare the length of the loops with the thickness of the double layer. Such an approach ought to be able to give some insight in the operative mechanism of bridging and the role played by salts. Only in this way is it possible to study the bridging quantitatively and to relate the properties of the adsorbed layer (thickness, segment density distribution) to double layer characteristics (surface potential, salt concentration and valency).

The aim of the present study is to examine critically the factors which influence the flocculation of colloidal particles by polymers, and especially the role of bridging. For that purpose experiments have been done with a well-defined system.

As a model colloid, *silver iodide* was chosen. From the work of the Dutch school many of the properties of AgI are known. Surface potential-surface charge relationships, in the presence of several electrolytes, are known from potentiometric titration (Lyklema and Overbeek 1961, Lyklema 1963). Critical coagulation concentrations have been measured for example by Kruyt and Klompé (1942) and Reerink and Overbeek (1954). The specific surface area can be determined by the capacitance method and by negative adsorption (van den Hul 1966, van den Hul and Lyklema 1967).

The polymer used was *polyvinyl alcohol* (PVA). This is a simple, flexible, uncharged polymer. Its concentration in solution is easily measured, which is important for good adsorption studies. By using samples of different acetate content the effect of hydrophobicity of the molecule can be studied; in fact the

solvent power of water is changed in this way. Moreover, the double layer properties of AgI covered with PVA can be compared with the AgI-butanol system (BIJSTERBOSCH 1965, BIJSTERBOSCH and LYKLEMA 1965) from which conclusions can be drawn about the orientation of segments in the first layer and the actual coverage of the surface.

The measurements reported in this thesis include:
characterisation of AgI and PVA; the adsorption of PVA on AgI; estimation of the layer thickness of adsorbed polymer; and flocculation in the presence of ions of different valencies. In chapter 6. an attempt will be made to extend the DLVO-theory to include extra terms accounting for the action of the polymer.

2. CHARACTERISATION OF MATERIALS

2.1. General procedure

All chemicals used were pro analyse quality. Water was distilled and percolated before use through a column of silver iodide to remove impurities which could interfere with the sol.

All glassware was cleaned with chromic acid, dilute nitric acid and tap water, in that order. After this tubes and vessels were steamed. Pipettes were rinsed for some hours with tap water. Finally all glassware was rinsed thoroughly with distilled, percolated water.

2.2. Silver iodide

2.2.1. *Preparation*

Three samples of silver iodide sol were used, designated A, B and C. The preparation closely followed the procedure given by de Bruyn (1942).

Sol A. A volume of 0.20 M $AgNO_3$ was added slowly to an equal volume of 0.22 M KI under vigorous agitation by a vibrating stirrer. The concentration of the sol thus obtained was 100 mmoles/l. The sol was electrodialysed, electrodecanted and aged in solution for 3 days at 80 °C. After ageing the electrodialysis and electrodecantation were repeated. Several preparations were added together to give a stock solution of 138 mmoles AgI/l.

Sol B. In this case a volume of 0.15 M $AgNO_3$ was added to a volume, twice as great, of 0.0825 M KI to give a sol of originally 50 mmoles/l. After two cycles of electrodialysis and electrodecantation the sol was aged and filtered through a glass filter (L 4, mean diameter of the pores 10–20 μm). The concentration of the stock solution was 139 mmoles/l.

Sol C. The preparation of sol C was identical to that of sol B, except that ageing was carried out between the first and second electrodecantation. The stock solution had a concentration of 640 mmoles/l.

It was found that after long ageing of concentrated sols much of the material coagulated; therefore filtration was applied for sols B and C and ageing for sol C was carried out before the second electrodecantation.

For most of the flocculation experiments a sol concentration of 10 mmoles/l was used. In table 2–1 the pI values of the different sols at this concentration

and the corresponding surface potentials are given. The pI of sol B is rather low because the iodide, liberated in the ageing process, was not removed by subsequent dialysis.

2.2.2. *Surface area and particle size distribution*

The surface area of all the samples has been determined by the *double layer capacitance* method. To that end the surface charge as a function of the surface potential was measured in the presence of 10^{-1} M KNO_3 and the surface charge per gram AgI was compared with the value per m^2 known from standard curves. The procedure resembles the method described by VAN DEN HUL (1966) and VAN DEN HUL and LYKLEMA (1967). The cell used for the potentiometric titration, and the procedure to obtain the surface charge as a function of the surface potential have already been described by LYKLEMA et al. (1961) and by BIJSTERBOSCH et al. (1965).

The values of the specific surface areas are also collected in table 2–1. The uncertainty of the values given is about 10%.

The specific surface area of sol C was measured also by the *negative adsorption* method (VAN DEN HUL 1966, VAN DEN HUL and LYKLEMA 1967). Originally, attempts were made to measure the negative adsorption of the concentrated sol by the dialysis procedure as described by DE HAAN (1964). However, it appeared that the KNO_3 concentration of this sol was too high (about 5.10^{-4} M). In the presence of high concentrations of univalent electrolyte, the negative adsorption of bivalent cations is hardly measurable. Therefore, the measurements were carried out on a AgI precipitate after washing out the KNO_3.

The procedure was as follows : a portion of sol C was coagulated by addition of $AgNO_3$ until the point of zero charge was reached. The precipitate was washed several times with water. Aliquots of this precipitate, containing about 5 g of AgI were placed in 25 ml glass stoppered cylinders and a calculated amount of KI solution was added to give a pI between 5 and 6. Then 5 ml 2.10^{-4} M K_2SO_4 were added and the volume brought to 25 ml with water. After rotating end-over-end for one day and standing at least for four days,

TABLE 2–1. *Properties of AgI sols*

sol	pI (sol concentration 10 mmoles/l)	Surface potential (mV)	Specific surface area (m^2/g)	
			capacity	negative adsorption
A	5.1	–320	7.8	–
B	4.3	–360	14.6	–
C	5.1	–320	11.3	10.9

the sulphate concentration of the supernatant solution was measured conductometrically. 7 ml of the sulphate solution were added to 7 ml isopropanol and the mixture was titrated with 5.10^{-4} M barium acetate. The resistance was measured with a Marconi Universal Bridge TF 2701. Reciprocal resistances, corrected for dilution, were plotted against ml barium acetate added to give the experimental equivalence point. Because of non-stochiometry this point is not equal to the theoretical equivalence point. A calibration curve of volume of barium acetate against concentration of sulphate was thus needed and was previously determined.

The specific surface area was calculated from the difference between the equilibrium and the initial concentration of sulphate according to eq. (9) of the paper by VAN DEN HUL and LYKLEMA (1967). The result was 10.9 m^2/g, in good agreement with the capacitance area (see table 2–1).

A complication that may occur in negative adsorption measurements is the possibility of double layer overlap (DE HAAN 1964, VAN DEN HUL 1966). The extent of overlap is determined by the ratio between the interparticle distance and the thickness of the double layer. The interparticle distance can be estimated from the concentration of AgI in the sediment, which was about 0.25 g/cm^3, and the particle radius. The radius R of monodisperse spheres follows from the surface area according

$$S = \frac{3}{dR} = \frac{0.53}{R} \tag{2-1}$$

where S is the specific surface area and d the solid density (i.e. 5.67 g/cm^3 for AgI).

Assuming hexagonal packing of monodisperse spheres, the interparticle distance was calculated to be 1550 Å. The ratio between this distance and the double layer thickness turned out to be about 8 in our case, corresponding to a decrease in negative adsorption of less than 10% according to DE HAAN (1964).

Since the uncertainty of the measurements is also about 10% double layer overlap was neglected.

In some cases a sample used for negative adsorption measurements was brought back to the point of zero charge, washed and used for further measurements. The surface area so found was the same within experimental accuracy. However, the surface area decreased rapidly to values of the order of 1–4 m^2/g when this procedure was repeated several times. Apparently irreversible aggregation of the particles occurs after several washing cycles.

The average particle size and the particle size distribution of sol C were determined in an experiment using the I.C.I.-Joyce Loebl *disc centrifuge*. The

apparatus and its operation have been described by BERESFORD (1967) and by JONES and MANLEY (1967). The principle of this centrifuge is as follows : In a rotating vertically mounted disc spin fluid is introduced followed by a small volume of the dispersion to be investigated. Precautions are taken to prevent turbulent mixing and streaming. The density of the spin fluid must be higher than that of the dispersant and lower than the particle density. After centrifuging for a preset time, at a given speed of revolution, the central part of the disc fluid is collected, thus giving the fraction of material with particle radii below a certain value, determined by the time and the speed of centrifugation, according to STOKES' law. The experiment is repeated with other centrifugation times. The fractions are analysed for solid content and a cumulative particle size distribution is obtained in this way.

In our case the AgI particles were dispersed in a mixture of 3 parts by volume of water and 1 part of methanol, and water was used as spin fluid. The concentration of silver in the undersize fractions was determined by dissolving the silver iodide in an ammoniacal solution of $K_2Ni(CN)_4$ and subsequent complexometric titration (FLASCHKA 1952, 1953).

The results are given in fig. 2–1. Few measurements have been performed in the smaller size fraction range, because accurate analysis is difficult in this region due to the low concentration of solid. If the experimental points in fig. 2–1 are extrapolated according to the dashed line, the distributive particle size distribution can be calculated, and from this the average particle radius. The

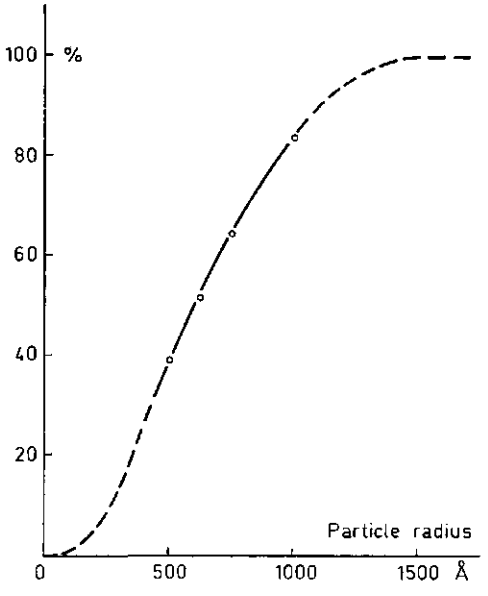

FIG. 2–1. The particle size distribution of AgI (sample C). Along the ordinate the undersize cumulative weight percentage is given

kind of average which is most interesting for our purpose is the volume-surface averaged radius; because this average is obtained by application of eq. (2–1) to heterodisperse systems. The volume-surface averaged radius is defined by:

$$\bar{R}_{32} = \frac{\Sigma_j n_j R_j^3}{\Sigma_j n_j R_j^2} = \frac{\Sigma_j w_j}{\Sigma_j w_j / R_j} \tag{2-2}$$

where n_j is the number of particles in fraction j and w_j the weight of each fraction. From eq. (2–2) and the distributive weight distribution, $\bar{R}_{32}$ was calculated as 480 Å. This is in very good agreement with the value of 470 Å, calculated from eq. (2–1) using $S = 11.3$ m^2/g.

In conclusion, it may be stated that the three different methods, used for the determination of the surface area agree very well with each other, despite the uncertainties involved in each method. The inaccuracy in the particle radius can be estimated to be about 10%. In all further calculations the value 500 Å will be adopted for the particle radius.

2.3. Polyvinyl alcohol

2.3.1. *Synthesis and properties*

Polyvinyl alcohol (PVA) is a water soluble polymer of relatively simple chemical structure. In a recent monograph, comprising the papers presented on a symposium on PVA the preparation, properties and applications of PVA have been described (Finch 1968). Properties and uses of fully hydrolysed PVA have been treated in a monograph by Pritchard (1970).

In the preparation of polyvinyl alcohol, vinyl acetate is first polymerised to polyvinyl acetate (PVAc). This polymer is subsequently hydrolysed to give polyvinyl alcohol containing a certain percentage of unreacted acetate groups. Schematically:

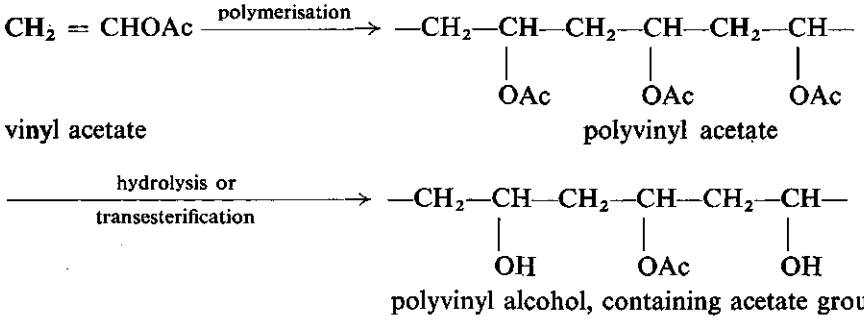

In this scheme – OAc denotes the $-O-\overset{\overset{O}{\|}}{C}-CH_3$ group

Instead of a true hydrolysis with acid or base, most industrial processes involve transesterification in the preparation of PVA from PVAc.

Polyvinyl acetate often is branched, but during hydrolysis the side chains split off and it would seem most probable that polyvinyl alcohol is unbranched (HACKEL 1968). The acetate groups along the chain are probably grouped together in blocks, especially when alkaline hydrolysis is applied (HACKEL 1968). The solubility of PVA depends strongly on the degree of hydrolysis. PVA containing only a few percent of acetate groups dissolves completely at 80°C. This temperature is necessary to break up the crystalline regions of solid PVA (MOORE and O'DOWD 1968). PVA with a higher acetate content (>10%) dissolves at room temperature because, due to the bulky acetate groups, less microcrystallites are present (PRITCHARD 1970). However, at higher temperatures phase separation occurs in solutions of PVA containing more than 10% of acetate groups.

The viscosity of the solutions does not change on storage, except in the case of fully hydrolysed PVA. In this case the viscosity and light scattering increase, indicating aggregate formation (TOJOSHIMA 1968, MATSUO and INAGAKI 1968, PRITCHARD 1970).

Properties of PVA, such as degree of tacticity and solubility, depend on the way of preparation (PRITCHARD 1970). LANKVELD (1970) showed that samples of PVA obtained from different sources may exhibit different surface activity.

2.3.2. *Types of PVA used and molecular weight*

The different samples of PVA used in this study are designated by two numbers, the first giving the approximate relative viscosity of a 4% aqueous solution at 20°C and the second the degree of hydrolysis. The PVA 16–98 was manufactured by Konam N.V., Amsterdam, and the other samples, listed in table 2–2, by Wacker, Germany. All these samples were kindly supplied to us by Konam N.V.; they were prepared from PVAc by transesterification.

The distribution of molecular weights is rather broad. The average molecular weights, quoted by the supplier without reference to the method of measurement and way of averaging are given in table 2–2. To check these values use was made of the MARK-HOUWINK relation :

$$[\eta] = k_1 \overline{M}^a \tag{2-3}$$

where $[\eta]$ is the intrinsic viscosity and $\overline{M}$ the viscosity-averaged molecular weight.

The constants k_1 and a were determined from viscosity measurements on

TABLE 2–2. Molecular weights and viscosities of PVA-samples

sample	$\bar{M}$ supplier	$\bar{M}$ eq. (2–3)	$[\eta]$ (dl/g)	k'
3–98.5	13,000	15,000	0.302	0.28
13–98.5	45,000	56,000	0.681	0.44
60–99	105,000	101,000	0.982	0.62
3–88	16,000	13,000	0.261	0.41
13–88	53,000	63,000	0.658	0.39
40–88	106,000	111,000	0.927	0.55
16–98	55,000			

some PVA samples, manufactured by Kurashiki, Japan, and supplied by Fresal, Amsterdam. The molecular weights, stated by this company without further references, were used for this purpose. The results are, at 30 °C : $k_1 = 8.7 \cdot 10^{-4}$ dl/g and $a = 0.61$ at an acetate content of about 2% and $k_1 = 8.7 \cdot 10^{-4}$ dl/g and $a = 0.60$ at an acetate content of 12%. These values differ only slightly from those stated by LANKVELD and are in good agreement with the values quoted by BERESNIEWICS (1959). Assuming the same k_1 and a for the PVA produced by Wacker, eq. (2–3) was used to calculate the molecular weight of these samples.

Viscosities were measured at 30 °C in Ubbelohde viscosimeters (design KPG, Jenaer Glasswerk Schott, Mainz) with an elution time for water of about 250 seconds, at 30 °C. COUETTE-HAGENBACH corrections were applied in accord with the tables supplied with the viscosimeters. Intrinsic viscosities were obtained by extrapolating the viscosity ratio excess to infinite dilution. Several relationships between viscosity ratio excess and polymer concentration have been suggested. The most common of these are the HUGGINS equation:

$$\frac{\eta_{re}}{c_p} = [\eta]_H + k'_H [\eta]_H^2 c_p \tag{2-4}$$

and the MARTIN equation:

$$\ln \frac{\eta_{re}}{c_p} = \ln [\eta]_M + k'_M [\eta]_M c_p \tag{2-5}$$

In these equations η_{re} is the viscosity ratio excess, c_p the polymer concentration and k' the HUGGINS constant. For reference to these equations see e.g. HUGGINS (1958). $[\eta]$ resp. k' were obtained by averaging arithmetically $[\eta]_H$ and $[\eta]_M$ resp. k'_H and k'_M. $[\eta]_H$ and k'_H were derived from a plot of η_{re}/c_p against c_p according to eq. (2–4) and $[\eta]_M$ and k'_M followed from a plot of $\ln \eta_{re}/c_p$ against c_p according to eq. (2–5). SAKAI (1968) showed that this procedure is the most

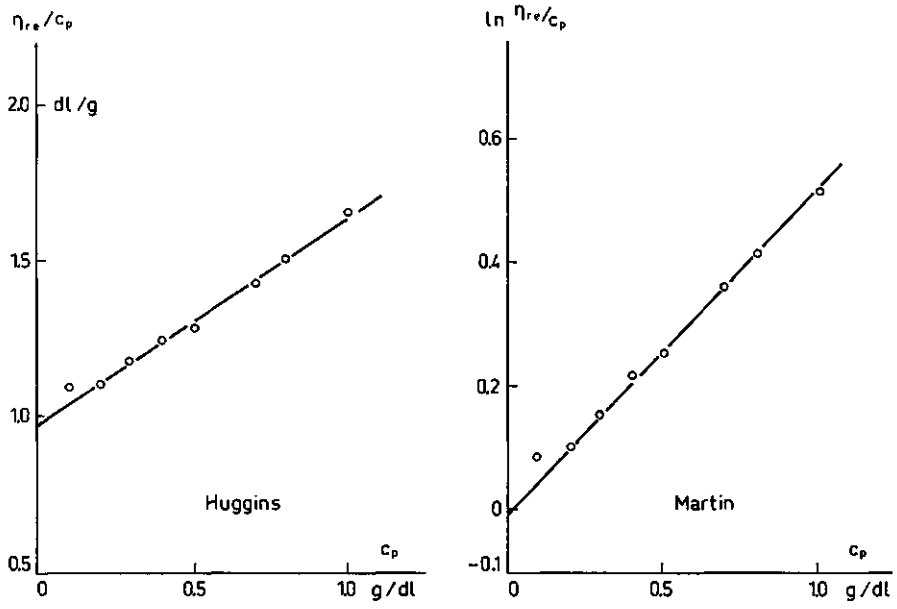

FIG. 2–2. HUGGINS and MARTIN plot for PVA 60–99 at 30 °C

reliable in obtaining the intrinsic viscosity and HUGGINS constant for polymers in good solvents. In our case $[\eta]_H$ and $[\eta]_M$ hardly differed. However, the differences between k'_H and k'_M amounted sometimes to as much as 25%.

A typical example of a HUGGINS and a MARTIN plot is given in fig. 2–2. The average values obtained for $[\eta]$ and k' are listed in table 2–2, together with the molecular weights calculated from eq. (2–3). The molecular weights agree rather well with those quoted by the supplier.

The values of k' will be discussed in 2.3.4.

2.3.3. *Configuration parameters*

The most important parameters describing the dimensions of flexible, linear polymer coils in solution are the root mean square *radius of gyration*, $(\overline{s^2})^{1/2}$, and the r.m.s. *end-to-end distance*, $(\overline{h^2})^{1/2}$. These quantities are related by:

$$\overline{s^2} = \overline{h^2}/6 \tag{2-6}$$

The dimensions of a chain can be related to its dimensions in so called Θ-conditions via

$$\overline{h^2} = \alpha^2 \, \overline{h_0^2} \tag{2-7}$$

where α is the linear expansion factor, increasing with increasing solvent power and $(\overline{h_0^2})^{1/2}$ is the r.m.s. end-to-end distance in a Θ-solvent. This quantity can

be calculated from random flight statistics (FLORY 1953, TANFORD 1961). The result is, for a chain with fixed bond length l, fixed valence angle, θ, and complete freedom of rotation about bonds:

$$\overline{h_{0F}^2} = m\, l^2 \frac{1 + \cos\theta}{1 - \cos\theta} \tag{2-8}$$

The index $_F$ denotes 'freedom of rotation'. m is the number of skeletal carbon atoms. For a polymethylene chain $\cos\theta = 0.333$, so $\overline{h_{0F}^2} = 2\,ml^2$. Real chains are restricted in rotation; this is accounted for by a factor σ:

$$\overline{h_0^2} = 2\,\sigma^2\, m\, l^2 \tag{2-9}$$

Thus σ represents the steric hindrance to rotation around a C–C bond and increases when the side groups of the chain become more bulky.

KUHN (1934) has pointed out that, in order to calculate chain dimensions, a polymer chain with fixed bond angles and restrictions to rotation about bonds can be replaced by an *equivalent chain* of the same contour length L consisting of i *statistical chain elements* of length l_s which are freely jointed together without bond angle restrictions. The end-to-end distance can then be written as

$$\overline{h_0^2} = i\, l_s^2 \tag{2-10}$$

i and l_s are further defined by using for the contour length L the planar zig-zag of the all-trans conformation with a distance of 2.53 Å between alternate carbon atoms (MORAWETZ 1965, p. 120). Then

$$i\, l_s = L = \frac{m}{2} \,.\, 2.53 \text{ Å} \tag{2-11}$$

By combining eqs. (2–10) and (2–11) with eq. (2–9) and taking $l = 1.54$ Å it follows that l_s is given by

$$l_s = 4\,\sigma^2 \frac{1.54^2}{2.53} = 3.75\,\sigma^2 \text{ (Å)} \tag{2-12}$$

The number of skeletal carbon atoms per statistical chain element, m/i, is

$$m/i = \frac{2l_s}{2.53} = 2.96\,\sigma^2 \tag{2-13}$$

Throughout this thesis the term '*segment*' will be used to denote a monomer unit of PVA, whereas an '*element*' refers to a statistical chain element consisting of several segments.

From viscosity measurements the chain dimensions can be deduced by use of the FLORY-FOX equation (FLORY 1953, p.611):

$$[\eta] = \Phi \frac{(\overline{h^2})^{3/2}}{M} \tag{2-14}$$

According to the original theory Φ should be an universal constant. However, Φ depends slightly on the solvent power; for a very good solvent $\Phi = 2.0 \cdot 10^{21}$ if $[\eta]$ is expressed in dl/g and in a Θ-solvent $\Phi = 2.55 \cdot 10^{21}$ (TANFORD 1961, p.401).

In the course of this study we shall use the concept of the *equivalent hydrodynamic sphere* (TANFORD 1961, p.344). The radius of this sphere is given by:

$$R_h = \xi (\overline{s^2})^{1/2} \tag{2-15}$$

In this concept a polymer coil is considered as a hydrodynamic particle in which the solvent is completely immobilised inside the volume defined by R_h, whereas outside R_h the solvent can flow completely freely.

The FLORY constant Φ is related to ξ through:

$$\Phi = \frac{0.1}{3 \cdot 6^{3/2}} \pi \, N_{Av} \, \xi^3 = 4.291 \cdot 10^{21} \, \xi^3 \tag{2-16}$$

where N_{Av} is AVOGADRO'S number.
$(\overline{h_0^2})^{1/2}$ can be obtained from eq. (2–14) by combining this equation with eq. (2–7):

$$[\eta] = K \alpha^3 M^{1/2} \tag{2-17}$$

with

$$K = \Phi \left(\frac{\overline{h_0^2}}{M}\right)^{3/2} \tag{2-18}$$

K is a constant for a given polymer.
The linear expansion factor α can be approximated by the FLORY equation (FLORY 1953, p. 600):

$$\alpha^5 - \alpha^3 = C_M \, (1/2 - \chi) \, M^{1/2} \tag{2-19}$$

where χ is the polymer-solvent interaction parameter. χ takes the value 0.5 under Θ-conditions and is lower in better solvents. C_M is a constant, defined by:

$$C_M = \frac{27}{2^{5/2}\,\pi^{3/2}} \frac{\bar{v}^2}{N_{Av}\,V_1} \left(\frac{\overline{h_0^2}}{M}\right)^{-3/2} = 0.858 \frac{\bar{v}^2}{N_{Av}\,V_1} \frac{\Phi}{K} \tag{2-20}$$

where $\bar{v}$ is the partial specific volume of the polymer and V_1 is the molar volume of the solvent.

By combining eqs. (2–17) and (2–19) the FLORY-FOX-SCHAEFGEN (FFS)-relation is obtained (see FLORY and FOX 1951, and KURATA and STOCKMAYER 1963):

$$\frac{[\eta]^{2/3}}{M^{1/3}} = K^{2/3} + 2C_M\,(1/2 - \chi)\,K^{5/3} \cdot \frac{M}{[\eta]} \tag{2-21}$$

Thus, by plotting $[\eta]^{2/3}/M^{1/3}$ against $M/[\eta]$ and extrapolating to zero molecular weight, K and χ can be calculated from the intercept and slope. $(\overline{h_0^2})^{1/2}$ follows from eq. (2–18) and the steric factor σ from eqs. (2–9) and (2–18):

$$\sigma^2 = \left(\frac{K}{\Phi}\right)^{2/3} \cdot \frac{M}{m} \cdot \frac{1}{2l^2} \tag{2-22}$$

Finally by use of eq. (2–7) α is obtained.

Equations (2–19) to (2–21) are approximate because eq. (2–19) is not valid in very good solvents. In moderately good solvents eq. (2–19) is a reasonable approximation and reliable values of K and hence of $(\overline{h_0^2})^{1/2}$ are obtained (KURATA and STOCKMAYER 1963). As will be shown in 2.3.4. water is a moderate good solvent for PVA so eq. (2–19) may be applied to our system. A second imperfection of the FLORY equation is the fact that C_M, as defined by eq. (2–20), is about twice as large as the corresponding constant in an exact series expansion for small α (STOCKMAYER 1955). For this reason the absolute significance of χ, obtained from the FFS equation is uncertain, but the relative values do give useful information on the polymer-solvent interaction.

Propositions for modifications and improvements of the FFS equation have been given in the literature (see the review by KURATA and STOCKMAYER, 1963). However, these methods offer merely a slight improvement in the curve fitting in most cases, except for polymers in very good solvents. For that reason we ignore them in the present treatment.

In fig. 2–3 the FFS plot is presented for PVA 88 and PVA 98.5. The molecular weights given in the third column of table 2–2 were used. Included in the plot are also points for some Kurashiki samples.

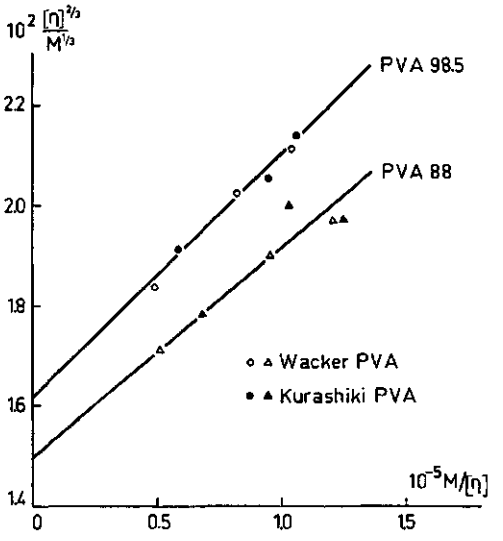

FIG. 2–3. FLORY-FOX-SCHAEFGEN plot for PVA

TABLE 2–3. Solution parameters of PVA

PVA-series	a	10^3K	σ	l_s (Å)	m/l	10^2C_M	$\frac{1}{2}-\chi$	χ
98.5	0.61	2.05	2.12	16.9	13.3	4.79	0.016	0.484
88	0.60	1.83	2.14	17.2	13.6	5.38	0.015	0.485

The values of the solution parameters are given in table 2–3. They are independent of the molecular weight. All units in this table are based on the value of $[\eta]$ in dl/g. Also included in table 2–3 are the exponents of the MARK-HOUWINK equation.

VAN KREVELEN and HOFTIJZER (1967) give the value $K = (2.2 \pm 0.3).10^{-3}$ for PVA, measured by a variety of authors, and calculate $2.09 \cdot 10^{-3}$ using a semi-empirical formula. This is in good agreement with our value for PVA 98.5.

To calculate the other parameters, a value of Φ must be chosen. We used for PVA in water, being a moderately good solvent (see 2.3.4.) $\Phi = 2.2 \cdot 10^{21}$. This corresponds with $\xi = 0.81$.

σ follows from eq. (2–22). The results are in reasonable agreement with the values given by KURATA and STOCKMAYER (1963): 2.04 for fully hydrolysed PVA and 2.12 for PVAc, indicating more restricted rotation in PVAc. In view of the small difference in σ between the non- and fully hydrolysed species no significant difference between PVA 88 and PVA 98.5 may be expected.

TABLE 2–4. Dimensions of PVA molecules in solution

sample	$(\overline{h_0^2})^{1/2}$ (Å)	$(\overline{h^2})^{1/2}$ (Å)	$(\overline{s^2})^{1/2}$ (Å)	α
3–98.5	120	127	52	1.06
13–98.5	231	259	106	1.12
60–99	310	355	146	1.15
3–88	107	116	48	1.08
13–88	236	266	109	1.13
40–88	310	360	148	1.16

Characteristics of the equivalent chain are obtained from σ using eqs. (2–12) and (2–13) and are included in table 2–3. It can be seen that one element of the equivalent chain consists of about 14 carbon atoms or 7 segments. The length of a statistical chain element is about 17 Å.

C_M was calculated from eq. (2–20) by substituting $\bar{v} = 0.77$ cm^3/g (BRANDRUP and IMMERGUT 1965) and $V_1 = 18$ cm^3/Mol. The values of $\frac{1}{2}-\chi$ and χ obtained from the slope of the FFS plot are discussed in 2.3.4. The order of magnitude agrees well with values quoted in the literature for PVA (DIEU 1954, SAKURADA et al. 1959, WOLFRAM et al. 1968).

The coil dimensions calculated from eqs. (2–18), (2–14), (2–6) and (2–7) are collected in table 2–4.

As can be expected α increases with increasing molecular weight.

The data given in tables 2–2, 2–3 and 2–4 are not unambiguous because no attempt was made to determine molecular weights by an absolute method. All figures are based on the molecular weight of the Kurashiki samples as given by the manufacturer. However, the close agreement with the values obtained in this way for M with the quotations of Konam led us to the conclusion that the analysis given provides data at least reliable enough for semi-quantitative interpretation. Moreover, values obtained for K, σ and χ agree satisfactorily well with literature values.

2.3.4. *Solvent power of water for PVA*

The quantities k' (HUGGINS constant), a (exponent in the MARK-HOUWINK equation), α (linear expansion factor) and χ (segment-solvent interaction parameter) can give, in general, useful information on the quality of the solvent.

For polymers in good solvents k' is usually of the order of 0.35, whereas in poorer solvents k' increases (TANFORD 1961, p. 392, MORAWETZ 1965, Ch VI). Under Θ-conditions values of about 0.5 are quoted (IMAI 1969, SAKAI 1970). Aggregation and branching both tend to increase k'. From table 2–2 it can be

seen that k' increases with M, in accordance with the fact that the solvent becomes poorer at higher molecular weight. However, the values of k' range from 0.28 to 0.62 for PVA 98.5; this is about the range between very good solvents and Θ-solvents. No conclusions regarding the solvent quality therefore can be drawn from these figures.

There is only a small difference in k' between PVA 13–98.5 and PVA 13–88. One should expect, on account of the higher percentage of hydrophobic groups in PVA 13–88, that k' should be higher in this case. This is not confirmed by experiment. TOJOSHIMA (1968) found the same trend in k' with acetate content. It is not quite clear what the reason is for this discrepancy. Perhaps the effect of better solvent power of water for PVA 13–98.5 is counteracted by a small tendency to aggregation in this polymer, possibly by formation of some intermolecular hydrogen bonds. For fully hydrolysed species this has been suggested by MOORE et al. (1968) and by PRITCHARD (1970), although the reasons for aggregation in water are not obvious. Moreover, it is doubtful to what extent k' is a reliable measure of solvent power for polar polymers (MOORE et al. 1957). For these reasons no definite conclusion can be drawn from the HUGGINS constant concerning difference in solvent power of water for the two types of polymer.

Sometimes the value of the exponent in the MARK-HOUWINK equation is also used as an indication for solvent power. a is not far from 0.5, the value under Θ-conditions. For very good solvents usually $a \simeq 0.8$ is found. It can be concluded that water is a moderately good solvent for PVA at 30 °C. The observed difference between PVA 13–98.5 and 13–88 is too small to permit reliable conclusions to be drawn as to the difference in solvent power at either degree of hydrolysis.

The same conclusions are valid concerning the magnitudes of α and χ. α is not far from unity and χ is close to 0.5 so water at 30 °C is a somewhat better solvent for PVA than a Θ-solvent. The differences in α and χ for the two types of PVA are again too small to permit definite conclusions.

Thus, summarising the results obtained, for PVA water is a moderately good solvent. Intuitively one should expect that water is a better solvent for PVA 98.5 than for PVA 88. However, if this difference exists it is too small to be detected definitely by our viscosity measurements. Another possibility still is that water is indeed a poorer solvent for PVA 88, but that this effect is counteracted by a slight aggregation in PVA 98.5.

2.3.5. *Examination of the possible ionic character of PVA*

In the preceding paragraph it was tacitly assumed that PVA is uncharged. In connection with the interpretation of stability and double layer studies, to be discussed later, it is important to know if this assumption is true. In order to

investigate whether or not the PVA molecule carried any charge, three experiments were carried out.

Firstly, it was investigated whether PVA, dissolved in a salt solution, moved under an applied electric field. A Kern-Aaran LK 30 electrophoresis apparatus was used. In this apparatus the displacement of the boundary between a polyelectrolyte solution and its equilibrium solution can be measured by an interferometric technique.

20 cm^3 of a solution of PVA 13–98.5 (0.5% by weight) were dialysed against 200 cm^3 10^{-2} N KCl. After equilibrium was reached the apparatus was filled and the boundary was observed. A small displacement took place towards the anode.

The first term in the equation of BOOTH (1950) (see also TANFORD 1961, p. 417) was used as an approximate formula to obtain the charge of the molecule. This first term is:

$$u = \frac{Ze}{6\pi\eta R} \frac{X(\kappa R)}{1 + \kappa R} \tag{2-23}$$

Here u is the electrophoretic mobility, Z the number of elementary charges (e) on the molecule, η the viscosity of the solvent, R the particle radius and κ the reciprocal DEBIJE-length. $X(\kappa R)$ is the well known HENRY function, which assumes the values 1.0 for small κR and 1.5 for large κR.

In the range between pH = 2.2 and 11, u was found to be about -3.10^{-6} cm^2/Vs. R was taken to be equal to R_h, the hydrodynamic radius. For PVA 13–98.5, $R_h = \xi(\overline{s^2})^{1/2} = 86$ Å. Then $\kappa R_h = 2.7$ and $X(\kappa R) = 1.1$. Using eq. (2–23) Z appeared to be about 1. If this value is realistic, one may conclude from the observed pH independency that per molecule one fully dissociated charge site is present, possibly a sulphate group coming from the initiator of the polymerisation. According to PRITCHARD (1970) PVA contains usually one carboxyl group per molecule, probably arising from chain termination on the ester part of the vinyl ester. Anyhow, for most purposes a polyvinyl alcohol molecule can be considered as virtually uncharged.

A further check on this conclusion followed from viscosimetry: the intrinsic viscosity of PVA 13–98.5 at ionic strength of 0.01 M does not depend on pH, indicating absence of weakly charged groups.

Finally the influence of salts on the viscosity of a PVA 16–98.5 solution was examined. KNO_3, $Ca(NO_3)_2$ and $La(NO_3)_3$ were chosen because the flocculation experiments were performed with these same salts. The results are given in fig. 2–4. There appears to be no effect till salt concentrations up to ~0.2 M. This agrees with published results for other salts (MAEDA et al. 1959, BIANCHI et al. 1967, SAITO 1969). At higher concentrations slight deviations occur. These

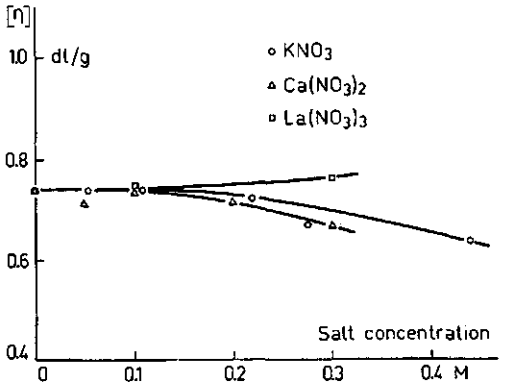

FIG. 2–4. Influence of the salt concentration on the intrinsic viscosity of PVA 16–98

may be interpreted in terms of influence of PVA on water structure (SAITO 1969) or in terms of hydrogen bonds (MAEDA 1959, PRITCHARD 1970) but again it is clear that PVA does not carry a substantial charge and can be regarded as an essentially non-ionic polymer.

3. THE ADSORPTION OF POLYVINYL ALCOHOL ON SILVER IODIDE SOL

In this chapter we shall consider in the main the *amount* of PVA adsorbed. In Ch. 4. we shall discuss some measurements to asses the *thickness* of the adsorbed layer.

3.1. General features of polymer adsorption

Due to the large number of segments, all of which are able to attach to the surface, the adsorption of polymeric materials is in several aspects different from the adsorption of low molecular weight substances. The adsorption of polymers at interfaces has been reviewed by Silberberg (1962b), Patat et al. (1964) and Stromberg (1967).

3.1.1. *Shape of the adsorption isotherm and reversibility of the adsorption*

In most cases the adsorption isotherm of polymers shows a high affinity character: at low concentrations nearly all of the added polymer is adsorbed. At higher concentrations the amount adsorbed increases only slightly with polymer concentration. A real plateau is not usually attained.

It takes a very long time to establish equilibrium between surface and bulk solution; adsorption increases with time until equilibrium is reached.

Desorption on washing with pure solvent does not occur in most cases. It follows that the adsorption is irreversible with respect to dilution as far as polymer molecules as a whole are concerned. The reason is that a polymer molecule is attached to the surface by many contacts. For desorption of a complete molecule to occur it is necessary that all of these attachments are broken simultaneously, which is statistically very unlikely and could take a very long time. This does not mean that polymer adsorption as such is irreversible: often by adding competitive adsorbates, or by changing the solvent power, desorption is achieved (Silberberg 1962b). On occasions displacement of low molecular weight polymers by molecules with higher molecular weight has been reported (Patat et al. 1964).

In spite of the apparent irreversibility of the adsorption only moderate adsorption energies per segment are involved, as is deduced from the usually small temperature dependence of the adsorption.

3.1.2. *Configuration of the adsorbed layer*

As mentioned before a homopolymer molecule is adsorbed with a large

number of segments in direct contact with the surface. The amount, which can be maximally adsorbed, usually exceeds the amount equivalent to one close-packed flat monolayer by a factor of two to five. It follows that only a fraction of the total number of segments is in the surface; the remaining part is forced to protrude into the solution. Thus an adsorbed polymer molecule consists of sequences of segments in the surface (*trains*), and stretches of segments only in contact with solvent (*loops*). The presence of these loops accounts for a rather thick layer.

The fraction of segments adsorbed is found to be of the order 0.2 to 0.5 at maximum adsorption. At low surface coverages, when this maximum adsorption is not yet attained, a relatively higher proportion of the segments can be in the surface, and less and/or smaller loops are present than at higher coverages. Hence the thickness of the adsorbed layer increases with coverage.

According to the theory of SILBERBERG (1968) the amount adsorbed and the configuration of the layer are virtually independent of the adsorption free energy per segment, provided that this is higher than about 1 kT.

3.1.3. *Influence of molecular weight and solvent power*

It is generally found that the adsorption of polymers on surfaces increases with molecular weight. Modern theories (SILBERBERG 1968, HOEVE 1970) predict that under Θ-conditions the maximum adsorption increases linearly with the square root of the molecular weight for degrees of polymerisation lower than several thousand. For very high molecular weights the amount adsorbed tends to a limiting value. In athermal solvents ($\chi = 0$) a much less pronounced dependence on molecular weight exists.

The amount adsorbed and the thickness of the adsorbed layer become higher when the solvent power decreases according to experimental findings. This is also predicted by theory (SILBERBERG 1968, HOFFMAN et al. 1970, HOEVE 1970). The physical interpretation of the lower adsorption and smaller thickness in good solvents is, according to HOEVE, that the polymer chains would be desorbed by strong osmotic pressures, if long loops did exist in good solvents. Therefore in a good solvent only small loops and relatively thin polymer films are possible.

3.2. EXPERIMENTAL PROCEDURES

3.2.1. *Adsorption measurements*

Portions of 2 ml of silver iodide sol were placed in 10 ml graduated glass stoppered cylinders. 3–6 ml of water or salt solution were added carefully from a burette, in such a way that a sharp boundary between the sol and the liquid

in top of it was formed. Then 5–2 ml of PVA solution were introduced by pipette to give a final volume of 10 ml with a certain polymer concentration. The purpose of the sharp boundary is to prevent irregular mixing of PVA and AgI. As will be shown in Ch. 5. irregular mixing has a great influence on flocculation.

Thereafter the contents of the cylinders were mixed by hand and the cylinders were rotated end-over-end during a preset adsorption time, in most cases one hour. Subsequently separation of AgI and supernatant solution was obtained by centrifuging 20 minutes at 20,000 rev/min in a Christ Universal KS III centrifuge. The PVA concentration in the supernatant was determined as described in 3.2.2.

During the course of the adsorption studies it was found that PVA adsorbs on the walls of the glassware. This adsorption is more or less reversible: by rinsing once or twice with water the PVA was removed from the glass walls. The adsorption of PVA 88 on glass appeared to be higher than that of PVA 98.5. To minimise interference with the adsorption on AgI a rather high concentration of sol was used in the adsorption experiments; in most cases the final concentration of silver iodide was 50 mmoles/l, giving a ratio of AgI area to glass area of at least 100. Furthermore, in the determination of the calibration curves (see 3.2.2.), tubes were used for each PVA concentration in which a PVA solution of the same concentration had been placed for two hours previously, and which had been allowed to drain upside-down for half an hour. It was assumed that in this way the appropriate amount of PVA had already been adsorbed on the walls of the glass.

3.2.2. *Determination of PVA concentration*

The concentration of PVA was determined colorimetrically by measuring the colour intensity of the complex of PVA with iodine in the presence of boric acid and potassium iodide. On adding these reagents the PVA molecule assumes a helical shape. Within the helix iodine is enclosed. The helix is stabilised by the boric acid (ZWICK 1965). The reaction is analogous to the well known reaction of starch with iodine.

To 6 ml of PVA solution (0–40 ppm) were added 4 ml of the reagent, containing 0.64 M H_3BO_3, 0.06 M I_2 and 0.018 M KI. The colour intensity of the complex was measured using a Unicam SP 600 spectrophotometer with 10 mm cells, at 6700 Å. If the procedure is carefully standardised as to temperature and time elapsed before measuring (ZWICK 1965) good straight calibration lines are obtained as shown in fig. 3–1. The reproducibility of the measurement is then within 2%. On the ordinate axis in fig. 3–1 the absorbance A is plotted, defined as $A = {}^{10}\log {}^{1}/_{\tau}$ in which τ is the transmittance. This definition follows recent proposals suggested in the literature (ANONYMOUS 1969).

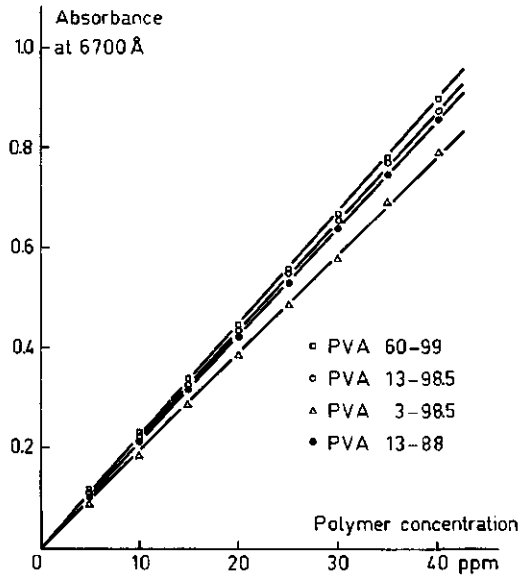

FIG. 3–1. Calibration lines (in the absence of salts) for the determination of PVA concentration

The concentration determination method described above, and slight modifications of it, have been succesfully applied by several workers (HORACEK 1962, CHENE et al. 1966, MONTE-BOVI 1969, SUGIURA et al. 1970, LANKVELD 1970).

The slope of the calibration line increases somewhat with molecular weight and decreases with higher acetate content; these findings are in agreement with those of ZWICK (1966). Moreover, the absorbance of the complex was found to depend on the concentration of other electrolytes present. It was found that the slope of the calibration line increases by 5% from 0 to 10 mmoles/l of KNO_3 and remains constant at still higher concentrations up to 150 mmoles/l. With increasing concentration of $Ca(NO_3)_2$ the slope decreases monotonically. The slope is about 20% lower at 50 mmoles/l of $Ca(NO_3)_2$.

Hence for every salt concentration a new calibration line had to be determined.

3.3. RESULTS AND DISCUSSION

3.3.1. *General*

The results of the adsorption measurements for four PVA samples on sol C at a sol concentration of 50 mmoles/l and a contact time of one hour are given in fig. 3–2. The values expressed in mg/m^2 are calculated using $S = 11$ m^2/g (see 2.2.2.); i.e. 1 mmole of AgI corresponds to 2.58 m^2. We shall discuss these

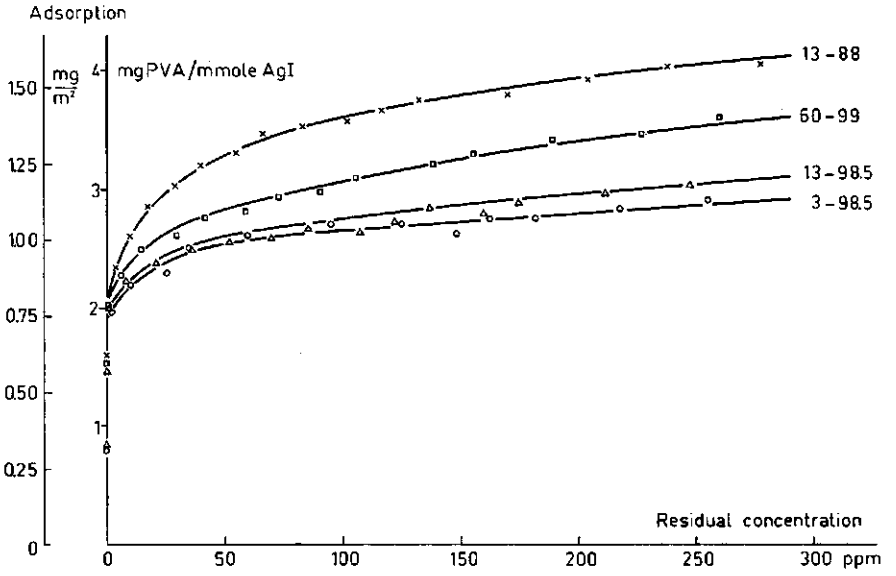

FIG. 3–2. The adsorption of polyvinyl alcohol on silver iodide (sol C); sol concentration 50 mmoles/l; time of adsorption 1 hour

and some other results below and compare them with general findings in polymer adsorption.

Shape of the isotherm. All adsorption isotherms are of the high affinity type: up to an amount adsorbed of about 0.75 mg/m² no PVA remains in solution. It is only at higher surface coverages that a partition of PVA between surface and bulk solution occurs. A real plateau is not reached.

Time effects. The results of fig. 3–2 were obtained with an adsorption time of one hour. Some experiments were carried out over longer times. It was found that the adsorption increases by about 20% in 24 hours, and somewhat more over still longer times. Obviously, the equilibrium state is not reached after 1 hour. Nevertheless, this time was chosen to enable a comparison of the adsorption results with the flocculation experiments to be made.

Desorption. Attempts were made to desorb the polymer from the surface by replacing the bulk solution, containing PVA, with pure water. No PVA present in solution could be detected, even after prolonged rotation of the cylinders.

Configuration of the adsorbed layer. From the compressibility of PVA in the water-paraffine interface LANKVELD (1970) concluded that the surface area per segment of PVA in a close-packed monolayer is about 25 Å². Assuming the same value on a AgI surface it can be easily calculated that the amount of

polymer in a close-packed monolayer would be 0.30 mg/m^2 for PVA 13–98.5. It follows that even for PVA 98.5 an amount of material is adsorbed equivalent to the amount in 3–4 monolayers. Thus at maximum adsorption one fourth of the total number of segments at most is adsorbed in the surface, and the polymer layer must be rather thick. At low coverage a higher proportion of segments can be adsorbed, giving a thinner layer. It will be shown in Ch. 4. that for PVA on AgI the polymer layer is indeed thin at low coverages and becomes thicker when the amount adsorbed increases.

Influence of molecular weight. The adsorption increases with molecular weight (fig. 3–2), but the increase is much less than the proportionality with $\sqrt{M}$, predicted by theory for low molecular weight polymers in Θ-solvents. One should expect this smaller dependence on M qualitatively, because water at room temperature is a moderately good solvent for PVA. However, it is remarkable that the difference in maximum adsorption between PVA 60–99 and 13–98.5 is higher than that between PVA 13–98.5 and 3–98.5. This is in contradiction with the theories mentioned. The reason for this discrepancy is not clear.

Effect of acetate content. The adsorption of PVA 13–88 is much higher than that of PVA 13–98.5 (fig. 3–2). This may be caused by two effects.

(i) According to theory the adsorption increases, the poorer the solvent.

(ii) It is probable that the GIBBS free energy of adsorption per segment is somewhat higher for PVA 88 than for PVA 98.5 on account of the more hydrophobic character of PVA 88.

Both effects could play a role.

In 2.3.4. it was concluded that only a small difference, if any, exists between the two types of PVA as regards the solvent power of water. However, in general the amount adsorbed depends strongly on solvent quality (SILBERBERG 1962b, 1968), so that a slight difference in solvent power could be responsible for a rather large difference in amount adsorbed.

On the other hand, one would expect that the adsorption free energy for a vinyl acetate segment on the hydrophobic AgI is higher than that for a vinyl alcohol segment. However, according to SILBERBERG (1968) the adsorption does not change substantially with increasing free energy of adsorption per segment. Therefore, one would tend to conclude that the small difference in the solvent power of water between the PVA's, rather than the difference in adsorption free energy per segment is responsible for the higher adsorption of PVA 88 (although we were not able to show this difference in solvent quality definitely in Ch. 2.). This conclusion is supported by the fact that the adsorption of PVA 88 on glass is higher than that of PVA 98.5 (see 3.2.1.), for it is hardly imaginable that the affinity of the acetate groups for glass is higher than that of hydroxyl groups. From this it follows also that the solvent quality is the important factor.

The higher adsorption of PVA 88 also leads to a greater thickness of the

adsorbed layer. This too will be shown in the following chapters.

Comparison with other work. Recently SUGIURA and YABE (1970) reported results of adsorption measurements of PVA on AgI. They found the same trends with respect to molecular weight and degree of hydrolysis of PVA. Two differences with our results emerge. Firstly, in their adsorption isotherms a real plateau seems to be attained. Secondly, the adsorption, expressed in mg/m^2, is about twice as high as that measured in the present study. However, it is not clear from their publication what the surface area used by SUGIURA and YABE was, and how they measured it. In this connection it should be repeated that in our case three different techniques yielded the same surface area (see 2.2.2.). This supports our values for the adsorption per m^2.

3.3.2. *Effect of the way of mixing of PVA and AgI on the adsorption*

One of the main variables in flocculation was found to be the way in which polymer and sol are mixed (see Ch. 5.). It was found that optimal flocculation takes place if the following mixing procedure is used: an amount of PVA is added to a portion of sol and after some time a second, equal, portion of sol is added to this mixture.

Investigations were carried out to see if there is also an effect of the way of mixing on the amount adsorbed. There appeared to be no influence on the final amount adsorbed, whether the sol was added to a PVA solution all at once or in two separate portions. However, it is probable that in the latter case the polymer is distributed unequally over the two portions of sol.

In some other experiments a given amount of PVA was added to one portion of AgI in two subsequent steps, the second part of the PVA being added 1 hour after the first. Again after 1 hour the total adsorption was measured. In this case the eventual adsorption was lower by about 10% compared with the adsorption of the same total amount of PVA added in one step to the AgI. This point will be discussed in 3.3.3.

3.3.3. *Reversibility of the adsorption*

From the increase of adsorption with time it can be deduced that at least some desorption of segments can occur. The molecules adsorbed in the early stages of the adsorption process will assume a relatively flat configuration on the surface. Thereafter the molecules must rearrange in order to enable more material to adsorb. Rearrangement implies desorption of segments from some sites. Hence the segment adsorption is, at least to some extent, reversible.

Another factor which can be responsible for the time dependence of the adsorption is the displacement of initially adsorbed molecules of low molecular weight by higher molecular weight species. As mentioned in 2.3.2. the molecular weight distribution of the PVA samples used is rather broad. In this case also

one may deduce that due to this type of rearrangement the adsorption of segments is reversible.

Still another argument stems from the adsorption of PVA in two steps (3.3.2.). The first part of the PVA will be adsorbed in a relatively flat configuration with a large fraction of segments in contact with the surface, in this way occupying a large fraction of the available surface area. The fact, that only one hour after addition of the second part of the PVA already 90% of the amount adsorbed on addition in one step is attached, is clearly indicative of segment desorption. It is likely, however, that the molecules from the second part are adsorbed with fewer segments attached and therefore the layer thickness may be greater, although the total amount adsorbed is somewhat lower. In experiments to be described in the next two chapters this picture is confirmed.

In most of the flocculation experiments, to be described in Ch. 5., measuring times were chosen of the order of one hour. This is much shorter than the time necessary for desorption of polymer molecules. Nor can a substantial rearrangement within the adsorbed layer take place, in view of the slow increase of the amount adsorbed with time. Hence for the purpose of interpreting the flocculation results the adsorption may be considered as irreversible.

3.3.4. *The interaction between a segment of PVA and the AgI surface*

In connection with the interpretation of our stability studies (Ch. 6.) an estimate for the adsorption free energy per CH_2—CHOH-segment is needed. Direct information on this quantity is not available but an assessment of at least the order of magnitude can be made on the basis of some general considerations.

The most common attachment mechanisms for polymers on surfaces are electrostatic bonding, hydrogen bond formation, VAN DER WAALS interactions and hydrophobic bonding. Only the last two possibilities need to be considered for the adsorption of PVA on AgI.

From potentiometric titration studies of AgI in the presence of low molecular weight aliphatic alcohols BIJSTERBOSCH et al. (1965) could deduce that these organic molecules are adsorbed on the surface with the hydroxyl group pointing towards the solution, whereas the hydrophobic part of the molecule is on the surface. The GIBBS free energy of adsorption was found to amount to about 4 kT per molecule for n-propanol and about 5.5 kT for n-butanol. The increment in adsorption free energy per CH_2-group is of the same order but higher than that given by TRAUBE's rule (see e.g. KIPLING 1965). Slightly lower increments in adsorption free energy per CH_2-group were measured by DAMASKIN et al. (1967) for the series n-propanol to n-hexanol on mercury. From this it would seem that the main contribution to the adsorption free energy of alcohols on AgI and Hg is due to hydrophobic bonding. This is also likely because the

difference in polarisability between a water molecule and a methylene group is rather small, so that the VAN DER WAALS contribution to the adsorption free energy is small. We conclude that the adsorption free energy per segment is to a large extent determined by its entropic part.

In view of the analogy in structure of these alcohols and a PVA segment it can be expected that the OH-group of a PVA segment, adsorbed on AgI, is directed also out of the surface. To estimate the adsorption free energy per segment the values found by BIJSTERBOSCH et al. (1965) and by DAMASKIN et al. (1967) have to be extrapolated to smaller chain lengths, notably ethanol. However, DAMASKIN et al. found that the differences in adsorption free energy per molecule between propanol and ethanol on mercury amounted to about 2 kT which is more than predicted by TRAUBE's rule, probably because the structure of the water around a hydroxyl group is changed in the vicinity of the surface. Thus one could infer that the adsorption free energy for ethanol on AgI would also be of the order of 2 kT per molecule. A PVA segment has a structure, similar to ethanol, except that the segments are linked together in a chain. Therefore there will be less room for neighbouring water molecules, the rearrangement of which upon adsorption determines the adsorption entropy. Moreover, the hydroxyl group will probably approach nearer to the surface than in the case of ethanol and the decrease in entropy will be greater than for ethanol, giving rise to a lower adsorption free energy. Taking all considerations together we conclude that the free energy of adsorption per segment is of the order of but definitely lower than 2 kT. In Ch. 6. we shall use the value of 1 kT for the GIBBS free energy of adsorption per segment of PVA adsorbed on AgI.

In addition to the factors mentioned, configuration entropy effects will also contribute to the adsorption free energy. These effects will not be considered here. In sec. 6.5.1. a method will be described to account for the configurational entropy changes.

3.3.5. *Influence of salt on the adsorption*

In fig. 3–3 the dependence of the adsorption on the nature and concentration of salt is shown. The polymer concentration (added 240 ppm) is chosen such, that roughly the same amount of polymer is present in solution as on the surface. The adsorption decreases somewhat when salt is present. However, the effect is only slight, maximally about 10% for KNO_3 and about 5% in the case of $Ca(NO_3)_2$.

In order to explain this effect one might imagine that due to competition between counterions and adsorbed segments in the STERN layer the polymer adsorption is lowered. However, this is unlikely because counterions are forced out of a AgI surface by butanol as has been deduced by BIJSTERBOSCH et al.

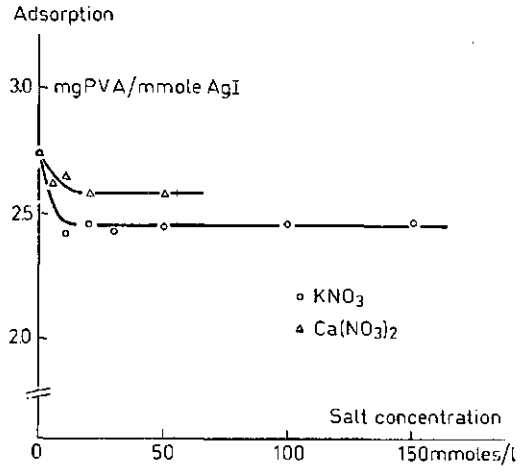

FIG. 3–3. Effect of the salt concentration on the adsorption of PVA 13–98.5 on AgI (sol C)
sol concentration 50 mmoles/1; polymer concentration (added) 240 ppm

(1965) and VINCENT et al. (1971) from the lowering of the double layer capacity. Also KOOPAL (1970) in our laboratory has found that, due to the presence of PVA, the double layer capacity decreases, indicating counterion desorption. Another explanation would be in terms of changes in solvent power; decrease of of adsorption could occur if an aqueous salt solution is a better solvent than water. However, from fig. 2–4 opposite trends are to be expected for KNO_3 and $Ca(NO_3)_2$. It is true that the concentration of counterions in the double layer near the surface is higher than in the bulk, but then one should expect even more of an increase in adsorption due to decreasing solvent power.

So we observe that the adsorption of PVA decreases somewhat with increasing salt content, but we cannot offer a satisfactory explanation. At the same time it should be noted that the magnitude of this effect is so small that it cannot play an important role in explaining the flocculation results.

3.4. CONCLUSIONS

The adsorption of polyvinyl alcohol on silver iodide is in general agreement with previous experimental findings on other systems and with the theories of SILBERBERG (1968) and HOEVE (1970).

The adsorption obeys a high affinity type adsorption isotherm. The (pseudo) maximum value of the amount adsorbed is of the order of 1 to 1.5 mg/m^2 and the fraction of segments adsorbed about 25%, depending on the molecular weight and the acetate content of the PVA. The amount adsorbed and the layer thickness increase with molecular weight, and decrease with increasing degree of hydrolysis of the PVA. The layer thickness is expected to be rather low for

low surface coverages and to increase with the amount adsorbed.

When PVA is added to AgI in two subsequent steps the amount adsorbed is only slightly lower than after one-step addition; yet the layer thickness is greater.

The adsorption of molecules as a whole is irreversible, but the segment adsorption is reversible, at least in part. For experiments with a time-scale of the order of 1 hour the adsorption may be considered as completely irreversible.

The GIBBS free energy of adsorption per segment of PVA can be estimated to be of the order of 1 kT by analogy with experiments with low molecular weight alcohols.

The adsorption is lowered by addition of salts. There is no obvious explanation for this effect, but it is very small.

4. ESTIMATION OF THE THICKNESS OF THE ADSORBED LAYER AND EVALUATION OF THE POLYMER DISTRIBUTION

In the previous chapter, measurements were described to obtain the amount of PVA adsorbed onto the particles in a silver iodide sol. With regard to the configuration of the polymer layer it was deduced that a relatively thin layer is present when only a small amount of polymer is adsorbed, whereas long loops occur at higher amounts adsorbed.

In this chapter some methods will be discussed to pursue these ideas more quantitatively by measuring the layer thickness as a function of the amount adsorbed. Moreover, from the electrical double layer properties of AgI in the presence of adsorbed PVA the volume fraction of polymer in the first layer adjacent to the surface can be estimated. The segment distribution in the adsorbed layer can then be evaluated by use of theoretical models available in the literature. This information is necessary for any quantitative interpretation of the flocculation results (Ch. 6.).

4.1. THE PROTECTION OF SILVER IODIDE SOLS BY POLYVINYL ALCOHOL

Polymers are able to protect sols against coagulation by salts. In this case there must exist, in addition to the double layer repulsion, a second contribution to the repulsion free energy in order to prevent coagulation under the influence of the VAN DER WAALS attractive forces. There is in fact a direct contribution due to the adsorbed polymer layer on the colloidal particles. Two mechanisms can be envisaged. Firstly, when two covered particles approach each other the adsorbed chains become restricted in the number of their possible configurations due to the presence of the second interface (*volume restriction repulsion*) (CLAYFIELD and LUMB 1966, MEIER 1967, HESSELINK 1971). Secondly, on account of the increase in polymer concentration between the surfaces an *osmotic repulsion* occurs (FISCHER 1958, MEIER 1967, HESSELINK 1971). Both these repulsive terms will become more important the thicker the polymer layer. Thus more salt will be needed to coagulate a covered sol as the layer thickness increases. The possibility arises of obtaining qualitative information concerning the extension of the adsorbed layer and the occurrence of long loops. The critical coagulation concentration can be used in this way as a qualitative measure of the thickness of the adsorbed layer.

4.1.1. *Experimental*

Polyvinyl alcohol was added to silver iodide using the sharp boundary method described in 3.2.1. After five hours of rotation end-over-end the amount adsorbed was measured as described in 3.2.

Coagulation values of KNO_3 were measured, five hours after the mixing of the AgI and the PVA, by the kinetic method introduced by REERINK and OVERBEEK (1954). The change of the absorbance of the mixture with time was measured for several salt concentrations c_s, and the initial slope of the plot of the absorbance against time was determined. The reciprocal of this slope may be shown to be proportional to the stability ratio W, and plots of log W against log c_s were obtained in this way. In the intersection of the two linear regions usually obtained in such a plot the critical coagulation concentration c_c was derived.

The experiments were carried out at a wavelength of 6620 Å, using a Vitatron UC 200 spectrophotometer with automatic recording. The final sol concentration in the spectrophotometer tubes was 0.2 mmoles/l. Coagulation values as a function of the amount adsorbed were determined for PVA's of two molecular weights and two degrees of hydrolysis.

4.1.2. *Results and discussion*

In fig. 4–1 coagulation values of KNO_3 for polymer covered AgI sols are plotted against the amount of PVA adsorbed (p_a in mg/m^2), for PVA 13–98.5,

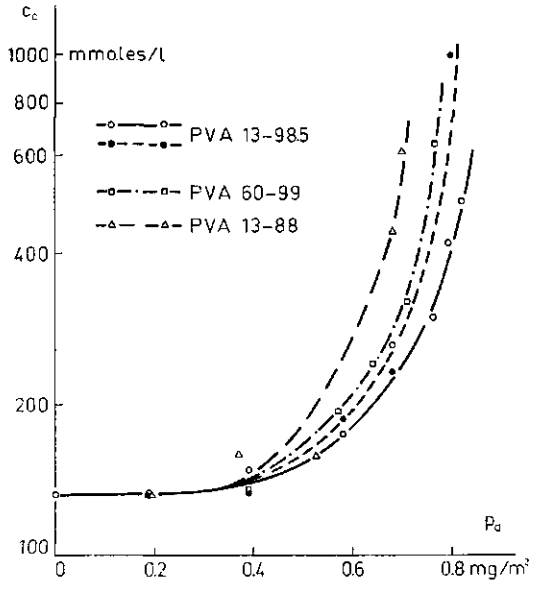

FIG. 4–1. Coagulation values of KNO_3 for AgI (sol C) covered by PVA.
The filled symbols refer to measurements in which PVA 13–98.5 was adsorbed in two steps.

60–99 and 13–88. Also included are some measurements in which PVA 13–98.5 was added in two equal steps to the AgI. In this case the contact time between the sol and the first step of PVA was 2.5 h, then the second part of PVA was added and again after 2.5 h c_c was measured.

As may be seen from fig. 4–1 no protection takes place at amounts adsorbed of less than 0.4 mg/m^2. One close-packed monolayer corresponds to about 0.3 mg/m^2 (3.3.1.). From comparison of these figures it would seem that up to $p_a = 0.4$ mg/m^2 the adsorbed polymer is lying flat or has only very small loops which do not contribute to the repulsion.

With increasing values of p_a loop formation becomes more extensive, leading to increased protection, as judged from the rise in critical coagulation value. At amounts adsorbed greater than 0.9 mg/m^2 apparently the loops are so long that the VAN DER WAALS forces are no longer effective in causing coagulation when the electrical double layer repulsion is removed by the addition of salt, and so a critical coagulation value cannot be measured. However, above $c_s =$ 2 M the sol is coagulated by the salting-out of the polymer.

The protection by PVA 60–99 is more effective than that by PVA 13–98.5, suggesting a thicker layer of polymer at equal p_a. A possible explanation of this fact will be discussed in 4.5.2.

The thickness of the adsorbed layer is higher for PVA 88 than for PVA 98.5. This is in accord with the theoretical expectation that the loops are longer in a poorer solvent (3.3.1.).

It is also apparent from fig. 4–1 that the protection is more effective if the polymer is added in two steps instead of all at once. The basis of this was discussed in 3.3.3. and arises from the formation of greater loops by the molecules of the second part of PVA. The surface is already covered rather completely by the PVA adsorbed in the first step so that fewer segments of the second part can attach to the surface.

In conclusion, the qualitative information on the configuration of the polymer layer obtained by the measurement of the coagulation values is in agreement with the inferences deduced from the adsorption measurements.

In the next two sections a more quantitative approach will be described.

4.2. THE VISCOSIMETRIC THICKNESS OF THE POLYMER LAYER

4.2.1. *Principle of the method*

The viscosity of very dilute dispersions of impenetrable, uncharged particles depends only on the volume fraction of solid according to the well-known EINSTEIN equation (EINSTEIN 1906). If a polymer is adsorbed onto the particles the effective volume fraction of the dispersed material and, thus, the viscosity

of the dispersion should increase. From this increase in viscosity the thickness of the polymer layer can be obtained (ROTHSTEIN 1964, ROWLAND et al. 1965, DOROSZKOWSKI et al. 1968). Experiments have also been carried out from which the thickness of a polymer layer adsorbed onto glass has been obtained from viscosity measurements in narrow glass capillaries (ÖHRN 1955, TAKEDA et al. 1956, HUQUE et al. 1959).

The dependence of the viscosity of a dispersion on the weight concentration of solids is given by eq. (2–4) for not too high concentrations. If the amount of solid is expressed in terms of the volume fraction, φ, eq. (2–4) reads (FRISCH et al. 1956):

$$\frac{\eta_{re}}{\varphi} = K_E + k' K_E^2 \varphi \tag{4-1}$$

As in eq. (2–4), η_{re} is the viscosity ratio excess and k' is the HUGGINS constant. K_E is the well-known EINSTEIN coefficient which depends on the shape of the particles. K_E takes the value 2.5 for solid uncharged spheres and is higher for anisodimensional particles. The value of K_E can be found from a plot of η_{re}/φ against φ according to eq. (4–1).

Eq. (4–1) is valid for a dilute dispersion of uncharged particles. With charged particles complications arise and the viscosity becomes dependent on the ionic strength of the solution. This is called the electroviscous effect. The *first electroviscous effect* is caused by the deformation of the double layer around the particles under shear. Due to this effect K_E becomes higher than the EINSTEIN value, especially at low ionic strength. The *second electroviscous effect* is caused by the interaction between the particles due to double layer overlap and effects k' rather than K_E. This effect also increases with decreasing ionic strength. Reviews concerning the electroviscous effect may be found in the literature (CONWAY et al. 1960, STONE-MASUI et al. 1968).

In the presence of adsorbed polymer the effective volume fraction increases by a factor f:

$$\varphi^* = f\varphi \tag{4-2}$$

φ^* is the effective volume fraction in the presence of adsorbed polymer.

The viscosity ratio excess of a covered sol, η_{re}^*, is found by substituting eq. (4–2) into eq. (4–1):

$$\frac{\eta_{re}^*}{\varphi} = K_E f + k' (K_E f)^2 \varphi \tag{4-3}$$

In a plot of η_{re}^*/φ against φ the intercept gives $K_E f$. If it is assumed that the

shape of the particles does not change on polymer adsorption K_E, obtained from eq. (4–1), can be used in turn to calculate f.

Assuming monodisperse spherical particles, the thickness of the polymer layer, Δ, follows from f:

$$\Delta = R(f^{1/3} - 1) \tag{4-4}$$

where R is the radius of the uncovered particle.

4.2.2. *Experimental*

The measurements were carried out with sol C. The volume fractions used were 0.025 and lower.

Firstly, it was checked whether the sol itself was Newtonian. For this purpose a capillary viscosimeter was used to which a variable pressure could be applied. It was found that the most concentrated sol was Newtonian up to an average shear rate of 5.10^3 s^{-1}.

Viscosities were measured at 25 °C in the same viscosimeters as described in 2.3.2. In these viscosimeters the average shear rate is about 10^3 s^{-1}, hence it was concluded that indeed the sol would show Newtonian behaviour in these viscosimeters.

In order to obtain the EINSTEIN coefficient K_E the viscosity of the AgI sols was measured at several volume fractions of solid, prepared by dilution of the most concentrated sol with water. This concentrated sol ($\varphi = 0.025$) contained about 2 mmoles/l of electrolytes, mainly KNO_3. The ionic strength was thus not constant in the dilution process. The reason for adopting this procedure will be discussed below. Some experiments with uncovered sols were also carried out in which the ionic strength was kept constant.

The polymer used in the layer thickness measurements was PVA 60–99. The polymer was brought in contact with the AgI again using the sharp boundary method to prevent irregular mixing. After mixing by hand the sol was rotated end-over-end for one hour and left for 15 hours.

Despite these precautions, some flocculation did occasionally occur. This was probably caused by the fact that, due to the high sol concentration, the mixing of the PVA and the AgI was not perfect (see Ch. 5.). Therefore the covered sol was passed through a glass filter (L 3, mean pore diameter $\sim 25\ \mu$m) to remove any aggregates. Hereafter the viscosity of every sol with a given ratio of PVA to AgI was measured in several dilutions. As stated, the ionic strength decreased upon this dilution. The sol concentration was determined by weighing after drying.

At the highest concentrations of PVA used some PVA remained in solution, altering slightly the viscosity of the dispersion medium. This was corrected for

by measuring the solution concentration of PVA; from this the viscosity of the dispersion medium was calculated, using the data of Ch. 2.

Originally attempts were made to perform all the experiments at a constant ionic strength of 5 mmoles/l of univalent electrolyte. However, it appeared that in this case the extent of the coagulation after mixing of PVA and AgI was so high, as to cause very irreproducible measurements. Therefore, the method of dilution with water was adopted, although this had the disadvantage of a variable ionic strength and, hence, also a variable electroviscous effect.

4.2.3. *Results and discussion*

In fig. 4–2 the reduced viscosity ratio excess η_{re}/φ is plotted as a function of the volume fraction for uncovered AgI (sol C). η_{re}/φ appears to be independent of φ ($k' = 0$), except for the lowest concentrations. The EINSTEIN coefficient K_E amounts to 4.4.

In experiments with AgI sols at constant ionic strength HARMSEN et al. (1953) found about 3.5 for K_E. This is higher than 2.5, the value for spherical particles, the difference probably being caused by the somewhat elongated shape of AgI particles. We found also 3.5 for K_E and a non-zero HUGGINS constant in experiments at constant ionic strength. Apparently the first electroviscous effect does not play a role in the range of ionic strengths used. However, at constant ionic strength the slopes of the curves of η_{re}/φ against φ increase with decreasing salt concentration, which is indicative for the occurrence of the second electroviscous effect.

The high value of 4.4 for K_E in experiments with variable ionic strength can be attributed to this second electroviscous effect. At constant ionic strength, lowering of φ should result in a lower reduced viscosity ratio excess η_{re}/φ. However, in our case the ionic strength decreased with decreasing φ, causing an increase of η_{re}/φ by the second electroviscous effect. Apparently these trends just compensate each other, giving rise to a constant value of η_{re}/φ, except for the lowest concentrations. In this case the increase in η_{re}/φ by the stronger double layer interaction is higher than the decrease caused by the lower solid content.

Thus in the range of volume fractions and ionic strengths used in our experiments the viscosity can be described by an EINSTEIN coefficient of 4.4 and a zero HUGGINS constant.

Results obtained with sols, to which PVA 60–99 was added, are presented in fig. 4–3. At low coverage the shape of the curves of η^*_{re}/φ against φ is the same as that for the sol without PVA, although, going to lower φ, the deviations from the horizontal line start at lower volume fractions. At higher amounts adsorbed the increase in reduced viscosity ratio excess due to the electroviscous effect disappears, possibly because the increase in η^*_{re}/φ due to the adsorbed polymer layer dominates.

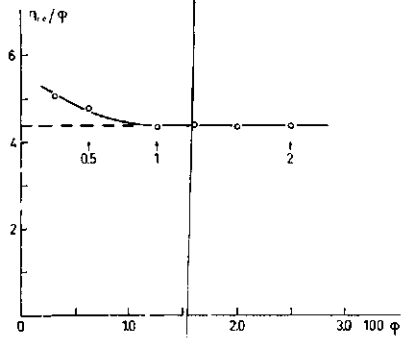

FIG. 4–2. The reduced viscosity ratio excess of silver iodide (sol C) as a function of the volume fraction of AgI. The figures at the arrows indicate the ionic strength in mmoles/l.

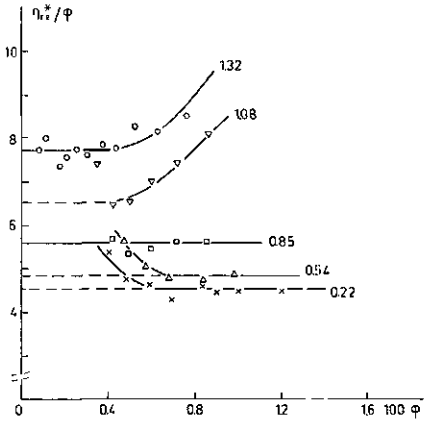

FIG. 4–3. The reduced viscosity ratio excess of silver iodide (sol C), covered with PVA 60–99, as a function of the volume fraction of AgI. The figures at the right indicate the amount of PVA adsorbed (mg/m²).

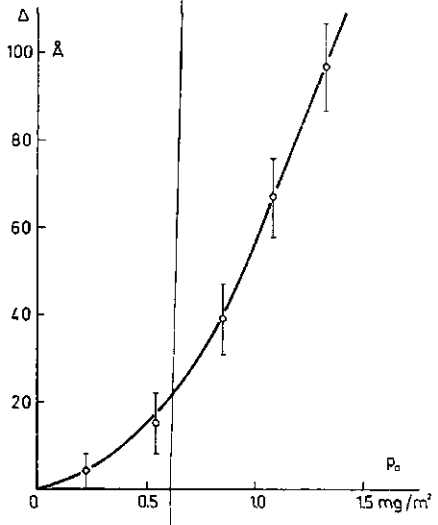

FIG. 4–4. Viscosimetric thickness of the layer of PVA 60–99 adsorbed onto AgI (sol C).

In the systems with the highest polymer concentrations deviations occur at high solid content. Here the increase in η^*_{re}/φ is probably caused by hydrodynamic interaction due to the rather thick polymer layer in these cases.

The intercepts of fig. 4–2 give the product of K_E and f. Using 4.4 for K_E the thickness Δ was calculated from equation (4–4). The results with the estimated uncertainties are plotted in fig. 4–4.

At low p_a the layer is thin, indicating that a high fraction of segments is

adsorbed. With increasing amount adsorbed the thickness increases rapidly, suggesting long loops protruding into the solution. In the (pseudo) plateau of the adsorption isotherm, at $p_a \simeq 1.35$ mg/m^2, the thickness is of the order of 100 Å. From a comparison with fig. 4–1 it would appear that strong protection against coagulation by salt is reached when the adsorbed layer is around 30 Å thick.

The results agree very well with the qualitative predictions mentioned before. In 4.5. the actual interpretation of the thickness values as found by the viscosimetric method will be discussed, and a quantitative comparison with the theory will be made there.

4.3. Estimation of the thickness of the polymer layer from electrophoretic measurements

4.3.1. *Principle of the method*

Charged particles move under the influence of an applied electric field. From the electrophoretic mobility the electrokinetic ζ-potential, that is the potential difference between the plane of shear and the bulk of the solution, can be derived.

When a polymer is adsorbed on a charged particle the plane of shear will be shifted outwards with respect to its position in the absence of polymer. The new distance of the plane of shear from the surface can be put equal, to a first approximation, to the thickness of the adsorbed layer.

In order to obtain the shift of the plane of shear due to the presence of adsorbed PVA it is necessary to make assumptions as to the potential distribution in the adsorbed layer. As PVA is uncharged (see 2.3.5.) the simplest approximation which can be made is that the PVA does not influence the charge distribution in the diffuse part of the double layer. The basis for this approximation is, that there is only slight interaction between PVA and salt (see 2.3.5., fig. 2–4). Furthermore, the volume occupied by polymer in the diffuse layer is only small. The potential distribution in the diffuse part of the double layer, $\psi(x)$, as a function of the distance from the surface, x, is then the same as that without adsorbed polymer and is, for symmetrical electrolytes and a plane double layer, given by:

$$\tanh \frac{ze\psi(x)}{4kT} = \tanh \frac{ze\psi_d}{4kT} \cdot e^{-\kappa(x-\delta)} \qquad (4\text{-}5)$$

where z is the valency of the ions in the double layer, δ the thickness of the Stern layer, ψ_d the Stern potential and κ the reciprocal Debije length. e, k

and T have their usual meaning. The layer thickness, Δ, is then found by substituting Δ for x and ζ for $\psi(x)$:

$$\tanh\frac{ze\zeta}{4kT} = \tanh\frac{ze\psi_d}{4kT} \cdot e^{-\kappa(\Delta-\delta)} \qquad (4\text{-}6)$$

This equation is valid only if the thickness of the polymer layer is higher than δ; thus it does not apply when p_a is zero or very small.

Eq. (4–6) offers the possibility of obtaining Δ from the measured ζ-potential, provided that a reasonable estimate for ψ_d can be found.

ζ can be calculated from the electrophoretic mobility which depends on the concentration of potential determining ions. At low pAg the mobility is positive; with increasing pAg the mobility decreases, reverses sign in the isoelectric point (iep) and becomes increasingly negative until a plateau is reached. From thereon the mobility does not depend on ζ any more due to relaxation effects (WIERSEMA et al. 1966). Hence it is impossible to obtain ζ from the mobility measured in the plateau region. As at low mobilities the experimental error is rather large, the most reliable ζ-potentials are obtained from the data at the onset of the plateau region. Thus the mobility at the beginning of the plateau was used to find the ζ-potential following the numerical calculations of WIERSEMA et al. (1966).

There is no direct method to find ψ_d. Although it is a good approximation to assume that PVA does not influence the potential distribution in the diffuse part of the double layer there is positive evidence that ψ_d is affected by PVA adsorption. In 4.3.3. one way of estimating ψ_d will be presented.

4.3.2. *Experimental*

Preliminary experiments to obtain the ζ-potential of the particles of sol C, covered by a varying amount of PVA 16–98, have been carried out by KOOPAL in our laboratory. The PVA and the AgI were mixed in the usual way; after dilution of the sol the pAg was adjusted in the cell described earlier (2.2.2.). The ionic strength was 10^{-3} N, obtained by addition of HNO_3. Electrophoretic mobilities were measured in an apparatus similar to that described by MACKOR (1951).

4.3.3. *Results and discussion*

In fig. 4–5 the results obtained by KOOPAL are summarised. The ζ-potential at the onset of the plateau region was calculated as described in 4.3.1. The surface potential (ψ_0) at the beginning of the plateau was derived from the difference between the pAg at this point and the iep using NERNST's law. In so doing the point of zero charge (pzc) and the iep are assumed, to a first approximation, to be equal. The STERN potential (ψ_d) at the onset of the plateau region

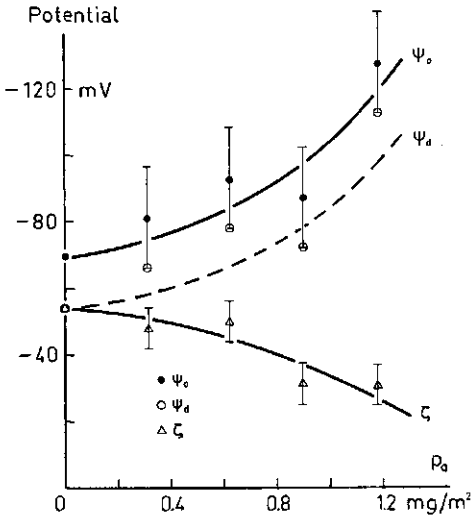

FIG. 4–5. Electrophoretic measurements on AgI (sol C) covered by PVA 16–98.
The ζ-potential, surface potential (ψ_0) and STERN potential (ψ_d) at the beginning of the mobility plateau as a function of p_a.

can be obtained from the surface potential if the potential drop across the STERN layer is known. If it is assumed that, for an uncovered AgI surface, ψ_d equals ζ the potential drop across the STERN layer amounts to 15 mV in this case.

It will be assumed that this same drop in potential also applies in the presence of PVA and is independent of p_a. In making this assumption two partially compensating errors are made. Firstly, ψ_0 increases with p_a and it can be expected that more specific adsorption of counterions occurs at higher surface potentials, causing the drop to increase with p_a. However, when more PVA is adsorbed on the silver iodide surface more competition takes place for specifically adsorbed ions, leading to a lower specific adsorption and a smaller potential drop across the STERN layer.

BIJSTERBOSCH et al. (1965) and VINCENT et al. (1971) have shown that desorption of counterions occurs when butanol is added to a AgI suspension.

Thus ψ_d was obtained by subtracting 15 mV from ψ_0. Δ was then calculated from eq. (4–6), using $\delta = 4$ Å. The results are plotted in fig. 4–6. The estimated uncertainties in the values given are rather high: at the highest Δ about 20% and for lower Δ much higher.

The thickness as a function of coverage, derived in this way for PVA 16–98, compares well with the viscosimetric thickness for PVA 60–99 (fig. 4–4). As will be shown in 4.5.2. the thickness, at equal p_a, does not depend very strongly on molecular weight.

At high amounts of adsorbed PVA the agreement is surprisingly good, in view of the very crude approximations used and the rather uncertain measurements. At low adsorption the electrophoretic thickness is higher than the vis-

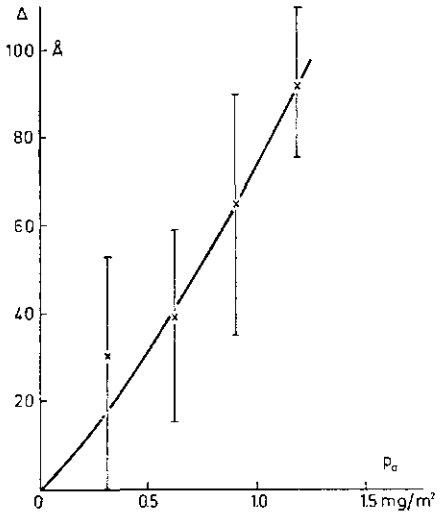

FIG. 4–6. The thickness of the layer of PVA 16–98 adsorbed on AgI (sol C), obtained from electrophoretic measurements.

cosimetric one. This is probably not significant because the experimental inaccuracy is greatest in this region.

Although the absolute figures obtained from the electrokinetic measurements are rather doubtful, they do give support to the viscosimetric experiments, described in 4.2. In the analysis on the polymer distribution in the adsorbed layer presented in 4.5. only the results obtained from viscosimetry will be used, because these results are more pertinent than those derived from electrophoresis.

4.4. THE COVERAGE BY POLYMER IN THE FIRST LAYER ON THE SILVER IODIDE SURFACE

In this section two methods will be applied to obtain information on the coverage in the first layer on the AgI surface. This coverage will also be needed to evaluate the polymer distribution in the adsorbed layer.

Polymer segments adsorbed in the first layer on the surface will alter the point of zero charge and will affect also the surface charge. Consequently, from these two double layer properties information can be gained concerning the coverage of the surface. As these experiments are aimed at inner layer properties, they are considered at a salt concentration of 0.1 M.

4.4.1. *The shift of the point of zero charge of AgI due to the adsorption of PVA*

Adsorption from solution of neutral molecules on a surface leads usually to a shift in the point of zero charge (Δpzc). This shift is primarily caused by a change in the chi-potential, the primary reason for this being the replacement of

water dipoles by the adsorbed molecules. In addition, secondary effects take place due to rearrangements of neighbouring water molecules and changes in the induced dipole moment in the solid phase. If specific adsorption occurs, its extent will also generally be affected by the adsorption of the neutral species, leading to a second mechanism of shifting the pzc. For AgI in the pzc specific adsorption is only slight, as can e.g. be judged from the small shift of the pzc due to adsorption of neutral electrolytes. Hence we shall interpret the shift solely via the dipole-replacement mechanism.

The shift in the pzc caused by small adsorbing molecules, Δpzc, is roughly proportional to the number of molecules adsorbed per unit area (n_a) (BIJSTERBOSCH et al. 1965). Thus:

$$\Delta\text{pzc} = \text{constant} \,.\, n_a \tag{4-7}$$

When PVA is the adsorbing molecule it may be assumed in first approximation that only the segments adsorbed in the first layer contribute to the shift of the pzc, the segments in the protruding loops being too far away to affect the inner layer properties. Each PVA segment consists of two parts, a methylene group and a CHOH-group. Formally, the shift due to adsorbed segments of PVA, Δpzc (PVA), can be split up into two parts:

$$\Delta\text{pzc (PVA)} = \Delta\text{pzc (CH}_2\text{)} + \Delta\text{pzc (CHOH)} \tag{4-8}$$

A crude estimation of the two separate contributions can be made from a comparison with the known shift caused by butanol (Δpzc(BuOH)) (BIJSTERBOSCH et al. 1965) and the shift in the presence of ethylene glycol (Δpzc(EG)) (DE WIT 1971). A surface completely covered by PVA segments is filled half by CH_2-groups and half by CHOH-groups. Then it can be assumed:

$$\Delta\text{pzc (CH}_2\text{)}^{\max} = \gamma_1 \,.\, \tfrac{1}{2}\Delta\text{pzc (BuOH)}^{\max} \tag{4-9a}$$

$$\Delta\text{pzc (CHOH)}^{\max} = \gamma_2 \,.\, \tfrac{1}{2}\Delta\text{pzc (EG)}^{\max} \tag{4-9b}$$

The suffix 'max' refers to a fully covered surface; γ_1 and γ_2 are parameters describing the relative contribution of CH_2- and CHOH-groups, respectively, to the shift of the pzc in comparison to the contribution of butanol and ethylene glycol molecules. Their magnitudes will be discussed below.

The fraction of the surface covered in the first layer by polymer segments, θ_p, is defined as:

$$\theta_p = \frac{n_p}{n_p^{\max}} \tag{4-10}$$

in which n_p is the number of segments of PVA adsorbed per unit area.

Combining eq. (4–10) with eqs. (4–7) to (4–9) it can be shown that

$$\theta_p = \frac{\Delta\text{pzc (PVA)}}{\Delta\text{pzc (PVA)}^{\max}} \tag{4-11}$$

or: $$\theta_p = \frac{2\Delta\text{pzc (PVA)}}{\gamma_1\Delta\text{pzc (BuOH)}^{\max} + \gamma_2\Delta\text{pzc (EG)}^{\max}} \tag{4-12}$$

From potentiometric titration of a silver iodide suspension in water in the presence of butanol, Δpzc(BuOH)^{max} was found to be 192 mV by BIJSTERBOSCH et al. (1965). Using the same technique DE WIT (1971) found a value for Δpzc (EG)^{max} of about 60 mV. KOOPAL (1970) measured for PVA 40–88 a shift of about 75 mV for amounts of adsorbed PVA about half the maximum and higher. It should be noted here that the amount of PVA, which can be adsorbed per m^2 onto the particles of a suspension of AgI is less than that on the particles of a sol by a factor of about two. This is probably due to the fact that it is not possible for the polymer molecules to penetrate into all the pores of the aggregates existing in the suspension.

It follows from KOOPAL's experiments that θ_p is already approximately constant when about half of the maximum amount of PVA is adsorbed. Using reasonable values for the parameters γ_1 and γ_2 the value of θ_p can be estimated from eq. (4–12).

As a first approximation it is assumed that $\gamma_1 = 1$, i.e. at equal surface coverage the shift caused by CH_2-groups is supposed to be the same as that caused by butanol. A butanol molecule adsorbs with its hydrocarbon end towards the surface (BIJSTERBOSCH et al. 1965). The hydroxyl groups, pointing towards the solution, are probably oriented randomly, so that the component of the dipole moment normal to the surface is very small. The effect of the adsorption of butanol molecules on the moment of the inner layer is than essentially the same as that of methylene groups, viz. the replacement of oriented water dipoles by dipole-less groups.

In the same way it may be assumed that the effect of replacing water molecules by the CHOH-groups of PVA is the same as that when water is replaced by the CH_2OH-groups of ethylene glycol. Then also $\gamma_2 = 1$.

Substituting these values in eq. (4–12) it is found that the coverage in the first layer, θ_p, is about 0.60. In view of the assumptions made this value is only approximative; it applies to amounts adsorbed greater than half of the maximum. At lower amounts adsorbed the coverage will be less.

4.4.2. *The surface charge of AgI in the presence of PVA*

When neutral molecules adsorb onto a charged surface the magnitude of the surface charge is influenced. The total surface charge can be considered as a linear combination of the surface charge of the uncovered surface and that at complete coverage. Both the conditions, constant cell E.M.F. (e.g. FRUMKIN

1926), and constant surface potential (BIJSTERBOSCH et al. 1965), have been proposed. We shall adopt the latter condition, since changes in the surface charge arising from changes in the pzc are then excluded. One may then write, again ignoring the effect of the loops:

$$\sigma_p = \sigma_0 (1 - \theta_p) + \sigma_p^{max} \theta_p \qquad \text{at constant } \psi_0 \tag{4-13}$$

Here σ_0 is the surface charge per cm^2 of un uncovered AgI surface, σ_p is that in the presence of PVA and σ_p^{max} is the value of σ_p at a (hypothetical) coverage of 100%. σ_0 and σ_p are measurable, but the value of σ_p^{max} can be assessed only by indirect means. The easiest way of estimating σ_p^{max} is again to compare it with σ_b^{max}, the surface charge of a AgI surface completely covered by butanol. It is assumed:

$$\sigma_p^{max} = \gamma_3 \sigma_b^{max} \tag{4-14}$$

γ_3 can be estimated by considering the integral capacity of the double layer per cm^2, i.e. the ratio between the surface charge per cm^2 and the surface potential. At constant ψ_0 eq. (4–14) is identical to:

$$K_p^{max} = \gamma_3 K_b^{max} \tag{4-15}$$

where K_p^{max} and K_b^{max} are the integral capacities per cm^2 when the surface is completely covered by PVA and butanol, respectively. At high ionic strength (10^{-1} M) the integral capacity of the double layer is determined almost completely by the STERN capacity. Moreover, when the surface is covered completely nearly all ions are forced out of the STERN layer so that only a small specific adsorption occurs. Therefore, to a good approximation:

$$K_b^{max} = \frac{\varepsilon_b^{max}}{4\pi\delta_b^{max}} \tag{4-16a}$$

$$K_p^{max} = \frac{\varepsilon_p^{max}}{4\pi\delta_p^{max}} \tag{4-16b}$$

and

$$\gamma_3 = \frac{\varepsilon_p^{max}}{\varepsilon_b^{max}} \cdot \frac{\delta_b^{max}}{\delta_p^{max}} \tag{4-17}$$

In these equations ε_b^{max} and ε_p^{max} are the dielectric constants of the STERN layer on the surface fully covered by butanol and polyvinyl alcohol, respectively, and δ_b^{max} and δ_p^{max} are the thicknesses of the STERN layers under the same conditions.

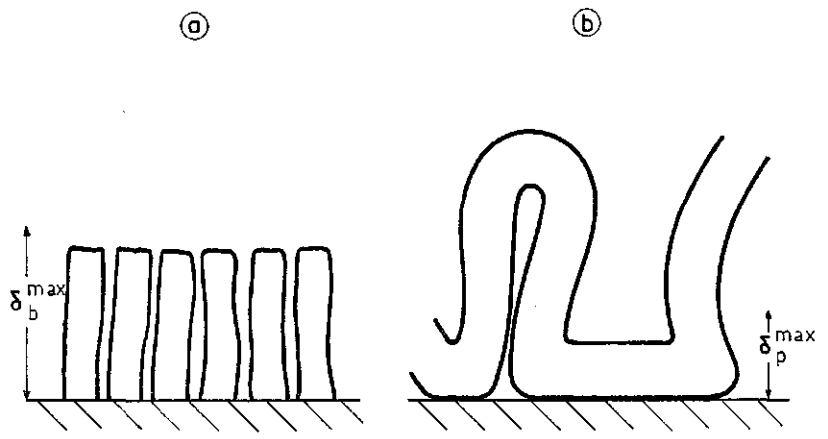

FIG. 4–7. Schematic representation of a surface completely covered by a) butanol or b) polyvinyl alcohol.

An estimation of the relative magnitude of these quantities can be found with the help of a schematic picture such as that given in fig. 4–7. The counter ions can approach somewhat nearer to a polymer covered surface than to one covered by butanol, so δ_b^{max} will be larger than δ_p^{max}. Moreover, probably $\varepsilon_b^{max} < \varepsilon_p^{max}$. Thus, according to eq. (4–17), γ_3 will be larger than 1, although it is very difficult to estimate by how much.

Combining eq. (4–13) and (4–14) it is found:

$$\theta_p = (\sigma_0 - \sigma_p)/(\sigma_0 - \gamma_3 \sigma_b^{max}) \tag{4-18}$$

For every value of ψ_0, σ_0 can be interpolated from the results of LYKLEMA et al. (1961, 1963) and of BIJSTERBOSCH et al. (1965); σ_b^{max} is also known (BIJSTERBOSCH et al. 1965) and σ_p has been measured by KOOPAL for several PVA's. A typical set of results is listed in table 4–1.

It can be concluded from table 4–1 that for the lowest considered value of γ_3 the surface is more than half covered. For the more realistic value $\gamma_3 = 1.5$, θ_p is found to be about 0.7. If γ_3 would be 2 the surface would be covered for 100% by PVA, which is unlikely.

About the same values for θ_p are found for PVA 16–98. For both PVA's θ_p becomes independent of p_a, as soon as p_a exceeds about half its maximum value. It must be stressed again that the maximally adsorbed amount per m^2 on the aggregates in a AgI suspension is lower than that on the particles of a sol. The value 0.35 mg/m^2, given in table 4–1, has to be compared with a maximum amount adsorbed onto the particles of a suspension of about 0.6 mg/m^2 for PVA 40–88.

TABLE 4–1. Coverage in the first layer on the AgI surface for PVA 40–88. Amount adsorbed: 0.35 mg PVA/m² of suspension

ψ_0 (mV)	Surface coverage (θ_p)		
	$\gamma_3 = 1$	$\gamma_3 = 1.5$	$\gamma_3 = 2$
–200	0.57	0.67	0.83
–250	0.58	0.75	1.03
–300	0.55	0.71	1.02
–350	0.51	0.68	1.01

In considering the results of the two electrochemical methods of obtaining a value for θ_p, it follows that θ_p must be higher than about 0.5, a value of 0.6 to 0.7 being a very reasonable estimation, in accordance with the most probable figures derived from both methods. For further calculations $\theta_p = 0.7$ will be adopted. This value applies then for amounts adsorbed of about half the maximum adsorption or more.

4.5. THE DISTRIBUTION OF POLYMER IN THE ADSORBED LAYER

In this section an attempt will be made to evaluate the polymer distribution in the adsorbed layer. Use will be made of theoretical models, in particular those of HOEVE (1965, 1970) and of HESSELINK (1969, 1971). By using the experimental results obtained in the previous sections of this chapter the parameters involved in these theories can be calculated. The resulting polymer distribution will be needed in the quantitative explanation of the flocculation results (Ch. 6.).

4.5.1. *Theoretical models*

An adsorbed homopolymer consists of *trains* on the surface and *loops*, protruding into the solution. In some cases there are possibly also *tails* present in the adsorbed layer. A tail can occur at the end of a molecule and is attached to the surface at one end as opposed to a loop, which is adsorbed onto the surface at two separate sites.

The polymer density distribution beyond the first layer results from the loops and the tails. According to HESSELINK (1969) the normalised density distribution of a loop, existing of i elements, $\rho_l(x)$, is given by:

$$\rho_l(x) = 12 \frac{x}{il_s^2} e^{-6x^2/il_s^2} \tag{4-19}$$

where x is the distance from the (plane) surface and l_s the length of a statistical element.

HOEVE et al. (1965) and ROE (1965a) derived a loop size distribution for a homopolymer, neglecting end effects and thus assuming that tails are absent. The number of loops of size i per unit area, n_i, is, in the notation of HESSELINK (1971), given by:

$$n_i = \frac{n}{\sqrt{\pi}} i^{-3/2} q e^{-q^2 i} \tag{4-20}$$

where n is the total number of elements in the loops per unit area. q is a function of the average number of elements per loop, $\bar{\imath}$, and can be written as:

$$q = \frac{b}{\bar{\imath}} \tag{4-21}$$

b is a numerical constant, approximately equal to 0.7 (HESSELINK 1971a).

If the loop size distribution, given by eq. (4–20), is valid an exponential density distribution follows for an adsorbed homopolymer. According to HESSELINK (1971a) the normalised distribution is:

$$\rho_h(x) = \frac{2q\sqrt{6}}{l_s} e^{-2qx\sqrt{6}/l_s} \tag{4-22}$$

A similar exponential distribution has been found by several authors (HOEVE 1965, ROE 1965b, 1966, RUBIN 1965, SILBERBERG 1968, MOTOMURA et al 1968, 1969).

HOEVE (1965, 1970) showed that at a distance δ from the surface, equal to the thickness of a polymer segment in the first layer, a discontinuity occurs. The density distribution then can be given as:

$$\rho(x) = \rho_0 \qquad \text{for} \quad 0 \leq x \leq \delta \tag{4-23a}$$

$$\rho(x) = K_H \rho_0 e^{-K_H \frac{v}{1-v} \frac{x-\delta}{\delta}} \qquad \text{for} \quad x > \delta \tag{4-23b}$$

Here K_H is a dimensionless constant, smaller than unity, which depends only on the flexibility of the polymer chain and v is the fraction of segments adsorbed, given by:

$$v = A_0/A_t \tag{4-24}$$

A_0 ($= \rho_0 \delta$) is the number of segments per unit area in the first layer and A_t

the total number of segments in the adsorbed layer per unit area.

Eq. (4–23b) is a slightly modified form of the equation given by HOEVE (1970) so as to make $\int_0^\infty \rho dx = A_t$. The equation is valid for small ν.

Eq. (4–23b) can be written as:

$$\rho(x) = K_H \rho_0 \, e^{-p_H (x - \delta)} \tag{4-25}$$

with

$$p_H = \frac{K_H}{\delta} \frac{\nu}{1 - \nu} \tag{4-26}$$

By comparing eq. (4–25) with eq. (4–22) the average number of elements per loop is found:

$$\bar{l} = \frac{2b\sqrt{6}}{l_s p_H} \tag{4-27}$$

As mentioned before eqs. (4–23) and (4–25) are valid if no tails are present in the adsorbed layer. ROE (1965b, 1966) and MOTOMURA et al. (1969) conclude, on theoretical grounds, that a considerable fraction of the adsorbed material can be present in one or two long tails. In that case eq. (4–25) must be modified. An attempt to do this will be made in 4.5.2. (eq. (4–32)). For one tail the distribution, analogous to eq. (4–19) has been given by HESSELINK (1969, eq. 12). A good approximation to his equation is (HESSELINK 1970):

$$\rho_t(x) = \frac{36}{7} \frac{x}{i l_s^2} e^{-18 x^2/7 i l_s^2} \tag{4-28}$$

Eqs. (4–19) and (4–28) apply under Θ-conditions, i.e. the linear expansion factor $\alpha = 1$. If α is different from unity the quantity il_s^2 $(= \overline{h_0^2})$ in these equations should be replaced by $\overline{h^2}$.

It should be noted again that eqs. (4–19), (4–22) and (4–28) are normalised so as to give unity on integration from $x = 0$ to $x = \infty$. The dimensions of ρ_t, ρ_h and ρ_t are cm^{-1}. However, eq. (4–23) is normalised such that the integral gives the total number of segments per unit area, A_t. The dimension of ρ is thus cm^{-3}.

4.5.2. *Evaluation of the polymer distribution*

If the polymer distribution is assumed to be exponential eq. (4–23) applies. The parameters in this equation can be obtained from the amount adsorbed (Ch. 3.), the polymer layer thickness (4.2.) and the coverage of the surface (4.4.) in combination with the volume of a PVA segment.

From monolayer studies on the oil-water interface LANKVELD (1970) showed that the surface area of a PVA segment is about 25 Å^2. From the density of solid PVA (1.3 g/cm^3) and the molecular weight per segment (44.6 for PVA 98.5) the segmental volume in the dry state can be calculated to be about 60 Å^3; in solution this volume is probably higher due to hydration. The thickness of an adsorbed segment, δ, is taken to be 4 Å, so the wet volume per segment is 100 Å^3.

The maximum value of A_0 would be, taking an area of 25 Å^2 per segment, 0.04 Å^{-2}. As $\theta_p = 0.70$ the value for A_0 will be 0.028 Å^{-2}. Then $\rho_0 = A_0/\delta =$ 0.0070 Å^{-3}.

With the molecular weight per segment the total number of segments per Å^2 follows directly from $p_a : A_t = 0.1345\ p_a$ if A_t is expressed in Å^{-2} and p_a in mg/m^2. Then ν follows from eq. (4–24).

The only unknown parameter in eq. (4–23b) then is K_H and the only datum not yet used is the layer thickness Δ. From an understanding of the values of the thickness as measured by viscosimetry it is possible to find K_H.

The polymer density in the adsorbed layer is a decreasing function of x. Near to the surface the water is completely immobilised, whereas in the outer regions of the adsorbed layer the water is more mobile. This continuously increasing mobility function can be formally replaced by a step function at a given polymer density ρ_{eff}, at which the mobility of the water suddenly increases from zero to the mobility of free water. This resembles closely the concept of the hydrodynamic radius of a free coil in solution (2.3.3.). The thickness Δ is then that distance from the surface where $\rho(\Delta) = \rho_{eff}$. Substituting this in eq. (4–23b) gives, after rearrangement:

$$\Delta - \delta = \frac{A_t - A_0}{K_H \rho_0} \ln K_H \rho_0 / \rho_{eff} \tag{4-29}$$

If a reasonable value for ρ_{eff} can be found, Δ as a function of A_t (or p_a) can be calculated for any value of K_H, and this can be compared with the experimental thickness as a function of p_a.

An estimate for ρ_{eff} may be found from a comparison with the polymer density at the hydrodynamic radius in a free coil. The density distribution in a Gaussian coil in solution, $\rho_c(r)$, is given by TANFORD (1961, p. 176) as:

$$\rho_c(r) = \frac{m}{2} \left(\frac{3}{2\pi}\right)^{3/2} \overline{(s^2)}^{-3/2} e^{-3r^2/2\overline{s^2}} \tag{4-30}$$

$\rho_c(r)$ is the number of segments per unit volume on a distance r from the centre of gravity, $m/2$ is the number of segments in the coil and $(\overline{s^2})^{1/2}$ the radius of gyration. Substituting for r the hydrodynamic radius, R_h, this equation becomes:

$$\rho_c(R_h) = \frac{m}{2}\left(\frac{3}{2\pi}\right)^{3/2}(\overline{s^2})^{-3/2}\, e^{-3/2\,\xi^2} \qquad (4\text{-}31)$$

where ξ is the ratio between the hydrodynamic radius and the radius of gyration, which for PVA is equal to 0.81 (see 2.3.3.). As $(\overline{s^2})^{1/2}$ is proportional to α/m, according to eqs. (2–7) and (2–9), $\rho_c(R_h)$ is proportional to $\alpha^{-3}\, m^{-1/2}$. The values for $\rho_c(R_h)$, calculated from eq. (4–31) are $2.9\cdot10^{-4}$, $1.3\cdot10^{-4}$ and $0.9\cdot10^{-4}$ Å^{-3} for PVA 3–98.5, 13–98.5 and 60–99, respectively. In an adsorbed layer ρ_{eff} is determined by the largest loops, which are probably shorter than the length of one molecule of PVA 3–98.5. Hence the value of ρ_{eff} will be larger than $\rho_c(R_h)$ for PVA 3–98.5.

It should be remembered that eq. (4–31) holds for a Gaussian distribution. However, in the adsorbed layer the distribution is exponential in most cases, so the procedure to obtain ρ_{eff} from comparison with a Gaussian coil is only approximative. Moreover, ρ_{eff} depends on the size of the loops, this is an additional uncertainty. For lack of a better measure for the layer thickness nevertheless the value of 5.10^{-4} Å^{-3} will be adopted for ρ_{eff}. Fortunately the thickness found by using eq. (4–29) is not very sensitive to ρ_{eff}. For $K_H = 0.8$ and $10^4\,\rho_0 = 70$ Å^{-3}, Δ is lowered by only 17% if the value of ρ_{eff} is assumed to be 50% higher.

According to eq. (4–29) the layer thickness is, at given amount adsorbed, independent of the molecular weight, provided that the same values of ρ_0 and ρ_{eff} apply for all molecular weights. From the results of the protection measurements (fig. 4–1) the extent of protection, and hence the layer thickness seem to depend somewhat on M. If ρ_{eff} for an adsorbed polymer layer were to decrease with M, then by analogy with the decrease of $\rho_c(R_h)$ with M in a free coil, this effect could be explained. However, in view of the difficulty in obtaining an accurate value for ρ_{eff} the same value will be used for all molecular weights. This is equivalent to the assumption that, at given amount adsorbed, the mean loop size does not depend on M. As at higher M more material is adsorbed the maximum layer thickness will still increase with molecular weight.

Another way in which Δ can depend on the molecular weight is by the occurrence of tails (see below). A large adsorbed molecule could also have long tails, resulting in a higher thickness.

In fig. 4–8 the theoretical thickness, calculated according to eq. (4–29), using $10^4\,\rho_{eff} = 5$ Å^{-3}, is plotted against the amount of PVA adsorbed for three values of K_H. In the same figure the viscosimetric thickness for PVA 60–99 is given. The theoretical lines are obtained assuming a constant coverage for the first layer on the surface ($10^4\,\rho_0 = 70$ Å^{-3}) for $A_1 > A_0$ or $p_a > 0.208$ mg/m^2. The lines are straight on account of the assumptions made, that ρ_0 and ρ_{eff}

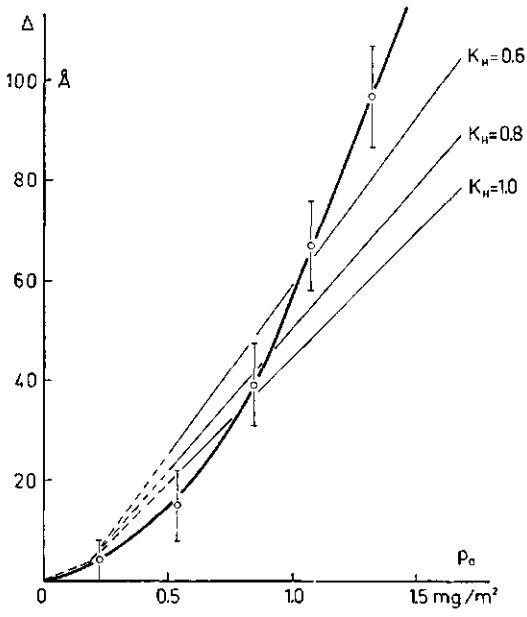

FIG. 4–8. The theoretical thickness calculated from eq. (4–29), compared with the experimental thickness measured by viscosimetry. The theoretical lines were calculated using $10^4\ \rho_0 = 70$ Å^{-3} and $10^4\ \rho_{eff} = 5$ Å^{-3}.

do not depend on the amount adsorbed, so that the logarithm in eq. (4–29) is independent of p_a. The assumption of constant ρ_0 is a good approximation at high p_a (see 4.4.1. and 4.4.2.), but becomes progressively less justified for $p_a <$ 0.5 mg/m^2. It is likely that ρ_0 increases with p_a in this region, resulting in a relatively more smoothed curve in the beginning; the kink at $p_a = 0.208$ mg/m^2 will then disappear. Moreover, for low p_a the fraction of segments adsorbed, v, is rather high, so that eqs. (4–23) and (4–29) do not apply. Therefore in the following discussion only the thickness at $p_a > 0.5$ mg/m^2 will be considered.

Keeping these restrictions in mind it can be seen that, for p_a less than 1 mg/m^2, the agreement between theoretical and experimental thickness is not too bad, in view also of the relatively large experimental error in Δ for low p_a. A definitive choice for the value of K_H is difficult to make as yet on account of the scarce experimental information. However, a value of 0.6 to 0.8 for K_H seems reasonable. It will therefore be assumed that at low amounts adsorbed the density distribution can be described by eqs. (4–23) and (4–25) with $K_H = 0.8$. As will be shown in the following chapter maximum flocculation occurs when p_a is about 0.9 mg/m^2. Under this condition the HOEVE distribution may be applied.

As an example some characteristics of the polymer distribution can now be calculated. For $p_a = 0.9$ mg/m^2 v is calculated to be 0.23 from eq. (4–24). p_H follows from eq. (4–26) and is found to be 0.060 Å^{-1}. The average number of elements per loop, $\bar{\imath}$, may then be obtained from eq. (4–27), using $l_s = 16.9$ Å

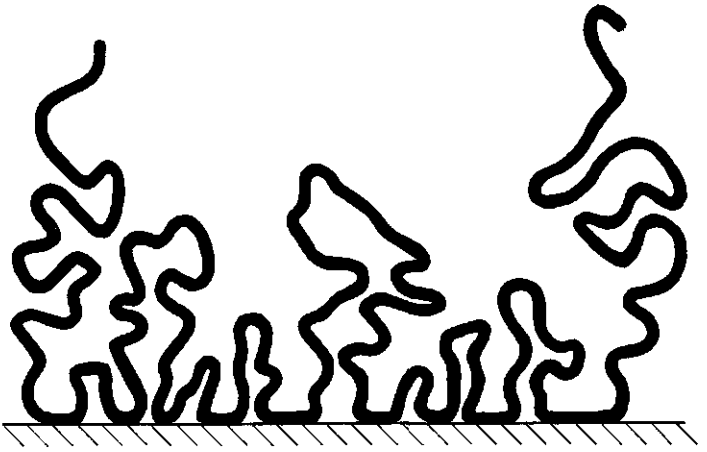

FIG. 4–9. Schematic representation of an adsorbed polymer layer at high coverage. The middle section of an adsorbed molecule assumes a distribution of loops according to HOEVE; beyond the first layer the segment density distribution is exponential. At the ends of a molecule tails can be present.

(see table 2–3). $\bar{\imath}$ turns out to be 3.4, so the average number of segments per loop is about 23.

At higher p_a values ($>$ 1 mg/m^2) eq. (4–29) is clearly inadequate: the layer thickness increases more rapidly than predicted by this equation. A possible explanation for this deviation could be the presence of tails in the adsorbed layer. The segments in a tail are less compressed in the direction of the surface than those in a loop, so that as the number of tails increases the thickness will also become higher. Physically it is not unreasonable that tail formation increases progressively with increasing p_a; at low amounts adsorbed there are, relatively, many adsorption sites available inducing the formation of short loops rather than long loops or tails. In fig. 4–9 a schematic representation is given of the configuration of an adsorbed polymer molecule at high coverage.

Making some simplifying assumptions the fraction of material present in the tails can be estimated. It will be assumed that each polymer molecule possesses two tails, both comprising a fraction $\frac{1}{2}\beta$ of the total number of segments in a molecule. The number of segments per Å^2 in the tails is then given by βA_t, that in the exponential distribution of the loops by $(1-\beta)A_t$. The number of carbon atoms in a tail is given by $\frac{1}{2}\beta m$, and accordingto eqs. (2–7) and (2–9) the end-to-end distance of a tail is $(\frac{1}{2}\beta\overline{h^2})^{1/2}$. The quantities m and $\overline{h^2}$ refer to a whole polymer molecule. For the sake of simplicity the linear expansion factor α is assumed to be the same for a tail as for a whole molecule.

Now with the help of eqs. (4–24) to (4–26) and (4–28) the segment density distribution is given, for $x > \delta$, by:

$$\rho(x) = K_H \rho_0 \, e^{-p_H (x - \delta)} + 4 A_t p_t x \, e^{-2 p_t x^2/\beta} \qquad (4\text{-}32)$$

in which now

$$p_H = \frac{K_H}{\delta} \frac{A_0}{(1-\beta) A_t - A_0} \text{ and } p_t = 18/7\overline{h}^2$$

For PVA 60–99 $(\overline{h^2})^{1/2}$ is 355 Å.

By supposing again that $10^4 \rho(\Delta) = 5$ Å^{-3} and making use of the viscosimetric thickness the value of β can be calculated from eq. (4–32) for any p_a. For example, for $p_a = 1.3$ mg/m^2 and $\Delta = 95$ Å, β turns out to be 0.36. Thus in an adsorbed layer of PVA 60–99 at $p_a = 1.3$ mg/m^2 each molecule can be thought to consist of two tails of 405 segments each, while the middle 1350 segments form an exponential distribution of loops.

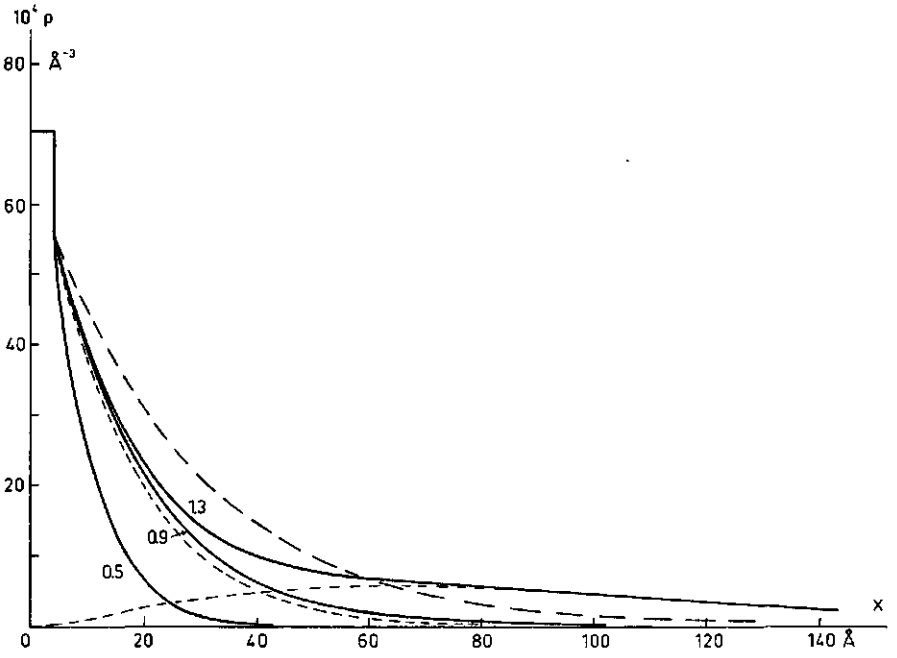

FIG. 4–10. The polymer density distribution in the adsorbed layer. The full lines give the distribution for $p_a = 0.5$, 0.9 and 1.3 mg/m^2. The curves for 0.5 and 0.9 mg/m^2 are calculated with the HOEVE formula (eq. 4–23) using $10^4 \rho_0 = 70$ Å^{-3}, $10^4 \rho_{eff} = 5$ Å^{-3} and $K_H = 0.8$. The curve for $p_a = 1.3$ mg/m^2 was calculated from eq. (4–21) with $(\overline{h^2})^{1/2} = 355$ Å (PVA 60–99) and $\beta = 0.36$.

The dotted lines represent the distribution in the loops (exponential) and in the two tails for $p_a = 1.3$ mg/m^2. The broken curve gives the HOEVE distribution for $p_a = 1.3$ mg/m^2 if no tails would be present.

In fig. 4–10 the polymer density distribution is plotted for three values of p_a. At $p_a = 0.5$ and 0.9 mg/m^2 the distribution is exponential beyond the first layer according to eq. (4–25). If no tails were present at $p_a = 1.3$ mg/m^2 the distribution would be given by the broken line. However, the thickness found is higher than accounted for by this HOEVE distribution, and therefore tails must be present. The dotted lines give the two contributions according to eq. (4–32) with $\beta = 0.36$, the full line for $p_a = 1.3$ mg/m^2 gives the total segment density. For distances higher than 60 Å the polymer density is determined largely by the tails.

The value obtained for β cannot be better than a very rough estimate. As mentioned before, the thickness Δ is rather insensitive to the value of ρ_{eff}, but in contradistinction to this β is very sensitive to the value chosen for ρ_{eff}, β becoming higher if ρ_{eff} is made higher. Moreover, β depends on the number of tails per molecule. The assumptions that the two tails of a molecule are equal in length and that every polymer molecule has equally long tails are certainly not correct. It is possible that some molecules have no tails and that others consist mainly of tails. Especially prior to the achievement of equilibrium it is to be expected that the recently arrived molecules protrude further into the solution than the molecules adsorbed in the early stages of the adsorption process. For all these reasons the absolute value of β is uncertain.

The order of magnitude of β is found to be of the same order as that proposed by ROE (1965b, 1966) and MOTOMURA et al. (1969) on theoretical grounds for adsorbed isolated chains. ROE states that at some critical value of the segmental adsorption free energy a molecule consists of three roughly equal parts: two tails and an exponential middle section. Here $\beta \simeq 0.67$. For higher values of the segmental adsorption free energy the contribution of the tails becomes less and is possibly of the order of 0.36. MOTOMURA et al. come to roughly the same conclusion as ROE. In our case the polymer molecules are certainly not isolated. However, from the experiments it seems unlikely that at low p_a long tails are present in view of the low thicknesses measured. In order to explain the thickness as a function of p_a, as measured in the present study, it seems necessary to assume the presence of tails only at high amounts adsorbed.

It has sometimes been reported in the literature (STROMBERG et al. 1963, KILLMANN et al. 1970) that the thickness increases considerably with increasing polymer concentration even after the (pseudo) plateau in the adsorption isotherm has been reached. This effect can not be explained if the polymer distribution is of the HOEVE type. However, if at high amounts of adsorbed polymer tails were to occur in the adsorbed layer the polymer density far out from the surface will be increased, and hence lead to the high experimental thickness found.

4.6. Conclusions

Several methods have been simultaneously applied to characterise the adsorption of PVA on silver iodide.

From protection measurements it would appear that the polymer layer is thin only when small amounts of polymer are adsorbed. The layer becomes thicker when the amount adsorbed increases. At low adsorption the polymer assumes a relatively flat configuration, whereas long loops, and perhaps also tails, will be present when more polymer is adsorbed. These qualitative findings were fully corroborated by quantitative measurements of the layer thickness. By measuring the viscosity of a sol the particles of which were covered by PVA, the thickness could be estimated from the increase in the effective volume fraction of the dispersed particles. In some electrophoretic measurements the lowering of the ζ-potential due to the adsorption of the polymer was used to calculate the shift of the plane of shear and hence the layer thickness. From both methods the layer thickness was found to be about 100 Å at the (pseudo) plateau of the adsorption isotherm.

From the shift of the point of zero charge due to polymer adsorption on the particles in a AgI suspension and from an analysis of the surface charge of AgI covered by PVA, in comparison with these quantities in the presence of butanol and ethylene glycol, the coverage in the first layer on the surface could be estimated. The fraction of the surface which is covered by PVA was found to amount to about 0.70 for amounts adsorbed higher than half the maximum adsorption. The data are not accurate enough to distinguish between samples with different molecular weights or acetate contents.

From these quantitative data about the surface coverage and the layer thickness it was possible to evaluate the polymer distribution in the adsorbed layer, by comparison with the theoretical one proposed by Hoeve. In connection with this it was necessary to specify the kind of thickness measured by viscosimetry.

For amounts adsorbed lower than 0.5 mg/m^2 the fraction of segments adsorbed is too high to use the theory by Hoeve. At p_a between 0.5 and 1.0 mg/m^2 the Hoeve distribution applies: then over the first 4 Å from the surface the polymer density is constant; at 4 Å it drops discontinuously to about 80% of its value on the surface and for larger distances from the surface the polymer density decreases exponentially. In principle, over this range of p_a, all the parameters occurring in the density distribution are known or can be estimated. At still higher amounts adsorbed the theory by Hoeve is no longer applicable; under these conditions there may well be tails present, not accounted for by the theory. The fraction of material present in tails is about 0.4 at maximum adsorption. This fraction is of the same order as predicted in the theories by

ROE and MOTOMURA et al. for isolated chains.

From the protection measurements it was deduced that with increasing molecular weight and with decreasing solvent power of water for PVA the layer thickness increases, in accordance with the expectation. The other experimental data are insufficiently detailed as yet to discriminate between PVA's of differing molecular weight and hydrophobicity. For this reason no attempts have been made to discuss these second order effects in the polymer distribution.

5. THE FLOCCULATION OF SILVER IODIDE SOL BY POLYVINYL ALCOHOL

In this chapter the conditions will be described under which a silver iodide sol can be flocculated with polyvinyl alcohol. It will be shown that the most important factors affecting the extent of flocculation are the way in which polymer and sol are mixed and the amount and type of salt present. In addition, the influence of the nature of the PVA on the flocculation was studied; these results and some kinetic studies will also be discussed.

5.1. THE WAY OF MIXING OF PVA AND AgI

5.1.1. *The optimal mixing procedure*

In the early stages of this study attempts were made to flocculate a silver iodide sol with PVA by adding the polymer from a pipette to a given volume of sol. Slight flocculation took place at some concentrations of PVA, but the results were very irreproducible. The extent of flocculation was found to depend particularly on the time elapsed between addition of polymer and the intimate mixing of sol and polymer. It was supposed that this irreproducibility was due to the irreversibility of the adsorption of polymer molecules (Ch. 3.); if local excesses of PVA are present in the solution it is possible that some AgI particles become more covered than others. This unequal distribution of PVA over the AgI particles may have consequences for the flocculation. This effect presumably depends on the way of mixing.

Therefore a standardised method was sought in which no irreproducible mixing of PVA and AgI would occur. This was achieved by using a separating layer of water or of a dilute salt solution. The procedure is as follows: to a portion of sol in a graduated cylinder this separating layer was added from a burette; the tip of the burette was placed against the inner wall of the vessel and the stopcock opened slightly; care was taken to avoid mechanical disturbance, so that a sharp boundary was formed between the sol and the liquid in top of it. After this the PVA solution was added carefully from a pipette. A three layer system was thus obtained (see fig. 5–1a). Mixing was then achieved by turning the cilinder upside down by hand. After some time the extent of flocculation was observed. The results using this mixing procedure were very reproducible; in this respect it was satisfying. However, it appeared that no flocculation at all took place any more.

Hence it was concluded that for flocculation to occur an inhomogeneous way

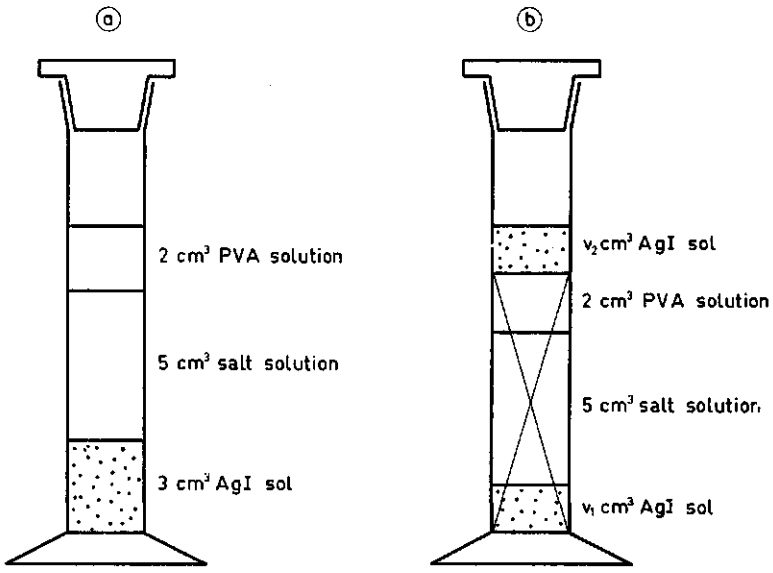

FIG. 5–1. The way of mixing of PVA and AgI.
a. One portion method b. Two portion method.
In the two portion method the second portion of sol (v_2) was added t_1 minutes after mixing of the polymer with the first portion of sol (v_1).

of mixing, leading to local excesses of polymer, is essential. Therefore a deliberate inhomogeneous way of mixing was applied (see fig. 5–1b). To a portion of sol a salt solution and a solution of polymer were added as described above. A certain time after mixing of the components a second portion of sol was added and the contents of the cylinder were mixed again by hand. It was now found that, depending on the PVA concentration and the ratio between the amounts of sol of the first and second portion, a very reproducible and efficient flocculation could be achieved. For this reason this two portion method was used throughout the flocculation studies.

It can already be noted therefore, that in a system containing a given amount of sol, either protection or flocculation can be brought about with a fixed amount of polymer, depending on the way in which the two are mixed. This important feature is typical for polymers and reflects ultimately the irreversibility of polymer adsorption.

5.1.2. *Experimental*

To a volume v_1 of sol a volume of salt solution and of PVA solution were added and mixing was performed as described in 5.1.1. After a given time of contact, t_1, to allow PVA to adsorb onto the AgI a second volume of sol, v_2, was

added; after mixing by hand the cylinders were rotated end-over-end during a certain flocculation time t_2. In some cases, especially at high salt or low sol concentrations, a sharp boundary between the sol and the salt solution could not be obtained because the density of the salt solution was higher than that of the sol. In these cases water was used as separating layer and the salt was added immediately before addition of the second portion of sol.

In all cases $v_1 + v_2$ was 3 cm^3; the final volume in the cylinders was 10 cm^3. The final concentrations of sol, salt and polymer (added) were varied and are denoted as c_{sol}, c_s and c_p, respectively. The fraction of sol in the first portion, $v_1/(v_1+v_2)$, is denoted by φ_1, that in the second portion by φ_2. A further important parameter is the amount of PVA added per mmole of AgI in the first portion, p_1. This quantity determines a.o. the thickness of the adsorbed layer on the first portion sol particles. It is expressed in mg PVA/mmole AgI.

As a measure of the extent of flocculation the absorbance, A, was used. The flocculated sol was centrifuged under mild conditions (two minutes at 900 rev./min) to settle any flocs formed; the absorbance of the supernatant solution was then measured in a Unicam SP 600 spectrophotometer. A low absorbance corresponds to a high extent of flocculation and vice versa. For $c_{sol} \sim 3$ mmoles/l the absorbance was measured, at a wavelength of 4300 Å (see below), in 1 mm cells; for lower c_{sol} longer path lengths were chosen and for higher c_{sol} the supernatant was diluted with water before the measurement of the absorbance. The results are presented in terms of the relative absorbance, A_{rel}, defined as the absorbance of the supernatant divided by that of the sol without added PVA.

As a typical example the relative absorbance of AgI (sol A, $c_{sol} = 3$ mmoles/l) flocculated by PVA 3–98.5 is given in fig. 5–2 as a function of v_1 at two wavelengths: 4300 Å (measured in 1 mm cells) and 6500 Å (in 5 mm cells). In this

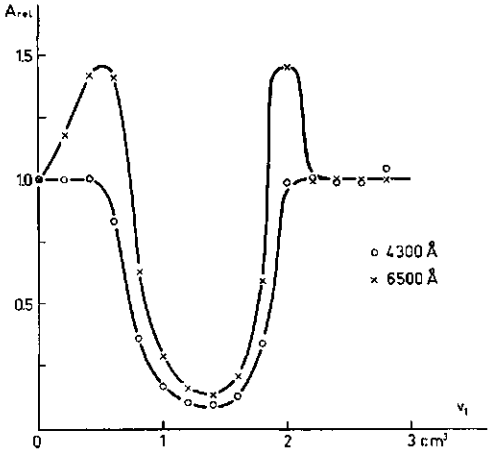

FIG. 5–2. The flocculation of AgI sol with PVA as measured by the relative absorbance. Sol A, PVA 3–98.5; p_1 = 2.5 mg PVA/mmole AgI; c_{sol} = 3 mmoles/1; c_s = 10 mmoles KNO_3/1; t_1 = 15 min; t_2 = 1 h.

experiment c_p was adapted such, that p_1, the polymer dosage per mmole of AgI of the first portion, was 2.5 mg PVA/mmole AgI. The detailed form of this type of curve will be discussed in 5.1.3.; for the moment it is sufficient to note that no flocculation occurs at $v_1 = 0$ or $v_1 = 3$ cm^3 and that maximal flocculation takes place at some intermediate value of v_1. The humps in the curve at 6500 Å apparently correspond to a situation where the sol is just on the verge of stability. The following explanation of the different shapes of the curves for the two wavelengths can be offered.

When the extent of flocculation is considerable, large flocs are formed which settle readily on centrifugation. On the other hand, with incipient flocculation only small flocs are present, some of which remain in the supernatant if the applied centrifugal force is small.

Around 6500 Å the scattering of light by small AgI particles is chiefly conservative: in this range the scattered intensity was found to be approximately inversely proportional to the fourth power of the wavelength, indicating that RAYLEIGH's law (see e.g. STACEY 1956, KERKER 1969) applies. Hence the scattered intensity is proportional to NV^2 where N is the number of particles of volume V. A larger average particle size will cause a larger scattering and a higher absorbance. In contrast with this around 4300 Å AgI shows an absorption peak; that is at this wavelength the light scattering is mainly consumptive. Consumptive absorption is much less sensitive to the particle size; the absorbance is now mainly determined by the amount of solid present.

These facts may explain the differences observed at 6500 and 4300 Å. Under conditions where a considerable fraction of the AgI is flocculated the flocs are so large that they settle easily during centrifugation. In this case the mean particle size in the supernatant is not much different from that in the unflocculated sol and the absorbance is, at both wavelengths, proportional to the amount of material present. The results at the two wavelengths are then consistent. However, when the sol is partially flocculated, small flocs are present in the supernatant, causing an increase in the absorbance at 6500 Å. As the amount of material remains constant the absorbance at 4300 Å does not change. Hence under these conditions different absorbances are observed at different wavelengths.

All absorbance measurements reported below have been carried out at 4300 Å. From the foregoing discussion it is clear that the absorbance at this wavelength is roughly proportional to the amount of material remaining in solution after centrifugation. Thus the relative absorbance of the supernatant is a real measure of the flocculation.

For the flocculation of AgBr with PVA and gelatin, LEVI and STEPANOVA (1965) reported absorbance against polymer concentration curves showing humps similar to the upper curve in fig. 5–2. They also used a centrifuging

technique. The wavelength at which their measurements were carried out is not given in their paper. The authors attribute the occurrence of the humps to a 'pseudo-stable state'. However, in view of the above it is possible that the shape of their curve is simply a consequence of the wavelength chosen.

5.1.3. *Flocculation results and discussion; the bridging model*

Results obtained with PVA 16–98 and sol A have already been reported (FLEER and LYKLEMA 1968). The results for other polymers are essentially the same as will be shown below.

In this section a study is made of the influence of the nature of the PVA and of the parameters p_1 and φ_1. To that end the values of the other relevant parameters had to be fixed. We chose: $t_1 = 15$ min, $t_2 = 1$ h, $c_s = 10$ mmoles/l of KNO_3 and $c_{sol} = 3$ mmoles/l of AgI. The influence that these parameters exert will be the subject of subsequent sections.

In fig. 5–3 the relative absorbance as a function of the volume of sol of the first portion, v_1, is given at constant added polymer concentration c_p for four different PVA's. It can be seen that the flocculation depends very strongly on v_1, that is on the way of mixing. In all cases it is clear that no flocculation occurs at $v_1 = 0$ or $v_1 = 3$ cm^3 i.e. when the total amount of sol is added at once to the polymer or conversely. For a given polymer concentration, optimal flocculation takes place at a certain ratio $\varphi_1 (= v_1/(v_1 + v_2))$ which varies with c_p. However, the value of p_1, the amount of the polymer added per mmole of AgI of the first portion, at the minima in the absorbance is approximately constant.

For PVA 13–98.5 (fig. 5–3b) at maximum flocculation p_1 is about 2.5 mg/mmole for all values of c_p. It is interesting to relate this value to the adsorption isotherm (fig. 3–2) and to the thickness of the adsorbed layer as deduced previously (fig. 4–4). It appears that at $p_1 = 2.5$ mg/mmole nearly all the polymer is adsorbed, resulting in the particles of the first portion of sol being nearly completely covered by a thick layer. Because only a very small fraction of the polymer remains in solution the particles of the second portion of sol remain virtually uncovered. It is thus possible to formulate a first condition for effective flocculation: a portion of sol in which the particles are fully covered may be flocculated on adding a second portion in which the particles are bare. This may be readily interpreted by the bridging model for flocculation: only if a considerable amount of polymer is adsorbed are the loops long enough (see Ch. 4.) for efficient flocculation. Moreover, for good bridging it is necessary that free surface is available on a second particle onto which the loops attached to a first particle can adsorb. This is the situation only if no excess polymer is present in the first portion of sol, because any free polymer molecules will adsorb much faster on the bare particles than any loops already adsorbed on another particle.

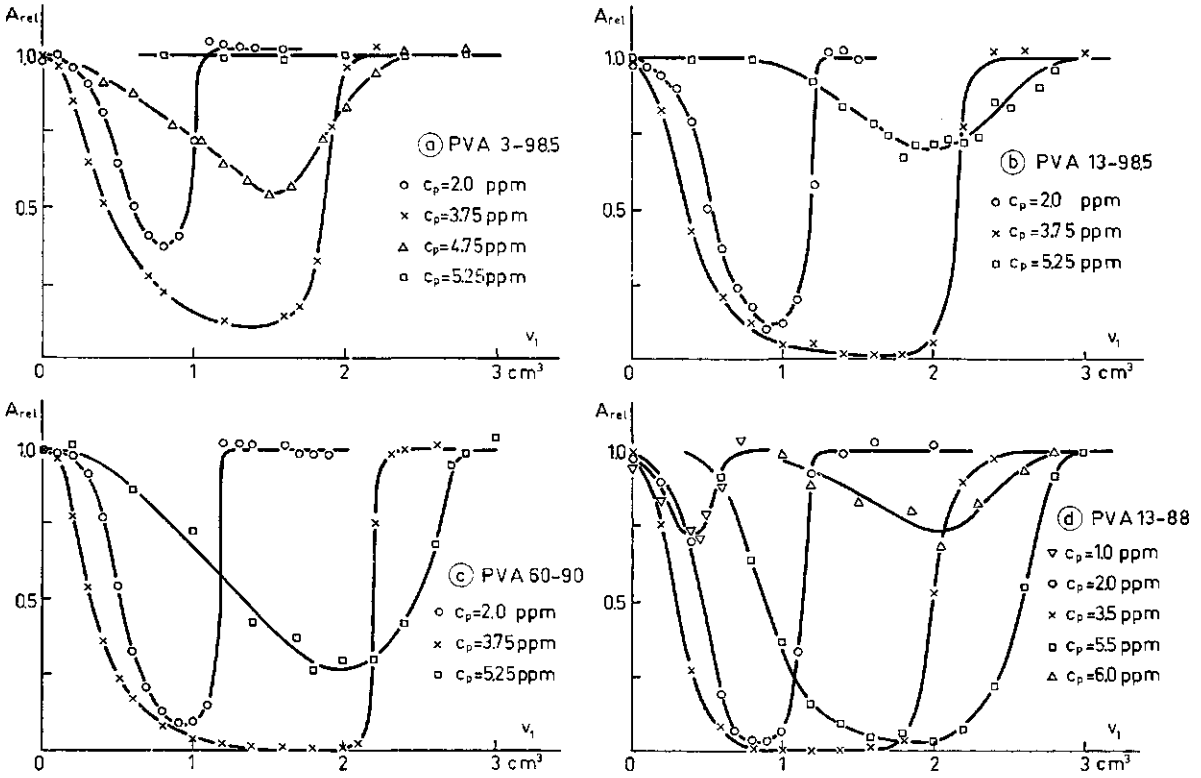

FIG. 5-3. Effect of the way of mixing on the flocculation of AgI by PVA at constant polymer concentration for four types of PVA.

c_{sol} = 3 mmoles/l; c_s = 10 mmoles KNO_3/l; t_1 = 15 min; t_2 = 1 h.

a, b and c: sol A; d: at c_p = 6 ppm sol C, at the other polymer concentrations sol B.

Thus the optimal value of p_1 can be considered as a compromise between two effects: with increasing p_1 the loops become longer, giving more efficient flocculation. However, if p_1 is too high too much polymer remains in solution, leading to fewer adsorption sites on the particles of the second portion; in this way bridging is impeded. From the discussion presented in Chs. 3. and 4. it is clear that the molecules adsorbed initially assume a relatively flat configuration on the surface, so that only a few molecules adsorbed on the bare particles can have a great influence on the efficacy of the flocculation.

From fig. 5–3b it can be seen that the depth of the minimum is largest for $c_p = 3.75$ ppm. In the minimum at this polymer concentration $v_1 = v_2$, thus $\varphi_1 = \varphi_2 = 0.5$. Evidently this is the second condition for effective flocculation: the number of covered particles should be equal to that of the bare ones. This would seem a reasonable conclusion if the flocculation is considered to be caused by Brownian encounters between covered and uncovered particles.

It is now possible to postulate a mechanism for the flocculation of AgI sols by PVA. The silver iodide particles are linked together by polymer bridges. This bridging is most effective if a given amount of the untreated sol is mixed with an equal amount of sol in which the particles are nearly completely covered by polyvinyl alcohol.

As an illustration of the importance of the way of mixing in fig. 5–4 a schem-

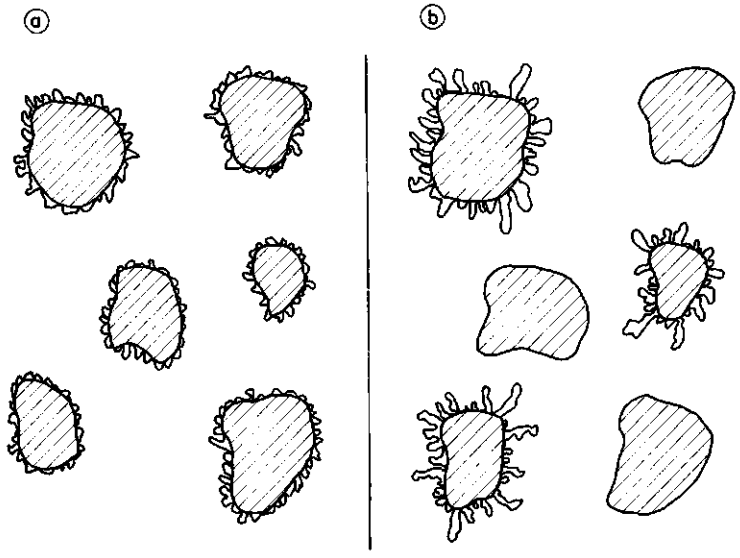

FIG. 5–4. Schematic representation of two ways of mixing.
a. One portion method; no flocculation.
b. Two portion method; effective flocculation.
The total amount of polymer and silver iodide is the same in both cases.

atic picture is given of the one portion method (fig. 5–4a) and the two portion method (fig. 5–4b) at equal total amounts of PVA and AgI. In the first case the adsorbed layer is too thin and no free surface is available, so that no bridging can occur. In the second case long loops are present which adsorb onto the free surface of newly added particles, leading to very effective flocculation.

The results for PVA's 3–98.5, 60–99 and 13–88 are essentially the same as those for PVA 13–98.5. This is also shown in fig. 5–3. The flocculation is somewhat more effective for higher molecular weights. The optimal value of p_1 is about 2.5 mg/mmole in all these cases, although there is a slight tendency for the optimal p_1 to increase with increasing molecular weight. This agrees with the corresponding increasing adsorption levels (fig. 3–2). With increasing acetate content the flocculating efficiency increases, as may be judged by a comparison of fig. 5–3d with fig. 5–3b. With PVA 13–88 slight flocculation already takes place at $c_p = 1$ ppm, in contradistinction to the case of 1 ppm PVA 13–98.5. This effect is even stronger at $c_p = 5.50$ ppm: also at this concentration, no flocculation is achieved with PVA 13–98.5.

On account of the higher adsorption plateau for PVA 13–88 one would expect that the optimal value of p_1 would be higher than that of PVA 13–98.5. This is not the case. The explanation is probably that, although the adsorption isotherm of PVA 13–88 shows a higher plateau, the high affinity is somewhat less pronounced: both isotherms leave the ordinate axis at about the same amount adsorbed (see fig. 3–2). Thus for PVA 13–88 the coverage of the particles of the second portion of sol plays a relatively more restricting role, thus compensating the favourable effect of the longer loops.

In fig. 5–5 the flocculation is shown as a function of φ_1 at $p_1 = 2.5$ mg PVA/mmole AgI, the optimal polymer dosage. In this experiment c_p was adjusted to v_1 in such a way that p_1 was constant. The curves obtained are nearly symmetrical around $\varphi_1 = 0.5$, so again it would appear that at optimal flocculation the number of uncovered particles is equal to that of uncovered ones. Flocculation is more effective, at given φ_1, if the molecular weight and the acetate content are increased. At high molecular weight and lower degree of hydrolysis of the polymer the way of mixing becomes somewhat less critical, as indicated by the broader range in φ_1 for which efficient flocculation takes place.

Flocculation results at $\varphi_1 = 0.5$ are given in fig. 5–6 as a function of p_1. It is striking that for all types of polymer the flocculation starts very steeply at about $p_1 = 2$ mg PVA/mmole AgI; this is the same polymer dosage at which the adsorption isotherms for all molecular weights leave the axis (fig. 3–2). Apparently the formation of loops, able to bridge, starts at the point where during adsorption it becomes difficult for the PVA molecules to find a site on the surface. At high polymer dosage flocculation becomes prohibited because the residual concentration of PVA, remaining in solution after adsorption on the

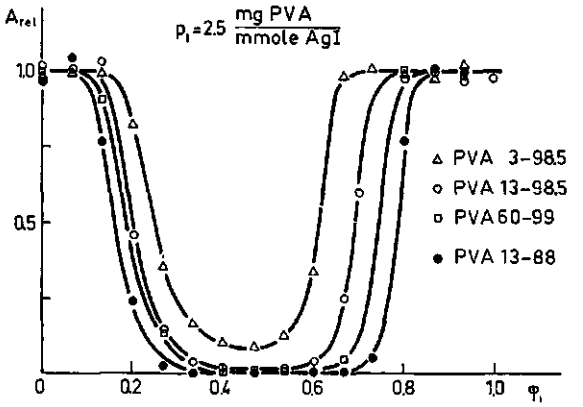

FIG. 5–5. The flocculation as a function of the ratio of the amounts of covered and uncovered sol at a constant polymer dosage of 2.5 mg PVA/mmole AgI of the first portion.
c_{sol} = 3 mmoles/l; c_s = 10 mmoles KNO_3/l; t_1 = 15 min; t_2 = 1 h.
The curve for PVA 13–88 has been measured with sol B, the others with sol A.

first portion of sol, becomes so high that the particles of the second portion become too covered. The value of p_1 at which this occurs increases with M and with acetate content (see fig. 5–6). This also agrees with the adsorption isotherms (fig. 3–2): at a certain residual concentration of PVA in solution the amount adsorbed and also the amount left in solution increase with increasing M and decreasing degree of hydrolysis; thus the polymer dosage, p_1, at which the second portion of sol is covered to a certain extent must increase also.

It should be noted that the explanation given here for the flocculation is only valid if the adsorption is irreversible with respect to polymer molecules as a whole. In a reversible system it should be irrelevant whether a completely covered and an uncovered particle are brought together, or two particles at half coverage: in both cases the flocculated state, corresponding to a minimum in the free energy, would be reached after a certain time. However, a system in which $\varphi_1 = 1$ and $p_1 = 1.25$ mg PVA/mmole AgI does not flocculate, even after several weeks of rotation end-over-end, reflecting again the irreversible character of the adsorption.

From the above discussion it is clear that bridging is essential for flocculation of AgI with PVA. At present the bridging mechanism for the flocculation of sols or suspensions with nonionic polymers, or polyelectrolytes of like charge as the particles, is generally accepted (LINKE and BOOTH 1960, KUZ'KIN and NEBERA 1963, LA MER and HEALY 1963, AUDSLEY 1965, SLATER and KITCHENER 1966, SOMMERAUER et al. 1968). However, from this study it is clear that bridging occurs only if the way of mixing is controlled carefully.

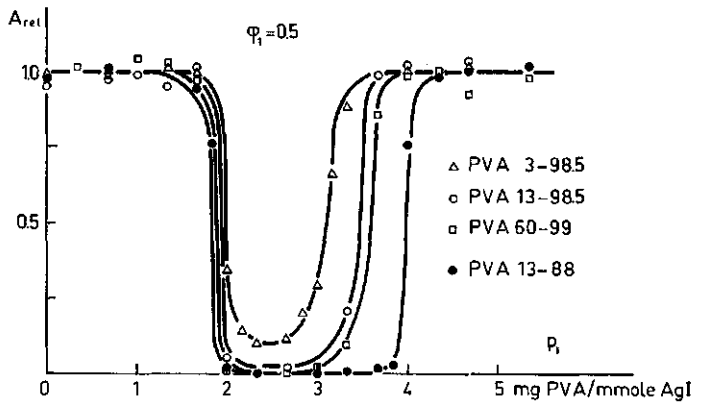

FIG. 5–6. The flocculation as a function of the polymer dosage to the first portion of sol at equal amounts of the first and second portion of sol.
c_{sol} = 3 mmoles/l; c_s = 10 mmoles KNO_3/l; t_1 = 15 min; t_2 = 1 h.
Sol A was used with PVA 3–98.5 and 60–99, sol B with PVA 13–88 and sol C with PVA 13–98.5.

NEMETH and MATIJEVIČ (1968) have objected to the bridging mechanism for the flocculation of AgBr sols with gelatin of like charge. They assume that by adsorption of gelatin the surface charge of AgBr decreases, by analogy with the results of BIJSTERBOSCH's (1965) work on the effect of butanol on AgI sols. They then suppose that normal coagulation by electrolytes takes place. One of their arguments is that the amounts of salt, with ions of different valencies, needed obey qualitatively 'the' SCHULZE-HARDY rule (see e.g. OVERBEEK 1952, p. 81). There are several flaws in this reasoning. Firstly, the surface charge of AgI does decrease in the presence of butanol, but the coagulation concentration for a sol with butanol covered particles is higher than that for a sol without butanol (VINCENT et al. 1971), thus the stability is enhanced instead of diminished. Moreover, the gelatin used by NEMETH et al. carries the same charge as the AgBr surface, so that, even if the surface charge were to decrease by gelatin adsorption, the effective charge of the covered particle increases, leading to stronger repulsion. Finally, the influence of electrolytes, as mentioned, does not necessarily imply a coagulation mechanism: in 5.3. it will be shown that, qualitatively, the same salt effects are found for the PVA-AgI system and that these can be in perfect agreement with the idea of bridging. In conclusion, also the destabilisation of AgBr by gelatin will presumably occur by bridging.

The results obtained in this section may be compared with the flocculation by commercial flocculants. Under practical conditions it is difficult to apply the optimal mixing procedure, although frequently local excesses of polymer will occur, leading to essentially the same flocculation mechanism as described

above. As the molecular weight of most commercial flocculants is very high, efficient flocculation can be obtained in spite of a less effective way of mixing; as shown for the flocculation of AgI sols by PVA, the way of mixing is less critical for higher molecular weights. Moreover, with higher molecular weights the irreversible character and the high affinity of the adsorption become more pronounced, promoting flocculation. Thus it seems probable that the trends found with the model system used have also validity in practical systems. In addition, with very high molecular weight flocculants simultaneous adsorption of a polymer molecule on two different particles might occur. Consequently, the efficiency of this type of flocculation depends very strongly on kinetic factors.

5.1.4. *Examination of some possible alternative explanations for the flocculation*

Although the preceding discussion demonstrates very clearly that all the flocculation phenomena of the AgI-PVA system can be explained by bridging, two possible alternative mechanisms will be considered, namely flocculation in the secondary minimum and heterocoagulation.

The potential free energy of two charged particles, surrounded by their double layer, as a function of the interparticle distance is characterised by a deep primary minimum at very short distances, and a shallow secondary minimum at large distances (VERWEY and OVERBEEK 1948). Assuming that the free energy curve in the presence of adsorbed polymer has a similar form as that for two uncovered particles, flocculation in the primary minimum is very unlikely due to the presence of the adsorbed layer: on account of the steric hindrance the particles are not able to approach each other closely enough. It would be possible that flocculation in the secondary minimum does take place, as has been shown to occur sometimes for the coagulation, especially for large particles (SCHENKEL and KITCHENER 1960). The depth of this minimum could possibly be modified by effects caused by the adsorbed polymer. In order to check this possibility, from the formulae given by VERWEY and OVERBEEK (see also 6.3.) the depth and the location of the secondary minimum were calculated. It appears that the depth is less than 1.5 kT and that the interparticle distance at the minimum is more than 400 Å at the critical salt concentration of KNO_3, 5 mmoles/l (see 5.3.). This distance is much greater than the thickness of the polymer layer, making it impossible for PVA to directly affect the secondary minimum. Moreover, systems coagulated in the secondary minimum are generally easily redispersible because the minimum is shallow. AgI, flocculated with PVA, can not be redispersed. So the presence of a secondary minimum can not offer a satisfactory explanation of the flocculation.

Another possibility would be the occurrence of heterocoagulation; i.e. an aggregation of particles with unequal ψ_d. In the literature it has been reported

(DEVEREUX and DE BRUYN 1963; HOGG, HEALY and FUERSTENAU 1966) that the repulsion free energy between two particles of unequal STERN potential is determined largely by the lower ψ_d, the more so if the difference between the two STERN potentials is large. In that case only a small salt concentration will be needed to destabilise a sol.

As mentioned in 5.1.3., the flocculation of AgI by PVA takes place by interaction of covered particles with uncovered ones. The STERN potential of a polymer covered surface will be somewhat lower than that of a naked AgI surface. In 6.3.1. it will be shown that at pI = 5 and a KNO_3 concentration of 5 mmoles/l reasonable estimates for the STERN potentials are –95 mV and –85 mV for an uncovered and a polymer covered surface, respectively. With the help of the approximate formulae given by HOGG et al. for spheres, or the numerical calculations of DEVEREUX et al. for flat plates it can be shown that the repulsion free energy in this case is about the same as that of two particles of $\psi_d = -90$ mV each, so that the electrostatic repulsion is still high enough to ensure stability, in contradistinction to experiment.

In conclusion, it can be stated that flocculation in the secondary minimum or heterocoagulation can not explain the flocculation results. Indeed bridging would seem the most probable mechanism. Due to this bridging and the presence of polymer between the particles some extra potential free energy terms are needed to evaluate the total potential energy of interaction as a function of the interparticle distance. An attempt to calculate these will be discussed in Ch. 6.

5.2. EFFECT OF THE TIME OF CONTACT BETWEEN PVA AND AGI

Polymer adsorption being a slow and irreversible proces, the actual configuration during flocculation studies will generally depend on the history of the PVA-AgI interaction. The contact time is one of the most important variables. It was studied in the following way.

For the conditions $p_1 = 2.5$ mg PVA/mmole AgI and $\varphi_1 = 0.267$ ($v_1 = 0.8$ cm^3) the time of contact, t_1, between PVA of three molecular weights and AgI was varied. The results are given in fig. 5–7a for values of t_1 shorter than 30 minutes and in fig. 5–7b for contact times longer than 1 hour. These experiments can provide some information about the rates of adsorption and rearrangement processes in the adsorbed layer; as all other variables are kept constant, only differences in the configuration of the adsorbed layer after the time of contact t_1 are reflected in the efficacy of the flocculation. A more efficient flocculation points to longer loops and a thicker adsorbed layer.

Firstly, it is clear from fig. 5–7 that the extent of flocculation increases with t_1 until a constant value of A_{rel} is attained. Apparently the layer thickness

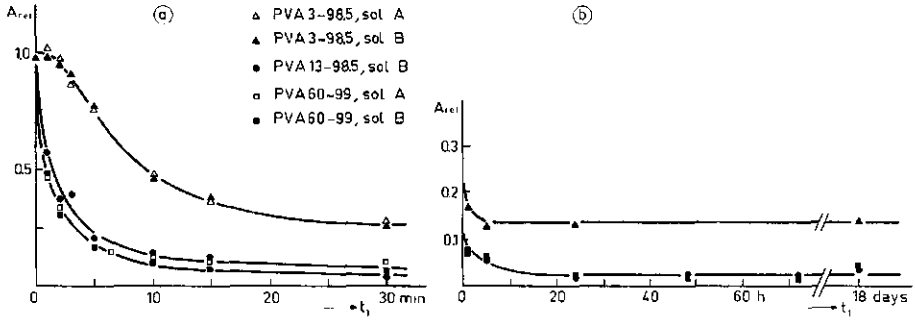

FIG. 5–7. The effect of the time of contact between PVA and the first portion of sol on the flocculation.
a. at short times b. at longer times
c_{sol} = 3 mmoles/l; c_s = 10 mmoles KNO_3/l; p_1 = 2.5 mg/mmole; v_1 = 0.8 cm^3; t_2 = 1 h.

increases steadily with time until a final layer configuration is reached. If one supposes that a molecule, arriving from the solution, is adsorbed initially by only few segments, but that after this first attachment more and more segments come into contact with the surface, one would expect that the number of long loops or tails decreases with time, leading to a less effective flocculation. This is not observed. It must be concluded that this process of rearrangement and progressive adsorption of one molecule is very fast and can not be measured with the method used here. Another possibility is that this rearrangement still takes place, but is dominated by the increase in the number of molecules adsorbed. As mentioned earlier (Ch. 3.) the amount adsorbed increases with time. Also slow replacement of smaller molecules by larger ones could play a role.

In the second place, it is somewhat surprising on first sight that the extent of flocculation increases more quickly with time for PVA 60–99 and 13–98.5 than for PVA 3–98.5 (fig. 5–7a), because it may be expected that the rate of adsorption of small molecules is faster than that of large molecules. However, what is measured by the flocculation is not the amount adsorbed, but the thickness of the layer. Apparently the thickness of the layer increases with time for high molecular weights. The difference between PVA 13–98.5 and 60–99 is very small, though.

It is probable that the rearrangement process is faster for a low molecular weight polymer than for larger molecular weights. This is confirmed by the curves in fig. 5–7b: the final configuration of the adsorbed layer is for PVA 3–98.5 reached after 5 hours, and for PVA 13–98.5 after about 24 hours. However, it

is possible that in the inner part of the adsorbed layer rearrangements occur, which are not reflected in the efficacy of the flocculation.

Similar measurements as described for $p_1 = 2.5$ mg PVA/mmole AgI and $\varphi_1 = 0.267$ were also carried out at the optimal flocculation conditions: $p_1 = 2.5$ mg/mmole and $\varphi_1 = 0.5$. Because the flocculation in this case is nearly complete A_{rel} is practically zero for all molecular weights at t_1 more than 10 minutes. At shorter times the same difference as mentioned above was found between PVA 3–98.5 and the samples of other molecular weight.

5.3. Effect of added electrolyte on the flocculation

All the experiments discussed in the preceding sections were carried out at a constant salt concentration of 10 mmoles/l KNO_3. Since in all colloid chemical phenomena the concentration and valency of the electrolytes are very important variables, it was decided to study to what extent the flocculation of AgI with PVA is dependent on the concentration and the type of electrolyte. These effects were considered at the optimum polymer dosage $p_1 = 2.5$ mg PVA/mmole AgI and the most effective way of mixing i.e. $\varphi_1 = 0.5$. For all the experiments presented in this section the time between adding PVA and the second portion of sol, t_1, was 15 minutes and the flocculation time, t_2, 1 hour.

In fig. 5–8 the relative absorbance of the supernatant is plotted as a function of the salt concentration for three electrolytes with cations of different valency and four types of PVA. From fig. 5–8 it follows that a certain critical concentrations is needed for flocculation to be effective: at low salt concentrations no flocculation at all takes place and with increasing c_s the absorbance decreases

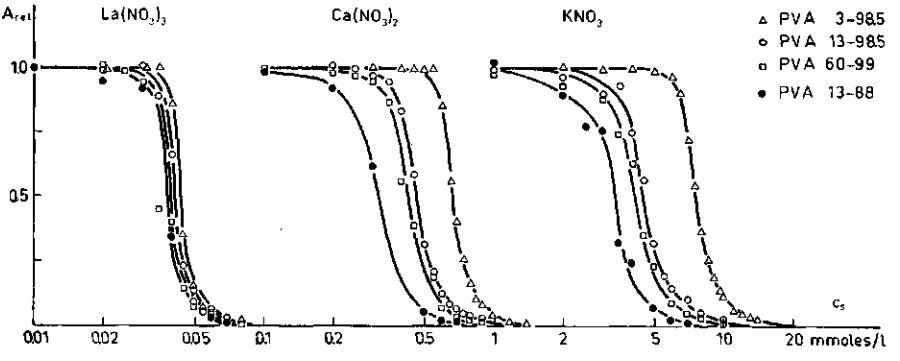

FIG. 5–8. Dependence of the flocculation on the salt concentration.
$p_1 = 2.5$ mg PVA/mmole AgI; $\varphi_1 = 0.5$; $c_{sol} = 3$ mmoles/l; $t_1 = 15$ min; $t_2 = 1$ h.
The experimental points are averages of measurements on sols A, B and C.

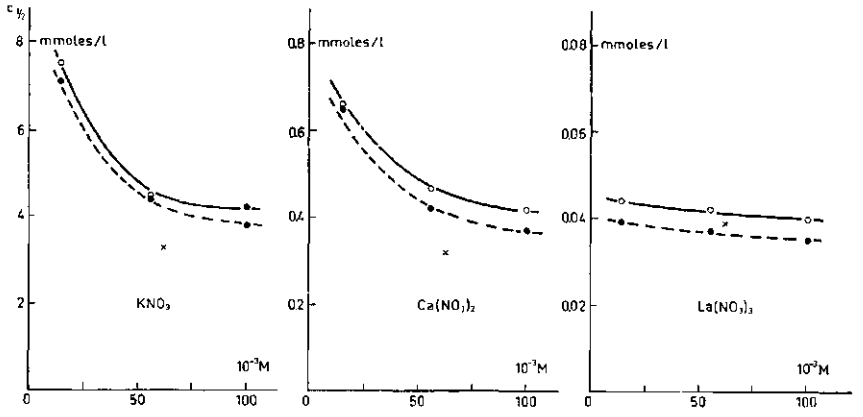

FIG. 5–9. The critical salt concentration at optimal flocculation conditions as a function of the molecular weight. Open circles: PVA 98.5, added in one step to the first portion of sol; full circles: PVA 98.5, added in two equal steps; crosses: PVA 13–88, added in one step.
Sol B; $p_1 = 2.5$ mg PVA/mmole AgI; $\varphi_1 = 0.5$; $c_{sol} = 3$ mmoles/l; $t_1 = 15$ min; $t_2 = 1$h.

rather suddenly until all the material is flocculated. We will define the critical salt concentration as that concentration at which half of the material is flocculated ($A_{rel} = 0.5$). This critical concentration will be denoted as $c_{\frac{1}{2}}$. $c_{\frac{1}{2}}$ is plotted as a function of the molecular weight of PVA in fig. 5–9 (full lines). Also given in fig. 5–9 is $c_{\frac{1}{2}}$ for the case in which the polymer is added in two equal steps to the first portion of sol, the second step being added 1 hour after the first (broken lines).

No flocculation is observed when no electrolyte is added; hence the flocculation process can be considered as a sensitisation.

Effect of the valency. From figs. 5–8 and 5–9 it can be seen that the influence of the valency of the cation is very large. For all types of PVA the critical salt concentration is around 5 mmoles/l for KNO_3, 0.5 mmoles/l for $Ca(NO_3)_2$ and 0.05 mmoles/l for $La(NO_3)_3$. This ratio of 100 : 10 : 1 is rather uncommon and does not resemble a power law of the valency as is often encountered in the coagulation of sols by electrolytes (OVERBEEK 1952, p. 303). The qualitative aspects of the SCHULZE-HARDY rule are obeyed. Thus the question arises what the function is of electrolytes in the flocculation of AgI with PVA.

Bridges between a covered and an uncovered particle can be formed only if the distance of closest approach between the two particles is not much higher than the thickness of the adsorbed layer. By adding electrolyte the double layer is compressed so that the distance of closest approach will be lowered, enabling bridging to occur. Counterions of higher valency can be more effective in reducing this distance of approach in two ways: firstly, the compression of the diffuse double layer is stronger because the attraction exerted on these ions by

the charged surface is larger and secondly, there is the possibility of stronger specific adsorption, reducing the STERN potential. Thus with ions of higher valency less salt will be needed to reduce the distance of closest approach to a certain value. A combination of the two effects could perhaps explain the ratio 100:10:1 found for $c_{\frac{1}{2}}$. An attempt to do this quantitatively will be described in Ch. 6.

Influence of the type of PVA. The critical salt concentration decreases with increasing molecular weight. This effect is most pronounced for PVA 13–98.5 in comparison to PVA 3–98.5; the difference between PVA 60–99 and PVA 13–98.5 is only small. If with higher M the loops are larger, then the layer thickness increases, so that bridges can be formed at larger interparticle distances than with a low molecular weight polymer and less salt will be needed. The small difference in $c_{\frac{1}{2}}$ between PVA 13–98.5 and PVA 60–99 indicates a roughly equal layer thickness in both cases. This is in agreement with the assumption that, at constant amount adsorbed, the layer thickness does not depend strongly on M (4.5.2.). Reasoning along these lines, the molecular weight of PVA 3–98.5 is too small for the assumption of a loop size distribution, which is independent of M, to be valid.

The flocculation with PVA 13–88 is more effective than that with PVA 13–98.5 as can be seen in figs. 5–8 and 5–9: less salt is needed for flocculation with PVA 13–88. This again points to a thicker adsorbed layer, as predicted earlier from the adsorption measurements (3.1.3.) and the protection experiments (4.1.2.). The same can be said for the adsorption of PVA in two steps; in this case the layer thickness must be higher than after addition of the polymer in one step as was concluded also in 3.3.2. and 4.1.2.

Specific effects. Some measurements have been carried out with other electrolytes. The results are given in table 5–1.

The trends found are the same as those found for the coagulation of negative sols by salts. For the nitrates a lyotropic sequence is found similar to that for uncovered AgI (OVERBEEK 1952, p. 307; LYKLEMA 1966). Also the effect of the valency of the co-ion is small. In both series the differences are only of minor importance compared to the influence of the valency of the counterion. The

TABLE 5–1. Critical concentrations (mmoles/l) of different electrolytes for the flocculation of AgI (sol B) with PVA 13–98.5.
$p_1 = 2.5$ mg PVA/mmole AgI; $\varphi_1 = 0.5$; $t_1 = 15$ min; $t_2 = 1$ h; $c_{sol} = 3$ mmoles/l.

nitrates		potassium salts		$La(NO_3)_3$	
$LiNO_3$	4.6	KNO_3	4.5	pH = 5	0.041
KNO_3	4.5	$\frac{1}{2}K_2SO_4$	3.9	pH = 7	0.03
$RbNO_3$	4.3	$\frac{1}{3}K_3Fe(CN)_6$	3.6	pH = 10	0.1

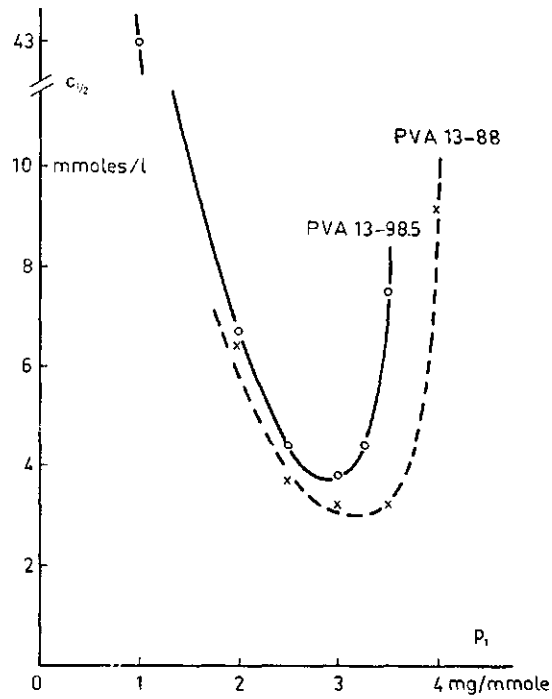

FIG. 5–10. Dependence of the critical salt concentration on the polymer dosage.
sol C; $\varphi_1 = 0.5$; $c_{sol} = 3$ mmoles/1; $t_1 = 15$ min; $t_2 = 1$ h.

similarity of the trends found with those reported for the coagulation in the literature strongly suggests that a similar mechanism is operative, i.e. presumably the specific effects are caused primarily by the influence of the ions on ψ_d.

The dependence of $c_{\frac{1}{2}}$ for $La(NO_3)_3$ on the pH points in the same direction. At intermediate pH (about 7 to 9) the lanthanum ion hydrolyses (OTTEWILL and SHAW 1968), giving rise to specifically adsorbing complexes, lowering ψ_d and decreasing $c_{\frac{1}{2}}$. At high pH a precipitation of lanthanum hydroxide occurs, increasing again the critical salt concentration.

The occurrence of these specific effects confirms the idea that the influence of salts must be explained from the compression of the diffuse double layer, in combination with the lowering of the STERN potential. Apparently specific adsorption occurs not only on uncovered AgI, but also on a polymer covered surface. This is not so surprising in view of our conclusion, arrived in sec. 4.4. that even at full coverage by PVA still about 30% of the STERN layer is void of segments.

Dependence of $c_{\frac{1}{2}}$ on the polymer dosage. In fig. 5–10 the dependence of $c_{\frac{1}{2}}$ on the polymer dosage to the first portion of sol, p_1, is given for PVA 13–98.5 and PVA 13–88. With increasing p_1 a strong decrease of $c_{\frac{1}{2}}$ is initially observed, indicating an increasing layer thickness. For PVA 13–98.5 the critical

concentration increases again at $p_1 > 3$ mg/mmole, because the particles of the second portion of sol become increasingly covered by PVA; more salt is then needed. The flocculation by bridging changes over to protection against salt at still higher p_1. For low p_1, $c_{\frac{1}{2}}$ raises until the coagulation value for an uncovered sol is reached. The curve for PVA 13–88 is similar: the minimum is lower and shifted to higher p_1 in accordance with the better flocculating power and the higher maximum amount adsorbed.

5.4. Kinetic aspects of the flocculation of AgI by PVA

All the experiments described up to now have been performed at a sol concentration of 3 mmoles/l and a flocculation time, t_2, of 1 h. By varying these parameters kinetic factors in the flocculation can be studied. Some experimental results obtained will be discussed in this section.

5.4.1. *The effect of the sol concentration and the flocculation time on the flocculation*

Influence of the sol concentration on the efficacy of the flocculation

The relative absorbance at the optimal polymer dosage $p_1 = 2.5$ mg PVA/mmole AgI as a function of φ_1 is plotted in fig. 5–11 for three sol concentrations: 0.3, 3 and 30 mmoles/l. The corresponding flocculation at $\varphi_1 = 0.5$ and varying p_1 is given in fig. 5–12. In these experiments PVA 13–98.5 was used; the electrolyte concentration was 10 mmoles/l KNO_3 and t_1 and t_2 were 15 minutes

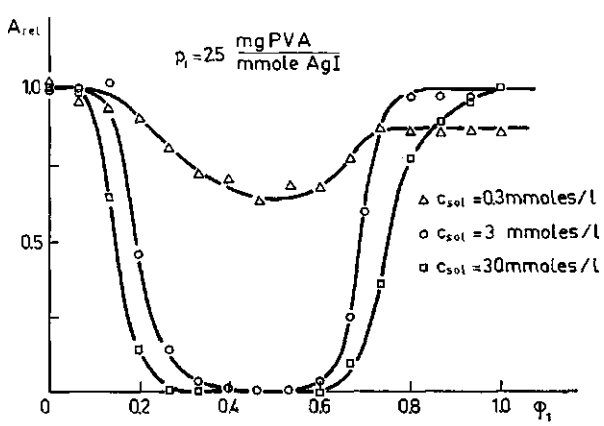

FIG. 5–11. The flocculation of AgI (sol A) by PVA 13–98.5 at different sol concentrations. $p_1 = 2.5$ mg PVA/mmole AgI; $c_s = 10$ mmoles KNO_3/l; $t_1 = 15$ min; $t_2 = 1$ h.

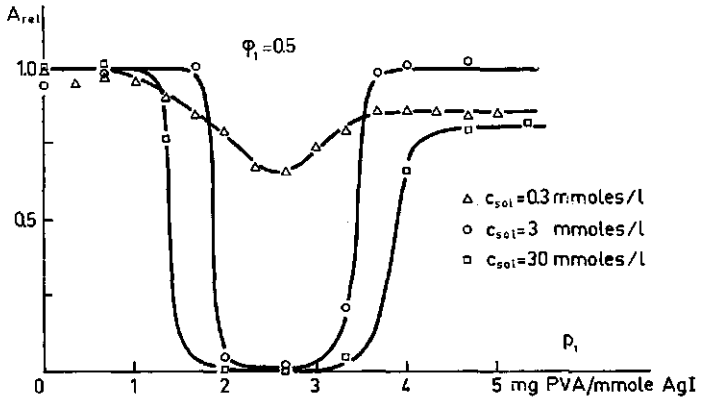

FIG. 5–12. The flocculation of AgI by PVA 13–98.5 at different sol concentrations.
$\varphi_1 = 0.5$; $c_s = 10$ mmoles KNO_3/l; $t_1 = 15$ min; $t_2 = 1$ h.
The curve for $c_s = 3$ mmoles/l was measured with sol C, the others with sol A.

and 1 hour, respectively. The curves for $c_{sol} = 3$ mmoles/l in figs. 5–11 and 5–12 are the same as those given in fig. 5–5 and 5–6. Similar curves at these three sol concentrations have been found for PVA 3–98.5 and PVA 60–99.

The efficacy of the flocculation depends strongly on c_{sol}: at $c_{sol} = 0.3$ mmoles/l the flocculation is very incomplete after 1 hour, while at $c_{sol} = 30$ mmoles/l all the material is flocculated around $p_1 = 2.5$ mg/mmole and $\varphi_1 = 0.5$. The most probable explanation for this sol concentration dependence is a kinetic one: as the sol concentration increases, the number of collisions per second between the particles increases also, leading to more bridges and more effective flocculation if the time of flocculation is fixed. Other experiments corroborating this idea will be discussed below.

It can be noted that at high p_1 a little flocculation takes place at $c_{sol} = 0.3$ and 30 mmoles/l (fig. 5–12). This is not observed in the experiments with $c_{sol} = 3$ mmoles/l. A possible explanation is the following: at low sol concentrations the polymer concentration is also very low. The polymer added in excess of 2.5 mg/mmole remains in solution and is responsible for the coverage of the particles of the second portion of sol, prohibiting flocculation in this way. However, at $c_{sol} = 0.3$ mmoles/l c_p is so low that the excess polymer adsorbs completely on the glass (see 3.2.1.). Upon addition of the second portion of sol this polymer will be released from the glass and attach itself to the bare AgI particles, but as this desorption is slow, some flocculation between the bare and covered particles may have occured before the bare particles are effectively protected. The anomaly in fig. 5–11 at high φ_1 can not be explained in this way; it is not yet quite clear what the reason is for the slight flocculation. At $c_s = 30$ mmoles/l a different phenomenon must take place; perhaps it is possible

TABLE 5–2. Critical salt concentrations of KNO_3 (mmoles/l) for the flocculation of AgI (sol A) by PVA at different sol concentrations.
$p_1 = 2.5$ mg PVA/mmole AgI; $\varphi_1 = 0.5$; $t_1 = 15$ min; $t_2 = 1$ h.

c_{sol} (mmoles/l)	0.3	3	30
PVA 13–98.5	10.2	4.5	1.7
PVA 60–99	9.8	4.2	1.3

that due to the high sol concentration and, consequently, the small interparticle distance simultaneous adsorption of one polymer molecule on two AgI particles occurs at high p_1, leading to some flocculation in spite of the fact that the optimal mixing procedure is not used. Anyhow, these anomalous flocculation effects are of minor importance, and no further attention will be paid to them.

Effect of the sol concentration on the critical salt concentration

It follows also from measurements of the critical concentration of salt that, at fixed t_2, the flocculation depends on the sol concentration. Table 5–2 gives the values of $c_{\frac{1}{2}}$ for KNO_3 measured at t_1 and t_2 of 15 minutes and 1 hour, respectively.

$c_{\frac{1}{2}}$ depends strongly on c_{sol} as can be seen from table 5–2. This effect can also be explained from kinetics: at high c_{sol} the number of encounters between the particles per second is higher than at low sol concentration so that in spite of the higher electrostatic repulsion the same extent of flocculation can be reached as with low c_{sol} and a higher salt concentration, corresponding to a low repulsion free energy.

The efficacy of the flocculation at varying flocculation time

If the sol concentration effect is indeed caused by kinetic factors the flocculation would be expected to become more extensive if the flocculation time is increased. This was experimentally corroborated, as shown in fig. 5–13. In fig. 5–13a the relative absorbance is plotted as a function of the flocculation time at $p_1 = 2.5$ mg/mmole and $\varphi_1 = 0.267$ ($v_1 = 0.8$ cm^3). These (less than optimal) conditions were chosen because at $c_{sol} = 3$ mmoles/l and optimal flocculation conditions the flocculation is too fast to be measured accurately with the technique used. In order to measure the flocculation rate at the optimal conditions $p_1 = 2.5$ mg/mmole and $\varphi_1 = 0.5$ a lower sol concentration must be chosen. Results are shown in fig. 5–13b for $c_{sol} = 0.2$ mmoles/l.

From fig. 5–13 it follows again that PVA 3–98.5 is less effective than PVA 13–98.5. The difference between PVA 60–99 and PVA 13–98.5 is only small.

The results presented in this section suggest strongly that the different

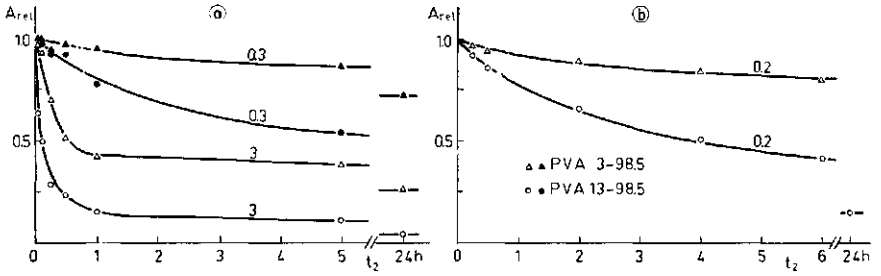

FIG. 5–13. The flocculation of AgI by PVA at constant sol concentration and varying flocculation time.
a. $p_1 = 2.5$ mg/mmole, $v_1 = 0.8$ ml ($\varphi_1 = 0.267$); sol B.
b. $p_1 = 2.5$ mg/mmole, $v_1 = 1.5$ ml ($\varphi_1 = 0.5$); sol C.
$c_s = 10$ mmoles KNO_3/l; $t_1 = 15$ min. The figures at the curves indicate the sol concentration in mmoles/l.

extents of the flocculation at different sol concentrations are caused by kinetic factors. By proper adjustment of the flocculation time to the sol concentration the flocculation efficiency will then be the same for all sol concentrations. This adjustment can be brought about provided the order of the flocculation reaction is known. To that order, a kinetic study at very short times was undertaken.

5.4.2. *Measurement of the initial flocculation rate*

A Durrum Stopped Flow spectrophotometer was used in a preliminary study of the initial rate of the flocculation. In this apparatus two solutions can be mixed within a very short time (10 ms for dilute aqueous solutions) and after mixing the transmittance as a function of time may be recorded on a storage oscilloscope; the picture obtained can be photographed and the initial slopes of the absorbance against time curves determined. These slopes are a measure for the rate of flocculation (REERINK and OVERBEEK 1954; see also 4.1.1.). Measurements with the Stopped Flow apparatus to determine the rate of coagulation of AgI in the presence of salts have been reported earlier (FLEER and LYKLEMA 1969). The construction of the apparatus is such, that only equal volumes of the solutions to be mixed can be handled.

Experimental procedure

The rate of coagulation of AgI sols in the presence of salts only has been measured by mixing of equal volumes of AgI sol and salt solution. The rate of flocculation, analogous to the one portion method (fig. 5–1), was studied by mixing a volume of sol with the same volume of a PVA solution, to which salt had been added. Simulation of the two portion method was achieved by using a volume of covered sol, to which salt had been added, and mixing this in the

apparatus with an equal portion of uncovered sol. The covered sol was prepared by adding PVA to AgI by the sharp boundary method (5.1.1.); the salt was added after one day of standing and this mixture was used for the measurements. Thus in all these kinetic measurements t_1 was 1 day.

If the sol concentrations of the covered and the uncovered portion were equal, then automatically $\varphi_1 = 0.5$. Other values of φ_1 were obtained by adjusting the concentration of the covered or the uncovered portion. All measurements were carried out with PVA 13–98.5 and sol C. The absorbance was measured at 8000 Å; at this wavelength the scattering of light by small AgI particles is conservative so that the absorbance increases with time. The path length of the cell used was 2 cm. Results are given in terms of dA/dt, expressed in $cm^{-1}s^{-1}$; the results are reduced to a path length of 1 cm. The initial value of dA/dt is proportional to the rate of flocculation or coagulation.

Results and discussion

Studies were made in the first place to see whether with this kinetic method a difference is again observed in the flocculation efficacy between the one portion method and the two portion method. It was found that, at $c_{sol} = 0.2$ mmoles/l and $c_s = 15$ mmoles/l KNO_3, dA/dt was $0.22 \cdot 10^{-4}$ cm^{-1} s^{-1} when the one portion method was used ($p_1 = 1.25$ mg/mmole; $\varphi_1 = 1$) whilst a value of $1.28 \cdot 10^{-4}$ cm^{-1} s^{-1} was found with the two portion method ($p_1 = 2.5$ mg/mmole; $\varphi_1 = 0.5$). Thus it is also found with this kinetic method that the two portion method is much more effective than mixing of PVA with one portion of AgI.

dA/dt as a function of c_s was measured at three sol concentrations, with the three salts used in earlier experiments. If the flocculation is a bimolecular process, as is the case with the coagulation, dA/dt should be proportional to c_{sol}^2. In fig. 5–14 $(dA/dt)/c_{sol}^2$ is plotted for the flocculation of AgI sols with PVA 13–98.5 (open symbols). Also some measurements are shown of the rate of fast coagulation, at the same sol concentrations, measured at $c_s = 200$, 5 and 0.5 mmoles/l for KNO_3, $Ca(NO_3)_2$ and $La(NO_3)_3$, respectively (filled symbols). The results are preliminary and not very accurate. Nevertheless some primary conclusions can be drawn.

With increasing c_s the flocculation rate increases, as expected, until a plateau is reached. Within the rather large experimental error dA/dt is proportional to c_{sol}^2, hence the flocculation can indeed be considered as a bimolecular process.

In 5.3. the critical salt concentration, $c_{\frac{1}{2}}$, was defined as that salt concentration at which, at a given flocculation time t_2, half of the material is flocculated. By analogy $c_{\frac{1}{2}}'$, derived from kinetic measurements, may be defined as to correspond to a system where the flocculation rate is half its maximum value. It can be seen from fig. 5–14 that $c_{\frac{1}{2}}'$ is independent of the sol concentration;

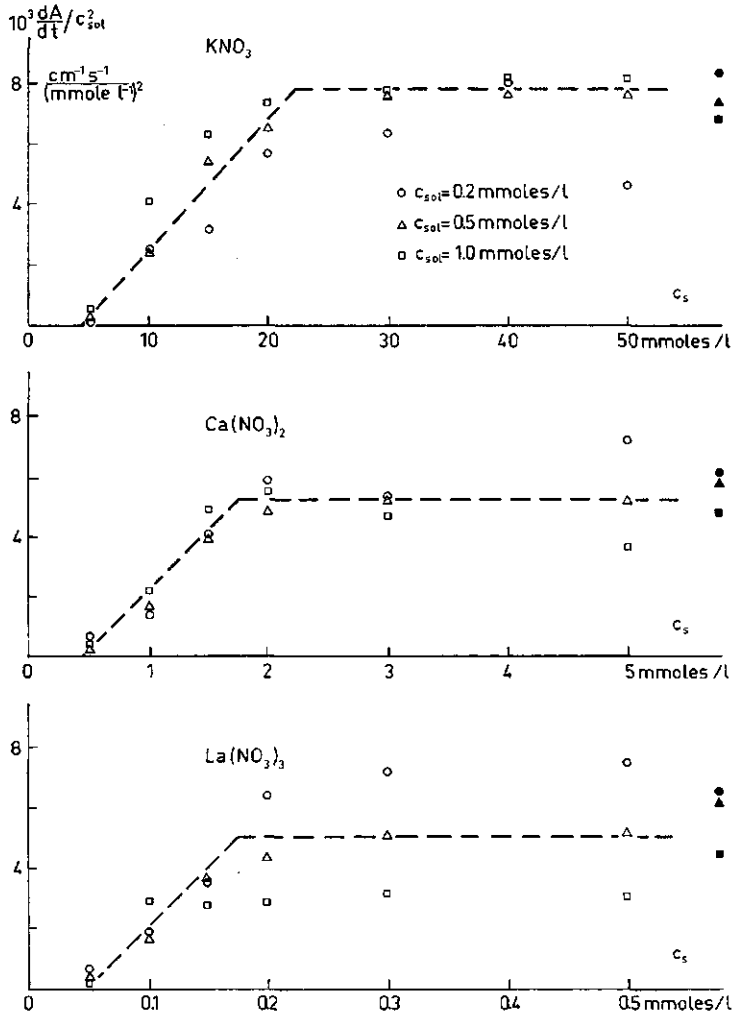

FIG. 5–14. The initial flocculation rate of AgI (sol C) with PVA 13–98.5 as a function of the salt concentration at different sol concentrations.
p_1 = 2.5 mg PVA/mmole AgI; $\varphi_1 = 0.5$; $t_1 = 1$ day.
The filled symbols give the rate of fast coagulation (without PVA) measured at 200, 5 and 0.5 mmoles/l KNO_3, $Ca(NO_3)_2$ and $La(NO_3)_3$, respectively.

probably the variation of $c_{\frac{1}{2}}$ with c_{sol} can be ascribed to kinetic effects. As is the case with $c_{\frac{1}{2}}$, $c_{\frac{1}{2}}'$ also appears to vary with the counterion valency according to approximately the ratio 100:10:1 for KNO_3, $Ca(NO_3)_2$ and $La(NO_3)_3$. The order of magnitude of $c_{\frac{1}{2}}'$ is the same as that of $c_{\frac{1}{2}}$ although the latter depends on the sol concentration and is therefore a less universal parameter.

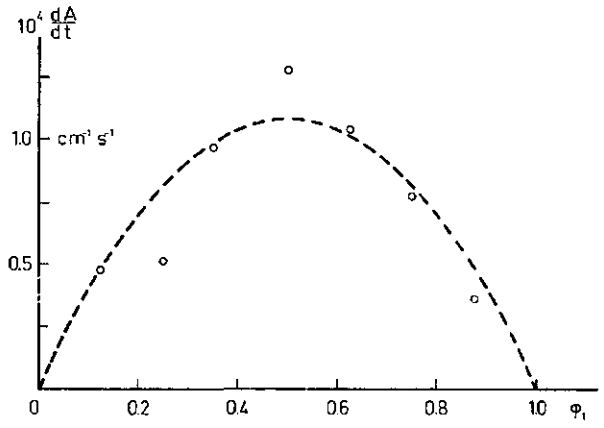

FIG. 5–15. The initial rate of flocculation as a function of φ_1 (two portion method). The broken line corresponds to $dA/dt = 4.3 \cdot 10^{-4} \varphi_1 \varphi_2$ cm^{-1}s^{-1}. PVA 13–98.5, sol C; c_{sol} = 0.2 mmole/1; c_s = 15 mmoles KNO_3/1; p_1 = 2.5 mg PVA/mmole of AgI.

If the flocculation is a bimolecular process the rate of flocculation in the two portion method should be proportional to $\varphi_1\varphi_2$ or to $\varphi_1(1-\varphi_1)$. In fig. 5–15 dA/dt is plotted as a function of φ_1 (c_{sol} = 0.2 mmoles/1, c_s = 15 mmoles/l KNO_3, p_1 = 2.5 mg/mmole). The broken line in fig. 5–15 is obtained by assuming dA/dt = constant. $\varphi_1(1-\varphi_1)$ in which the constant was taken to be $4.3 \cdot 10^{-4}$ cm^{-1} s^{-1}. It appears that the experimental points agree rather well with this theoretical line, indicating again that the flocculation between covered and bare particles is a bimolecular process.

An interesting point emerges from a comparison between the rate of fast flocculation with the two portion method and the rate of fast coagulation. At φ_1 = 0.5 only half of the collisions can be effective because encounters between two bare particles or between two covered particles cannot lead to flocculation. If no repulsive forces would act between the particles one should expect that the rate of fast flocculation is half of the rate of fast coagulation at the same c_{sol}. This is not observed: the two rates seem to be about equal (fig. 5–14). The reason for this is not clear. Perhaps the collision diameter of a covered particle is somewhat higher than that of an uncovered particle, but then also the diffusion coefficient will be lower. It seems unlikely that this effect can explain a factor of two in the flocculation rate. Another possibility is that the flocs formed in the flocculation process are more compact than the aggregates in a coagulating sol (see 5.5.) so that the time dependence of the absorbance is greater for a flocculating than for a coagulating system. This also, however, cannot be a satisfactory explanation.

In connection with this it is worth mentioning that it is generally found that the absolute rate of coagulation is too low in comparison with its theoretical value. This effect has not yet been fully explained (SPIELMAN 1970, HONIG et al. 1971).

GREGORY (1970) found that the rate of flocculation of negative polystyrene latices with cationic polyelectrolytes was about the same if a two portion method analogous to that described in 5.1. was applied as that measured using a one portion method. In this case perhaps the reason is that a covered and an uncovered particle are oppositely charged; due to the electrostatic attractive forces the rate of flocculation measured with the two portion method will be enhanced.

Another interesting fact is the higher rate of the flocculation as well as of the coagulation in the presence of KNO_3 in comparison to those when $Ca(NO_3)_2$ or $La(NO_3)_3$ are the electrolytes used. This observation has been found previously by TROELSTRA (1941, 1943) for a coagulating system. The same kind of difference is also reflected in measurements of the sediment volume (see 5.5.).

5.4.3. *Determination of the critical salt concentration if the flocculation time is adjusted to the sol concentration.*

At a constant flocculation time the critical salt concentration depends on the sol concentration (table 5–2). In 5.4.1. and 5.4.2. it was shown that this has a kinetic origin. However, if the time of flocculation, t_2, is properly adapted to c_{sol}, $c_{\frac{1}{2}}$ should become independent of c_{sol}. The question arises as to how t_2 should be adjusted to c_{sol}.

The criterium used in the flocculation experiments is the relative absorbance. If the wavelength is chosen in such a way, that mainly consumptive absorption of light occurs the absorbance, in a homodisperse system, can be assumed to be proportional to NV, where N is the number of particles of volume V. A_{rel} is measured after centrifugation; if it is assumed that only the 1 to j_{cr}-fold particles remain in the supernatant (if $j_{cr} = 1$ only primary particles would remain and all larger particles settle out) it follows:

$$A_{rel} = \sum_{j=1}^{j_{cr}} jN_j/N \tag{5-1a}$$

in which N_j is the number of j-fold particles and N the number of primary particles. In deriving (5–1a) the approximation was made that $V_j = jV$.

In the case in which mainly conservative light scattering occurs the absorbance in proportional to NV^2, and, if it is assumed that the scattering of an aggregate is the same as that of a sphere of equal weight, the relative absorbance after centrifugation is given by:

$$A_{rel} = \sum_{j=1}^{j_{cr}} j^2N_j/N \tag{5-1b}$$

In 5.4.2. it was found that the flocculation is bimolecular. In that case, for fast

flocculation, N_j/N can be calculated with the theory of VON SMOLUCHOWSKI (1916, 1917):

$$\frac{N_j}{N} = \frac{(t_2/t_{\frac{1}{2}})^{j-1}}{(1 + t_2/t_{\frac{1}{2}})^{j+1}} \tag{5-2}$$

t_2 is the time of flocculation and $t_{\frac{1}{2}}$ is the time, in which, during fast flocculation the number of particles is just halved. $t_{\frac{1}{2}}$ is inversely proportional to the number of primary particles, thus to c_{sol}.

If a certain electrostatic repulsion exists the flocculation is retarded by a factor W, the stability ratio (FUCHS 1934). W depends a.o. on the salt concentration and valency. A comprehensive survey of the theories of VON SMOLUCHOWSKI and FUCHS has been given by OVERBEEK (1952, Ch. VII). For slow flocculation eq. (5–2) can be written as:

$$\frac{N_j}{N} = \frac{(t_2/Wt_{\frac{1}{2}})^{j-1}}{(1 + t_2/Wt_{\frac{1}{2}})^{j+1}} \tag{5-3}$$

By combining eq. (5–1a) or (5–1b) with eq. (5–3) it can be seen that, independent of the type of light scattering law valid, A_{rel} solely depends on $t_2/Wt_{\frac{1}{2}}$, so on $t_2 c_{sol}/W$. If the flocculation time is adapted in such a way that $t_2 c_{sol}$ becomes constant a value of A_{rel} should be found for each c_s, which is independent of c_{sol}. Thus $c_{\frac{1}{2}}$ should be independent of sol concentration, provided t_2 is inversely proportional to c_{sol}.

The validity of this conclusion was verified in experiments using PVA 13–98.5 at $p_1 = 2.5$ mg/mmole and $\varphi_1 = 0.5$ at different sol concentrations. The results are given in table 5–3. It is clear that indeed the dependence of $c_{\frac{1}{2}}$ on c_{sol} at constant t_2 is a kinetic effect; if the flocculation time is adapted the critical salt concentration is found to be virtually independent of c_{sol}. It should be noted that the values, given in table 5–3 at $t_2 = 1$ hour are somewhat lower than

TABLE 5–3. The critical salt concentration $c_{\frac{1}{2}}$ (mmoles/l) at different sol concentrations (mmoles/l) and varying flocculation time. PVA 13–98.5, sol C; $p_1 = 2.5$ mg PVA/mmole AgI; $\varphi_1 = 0.5$; $t_1 = 1$ day.

c_{sol}	KNO_3		$Ca(NO_3)_2$		$La(NO_3)_3$	
	$c_{\frac{1}{2}}$		$c_{\frac{1}{2}}$		$c_{\frac{1}{2}}$	
	$t_2 = 1$ h	$t_2 = 3/c_{sol}$ h	$t_2 = 1$ h	$t_2 = 3/c_{sol}$ h	$t_2 = 1$ h	$t_2 = 3/c_{sol}$ h
0.2	10.0	4.0	1.05	0.42	0.092	0.040
0.5	6.3	4.1	0.70	0.40	0.060	0.042
1	5.0	3.9				
3	3.5	3.5	0.37	0.37	0.037	0.037

the corresponding figures for PVA 13–98.5 in table 5–2. The differences are caused by the different contact times t_1.

One may wonder why the critical flocculation concentration depends on the sol concentration, whilst the critical coagulation concentration is usually independent of c_{sol}. This difference is caused by the method of measuring chosen: $c_{\frac{1}{2}}$ was determined in a situation in which half of the material is flocculated. If the same method were to be applied for coagulation, a similar dependence of the coagulation value on c_{sol} should occur. As shown in 5.4.2. the critical flocculation concentration determined with the rate of flocculation method is independent of c_{sol}, as is the critical coagulation concentration.

Summarising the results obtained in this section, from measurements of $c_{\frac{1}{2}}$ at varying sol concentrations and adjusted flocculation times it can be concluded that the dependence of the critical salt concentration on the sol concentration is due to kinetic effects.

5.5. The sediment volume of flocculated and coagulated silver iodide

Generally it is found that flocs formed after flocculation are looser and less compact than coagulated flocs (e.g. Linke and Booth 1960, La Mer and Healy 1963). This open structure is an important feature for soil structure improvement. Some experiments were carried out to investigate this for silver iodide flocculated by PVA.

For the measurements of sediment volumes wide-necked tubes tapering to a narrow cylindrical end were used. The volume of the narrow part of the tubes was about 2 cm^3 and its length about 8 cm. The total volume of the tubes was 10 cm^3.

For the measurements with coagulating systems salt solution was simply added to the sol in the tubes. For the flocculation measurements the two portion method was used with $p_1 = 2.5$ mg PVA/mmole AgI and $\varphi_1 = 0.5$. Salt was added just prior to the second portion of sol to prevent coagulation of the first portion of sol. Mixing was achieved with the aid of a small stirring rod. The sol concentration used was 30 mmoles/l AgI; the quoted sediment volumes apply to 0.30 mmole of AgI.

Sediment volumes as a function of time are given in fig. 5–16 for the coagulation with KNO_3, $Ca(NO_3)_2$ and $La(NO_3)_3$ and for AgI flocculated by PVA 13–98.5 in the presence of the same salts at lower concentrations. In contradistinction to what is often reported in the literature, the sediment volume after flocculation is smaller than that of a coagulated sol, at least at relatively short sedimentation times. The final sediment volume is reached rather fast in the case of flocculation, while the sediment of a coagulated sol continues to con-

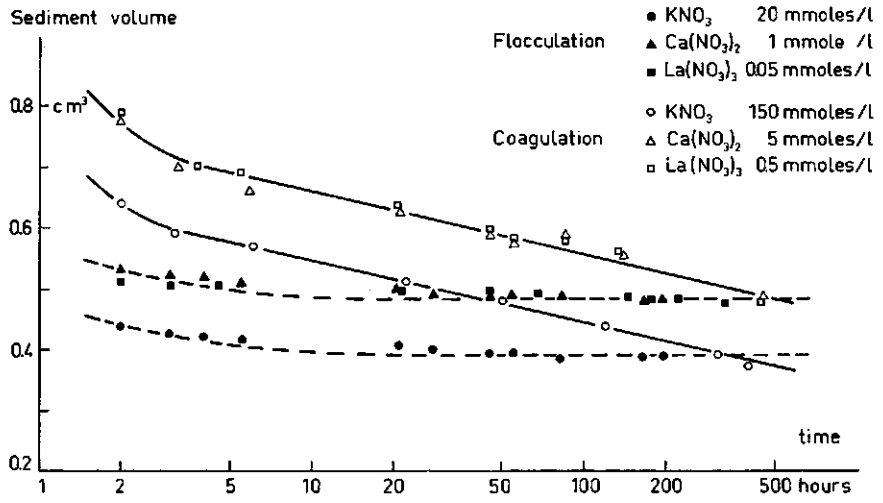

FIG. 5–16. The sediment volume of 0.30 mmole AgI (sol C) after coagulation (filled symbols) and flocculation with PVA 13–98.5 (open symbols) in the presence of different salts. For the flocculation the two portion method of mixing was applied ($p_1 = 2.5$ mg PVA/ mmole AgI, $\varphi_1 = 0.5, t_1 = 15$ min).

centrate with time: in this case the sediment volume seems to decrease exponentially with time for flocculation times between some hours and some hundreds of hours.

For a flocculated, as well as for a coagulated, system it appears that the sediment volume in the presence of KNO_3 is lower than that in the presence of $Ca(NO_3)_2$ and $La(NO_3)_3$. For coagulation this has already been reported and explained by TROELSTRA (1941, 1943).

The sediment volumes of flocculated AgI sols after 200 hours are plotted as a function of the salt concentration in fig. 5–17. It can be seen that the sediment

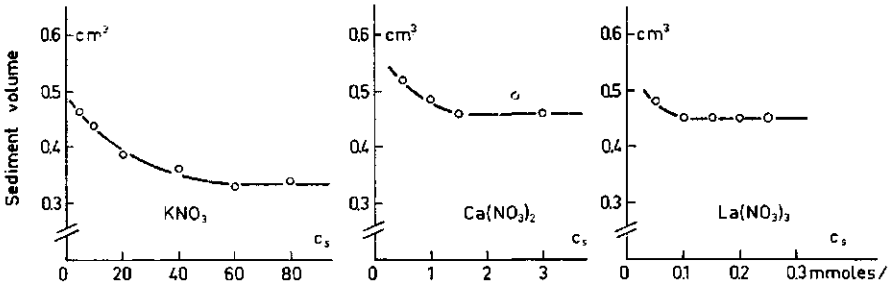

FIG. 5–17. The sediment volume after 200 h of standing of 0.30 mmole AgI (sol C) flocculated with PVA 13–98.5 as a function of the salt concentration. $p_1 = 2.5$ mg PVA/mmole AgI; $\varphi_1 = 0.5; t_1 = 15$ min.

volume becomes constant at high salt concentrations. This is to be expected: at high c_s electrostatic repulsion is no longer present and a further increase of c_s is without consequence. That higher sediment volumes are found at lower c_s is contrary to what was found for coagulation in the presence of KNO_3: in the latter case the sediment volume increases with c_s until the value in the presence of $Ca(NO_3)_2$ and $La(NO_3)_3$ is attained; for the latter salts no concentration dependence was found. The results found for a coagulated system agree with those given by TROELSTRA.

The observed trends are partly at variance with traditional expectations and an obvious explanation can not be offered. Below a few considerations and speculations are given.

It should be born in mind firstly that the sediment structure of coagulated flocs, as well as of flocculated ones, is a very loose one; the volume fraction of solids is not more than about 3%. Thus strictly a 'compact' sediment is not really dense. The particles must be arranged in more or less linear strings of beads, or in relatively compact sub-clusters arranged in a very loose packing.

Perhaps the fast attainment of the final sediment volume of a flocculated system can be explained by distinguishing two consecutive steps in the process: an initial floc forming process, followed by a rearrangement within the sediment. Flocculated particles are connected together by many polymer bridges with linkages in all directions; each particle is in contact with many others through the long, flexible loops. In this way in the first hours of the flocculation a rather compact sediment can be formed. Due to the large number of connections and the irreversible character of the adsorption any rearrangement process can not take place. In a coagulated floc, on the other hand, specific contacts between two surface sites on adjacent particles play the major role and rearrangement can occur somewhat more easily by sliding of the particles along each other, resulting in a continuing compression of the sediment. The occurrence of specific contacts in a coagulated floc explains also, according to TROELSTRA, the difference in sediment volume between KNO_3-flocs and those in the presence of higher charged cations; the high-valent ions form stronger interparticle contacts so that the aggregates do better resist the force of gravity tending to build up a dense packing.

The difference between K^+ on the one side and Ca^{++} and La^{+++} on the other in flocculation is not easily explained in this way, because no direct surface-surface contacts exist. Possibly the net repulsion between the particles is highest in the presence of KNO_3, so that in the initial stages of the floc forming process the flocculation is somewhat slower; more rolling of the particles over one another is then possible, leading to a denser sediment.

Neither is it very clear why the sediment volume of a flocculated sol decreases with increasing salt concentration. If c_s becomes higher the repulsive forces

between two particles become lower; perhaps due to this the interparticle distance will decrease. However, these are only speculations.
Ultimately, in view of the open sediment structure, it is doubtful to what extent the small effects discussed above really reflect the interaction between two particles.

5.6. Conclusions

In order to obtain efficient flocculation of a silver iodide sol with polyvinyl alcohol the way of mixing must be carefully considered. Effective flocculation takes place only if an amount of sol, the particles of which have adsorbed nearly the maximum amount of polymer, is mixed with an equal amount of untreated sol.

All observed flocculation phenomena can be fully explained by a bridging mechanism: loops extending from covered particles adsorb onto bare particles and in this way a network is formed of AgI particles interconnected by polymer bridges. The way of mixing is so critical only because the adsorption of polymer molecules is irreversible.

In the absence of salt no flocculation occurs. A small amount of electrolyte is needed, but far less than the coagulation value. Hence the flocculation should be referred to as sensitisation. A sol in which all the particles are covered with polymer is protected against coagulation by salts, but not against flocculation with newly added sol provided some electrolyte is present.

A critical salt concentration for the flocculation can be defined; this critical concentration depends very strongly on the valency of the counterion. The ratio between the critical concentrations was found to be 100:10:1 for KNO_3, $Ca(NO_3)_2$ and $La(NO_3)_3$, respectively. The function of the salt is to reduce the distance of closest approach between a covered and an uncovered particle so that bridges can be formed. The dependence of the critical concentration on the valency is explained in terms of the compression of the diffuse part of the double layer, in combination with specific adsorption. This is confirmed by some experiments in which the effect of the nature of the counterion was studied: the observed trends are qualitatively the same as those found with the lyotropic sequence in coagulation.

With increasing molecular weight the efficacy of the flocculation increases. However, the difference between PVA 13–98.5 and PVA 60–99 is very small, indicating that the layer thickness and the loop size distribution are similar for these two molecular weights. PVA 13–88 is more effective than PVA 13–98.5, in agreement with the higher layer thickness found for the former polymer; this has been deduced already from the adsorption and protection experiments.

Flocculation is more efficient if the time of contact between the polymer and the first portion of sol is increased; this could indicate a layer thickness increasing with time. Apparently the flattening of long loops or tails, formed in the initial stage of the adsorption process is compensated for by additonal adsorption or by the displacement of small polymer molecules by larger ones.

At fixed flocculation time the efficacy of the flocculation increases and the amount of salt needed decreases with increasing sol concentration. It can be shown that these effects have a kinetic origin. From measurements of the initial rate of flocculation it was deduced that flocculation is a bimolecular process. It was demonstrated that the critical salt concentration is independent of the sol concentration if the flocculation time is adapted in the proper way to the sol concentration. Some experiments have been done to measure the volume of the sedimented flocs. Contrary to what is generally found, it would appear that the flocs of a flocculated sol are more compact than those formed by coagulation.

6. THE FREE ENERGY OF INTERACTION BETWEEN A POLYMER COVERED AND A BARE PARTICLE

6.1. INTRODUCTION

In Ch. 5. it was shown that a silver iodide sol is flocculated by polyvinyl alcohol only if several critical conditions are fulfilled. One important condition appears to be the way of mixing of polymer and sol, the most efficient flocculation occurring if equal amounts of covered and uncovered particles are mixed. This effect could be explained satisfactorily. Another necessary condition for flocculation was shown to be the presence of a critical amount of salt. This critical flocculation concentration depends strongly on the valency of the counterions. In sec. 5.4. it was argued that the function of the salt is to lower the double layer repulsion so as to give a smaller distance of closest approach. In order to explain quantitatively the influence of the concentration and valency of electrolytes on the flocculation the interaction free energy between a covered and an uncovered particle has to be calculated as a function of the interparticle distance. An attempt to do this will be described in this chapter. In view of the complexity of the system only a very rough estimation of the various contributions can be obtained.

The classical factors determining the stability of colloidal systems, if no polymer is present, are the *van der Waals attraction free energy* (V_A) and the *double layer repulsion free energy* (V_R). DERYAGIN and LANDAU (1941) and VERWEY and OVERBEEK (1948) have formulated a theory to calculate these free energy terms. Formulae for V_A are available for various geometries. Exact values of V_R for flat plates can be obtained from the numerical tables given by VERWEY and OVERBEEK (1948) and by DEVEREUX and DE BRUYN (1963); approximative analytical expressions have been given for flat and spherical particles. The VAN DER WAALS attraction and the double layer repulsion will also play a role in the case of flocculation by polymers. In 6.2. and 6.3. their contribution will be calculated for the system AgI with PVA.

In the presence of adsorbed polymer extra terms are needed, because destabilisation of the system occurs at salt concentrations, at which the double layer repulsion is much higher than the VAN DER WAALS attraction. Thus, if only these factors were to be present, the system would be stable. In Ch. 5. it was concluded that bridging of polymer between two particles takes place. Due to this bridging extra interaction terms are introduced. Two consequences of bridging can be envisaged.

(i) The outermost segments of the adsorbed layer on one particle will adsorb

on the other particle, resulting in a decrease in free energy due to the gain in segmental adsorption free energy. This effect will be denoted as the *adsorption attraction free energy* (V_{Aa}). With decreasing interparticle distance the number of adsorbed segments increases, hence V_{Aa} will become more important. To calculate V_{Aa} (see 6.4.) use will be made of the segmental adsorption free energy estimated in 3.3.4. and of the segment density distribution (4.5.2.).

(ii) On adsorption of the first segments of a *loop* onto the second surface the loop is replaced by two *bridges*. The number of possible configurations of the two bridges will be less than that of the free loop due to the anchoring of the ends of the bridges. This results in a *configurational repulsion free energy* due to bridging (V_{Rb}). With decreasing interparticle distance more segments of a loop will adsorb and more loops become involved in the adsorption process, so that this configurational repulsion increases also with decreasing distance.

V_{Aa} and V_{Rb} necessarily occur simultaneously, and it would seem attractive to take the two terms together. However, it turns out that it is easier to separate them formally; it is then assumed that they can be added to give the free energy change due to the presence of the polymer, V_{pol} (6.6.).

In addition to the configurational entropy loss, accounted for in V_{Rb}, an osmotic effect could play a role, due to the increase in segment concentration between the two particles. It will be shown in 6.5.3. that the osmotic repulsion free energy will probably be rather small in our case. Therefore it will be neglected.

In the evaluation of V_{Aa} and V_{Rb} as a function of the interparticle distance a number of simplifying assumptions will be necessary. Use will be made of the segment density distribution derived in 4.5.2. and of the theory of HESSELINK (1971). This is only possible if the flat geometry is adopted. For that reason V_A and V_R will also be considered for flat plates.

All the results of the free energy calculations will be presented in the units $kT/100^2$ Å^2, i.e. in terms of the interaction between a plate of area 100^2 Å^2 and an infinite plate. The average radius of the AgI particles, assuming them to be spheres, is 500 Å (see 2.2.2.). It is difficult to correlate the free energy of interaction of two spherical particles with that of two flat plates, because it is not known what the 'equivalent flat area' of a AgI particle is. Moreover, this area would probably depend on the type of interaction. However, the magnitude of the 'equivalent flat area' of the AgI particle will be probably of the order of (5–10). 10^4 Å^2; hence, to get the interaction free energy in kT per pair of particles the value calculated for flat particles and expressed in $kT/100^2$ Å^2 must be multiplied by a factor of 5 to 10.

Two general assumptions will be made in this chapter. Firstly, the distribu-

tion of ions in the diffuse part of the double layer is considered to be unaffected by the presence of the polymer. As the viscosity of PVA is hardly influenced by salts (2.3.5.) it may be assumed that no specific interactions occur between the ions and the polymer, and the only possible effect of PVA on the ionic distribution is due to the volume occupied by the polymer. However, except for the first layers on the surface the polymer volume fraction is low, so the effect will be small. This assumption implies that the double layer repulsion between a covered and an uncovered particle is modified only through the influence of PVA on the potential of the diffuse part of the double layer, ψ_d.

The second assumption is based on the same viscosimetric measurements: it is supposed that the influence of salts on the polymer configuration is negligible. The validity of this approximation also follows from the fact that the amount of adsorbed PVA depends only very slightly on the salt concentration (3.3.5.). On account of this second assumption V_{Aa} and V_{Rb} are considered to be independent of the concentration and nature of the salts present.

In view of the other and relatively more serious approximations made in this chapter these two assumptions are well justified.

6.2. The van der Waals attraction

The attraction free energy between two plates embedded in a medium at an interparticle distance H, ignoring retardation effects, is given by the following equation (de Boer 1936, Verwey and Overbeek 1948):

$$V_A = -\frac{A_{12}}{12\pi H^2} \tag{6-1}$$

A_{12} is the Hamaker constant for particles of material 1 in a dispersion medium 2. For AgI in water we will adopt the value of $2.5 \cdot 10^{-13}$ ergs, recently found by Vincent et al. (1971).

In our case one complicating factor arises. One of the particles is covered with a layer of PVA, which might influence the van der Waals attraction (Vold 1961). However, the polymer layer is diffuse and the PVA is strongly hydrated. To a good approximation the Hamaker constant of the adsorbed layer may be put equal to that of water. Sonntag (1968) has previously made the same assumption for adsorbed layers of protective colloids. In that case eq. (6-1) remains valid if PVA is adsorbed on the AgI surface.

The plot of V_A against H is given in fig. 6–9. In anticipation of the discussion to come it may be stated that V_A is rather small in comparison with the other contributions to the interaction free energy. Hence, neglecting the influence of

the adsorbed layer on the VAN DER WAALS attraction free energy cannot lead to any serious error.

6.3. THE DOUBLE LAYER REPULSION

The electrical double layer repulsion free energy is taken from the DLVO theory. As V_R depends relatively strongly on the potential ψ_d of the diffuse part, this quantity has to be evaluated first.

6.3.1. *Estimation of the Stern potential*

The salt concentrations at which flocculation occurs were found to be of the order of 5, 0.5 and 0.05 mmoles/l for KNO_3, $Ca(NO_3)_2$ and $La(NO_3)_3$, respectively. In order to obtain V_R the values of the STERN potential under these conditions have to be known.

One way of finding ψ_d is to calculate it from the charge in the diffuse double layer, σ_d, by use of the GOUY-CHAPMAN theory (see e.g. OVERBEEK 1952, p.130). According to this theory the relation between σ_d and ψ_d is:

$$\sigma_d = -\sqrt{\frac{2\varepsilon n_s kT}{\pi}} \sinh \frac{ze\psi_d}{2kT} \tag{6-2}$$

where n_s is the number of counterions per unit volume, ε the dielectric constant and e, k and T have their usual meaning. Eq. (6–2) is valid for symmetrical electrolytes.

σ_d can be estimated from the surface charge σ_0, which in turn can be obtained from interpolations and/or extrapolations of potentiometric titration data for AgI in the presence of butanol and polyvinyl alcohol (see table 6–1). For AgI in the presence of $La(NO_3)_3$ no suitable information is available, and for AgI with $Ca(NO_3)_2$ only some preliminary unconfirmed data have been obtained (VAN DER LINDE 1971).

In table 6–1 the data used for the estimation of ψ_d for uncovered AgI and for AgI covered with butanol and PVA, respectively, at pI = 5.2 have been collected. The values given in this table for AgI in the presence of $Ca(NO_3)_2$ are rather unaccurate extrapolations.

The figures for σ_d/σ_0 are estimates, in line with the results for higher salt concentrations of LYKLEMA (1966) and VINCENT et al. (1971). σ_d/σ_0 increases with decreasing salt concentration and increasing adsorption of neutral species. Fortunately the value of ψ_d in this region is rather insensitive to changes in σ_d, and hence in σ_d/σ_0. Thus in spite of the difficult interpolations and extrapolations used the value of ψ_d may be expected to be accurate to within about 10 mV.

TABLE 6–1. Estimation of ψ_d for AgI at pI = 5.2 from titration data

Salt and concentration	σ_0 (μC/cm^2)	$-\sigma_d/\sigma_0$	σ_d (μC/cm^2)	ψ_d (mV)	System	References
	–2.85	0.9	2.56	–95	AgI	a, b, c
KNO_3, 5.10^{-3} M	–1.90	0.95	1.80	–78	AgI + 0.65 M butanol	b
	–2.30	0.95	2.18	–87	AgI + PVA [1]	c
$Ca(NO_3)_2$, 5.10^{-4} M	–3.75	0.5	1.88	–68	AgI	d
	–2.05	0.75	1.54	–63	AgI + 0.65 M butanol	d

[1] These values are averages for PVA 16–98 (0.28 mg PVA adsorbed/m^2 of suspension of AgI) and for PVA 40–88 (0.35 and 0.47 mg/m^2). It should be remembered that the maximum amount of PVA which can adsorb on the particles of a suspension of AgI is about 0.6 mg/m^2 (see 4.4.2.).

References: a. LYKLEMA (1963), b. BIJSTERBOSCH et al. (1965), c. KOOPAL (1970), d. VAN DER LINDE (1971).

The concentration of butanol, 0.65 M (see table 6–1), was chosen to give a coverage in the first layer on the surface comparable to that in the presence of PVA. From the values for ψ_d it would again appear that butanol influences the properties of the non-diffuse part of the double layer more strongly than PVA. The same conclusions were reached in 4.4.

It can be seen from table 6–1 that ψ_d for an uncovered AgI surface in the presence of 5.10^{-3} M KNO_3 is –95 mV, and that of a PVA covered surface about –10 mV lower. From the numerical tables given by DEVEREUX and DE BRUYN (1963) it may be deduced that in this range of ψ_d the repulsion free energy between two particles with STERN potentials ψ_{d_1} and ψ_{d_2}, respectively, is equivalent to that between two particles with equal ψ_d, the value of which is the arithmethic average of ψ_{d_1} and ψ_{d_2}. Hence, in order to calculate V_R the STERN potential for both particles may be taken as –90 mV in the presence of 5.10^{-3} M KNO_3. From a comparison with the values for a butanol covered surface –75 mV was adopted for 5.10^{-4} M $Ca(NO_3)_2$ and, more or less arbitrarily, a value of –60 mV was assumed for the average ψ_d in the presence of 5.10^{-5} $La(NO_3)_3$.

It will be supposed further that these values are independent of the salt concentration in the range around the critical flocculation concentrations.

6.3.2. *Calculation of the double layer repulsion free energy*

For the electrostatic repulsion free energy due to double layer overlap VERWEY and OVERBEEK (1948) have given exact tables, calculated with the assumption of constant potential during particle approach. From these tables the repulsion free energy as a function of the interparticle distance can be found for any ψ_d by interpolation. In addition, VERWEY and OVERBEEK derived

an approximate analytical formula for the repulsion free energy per unit area, V_R:

$$V_R = \frac{64 n_s kT}{\kappa} \gamma_d^2 e^{-\kappa H} \tag{6-3}$$

where H is the interparticle distance, κ the reciprocal DEBIJE length and $\gamma_d = \tanh(ze\psi_d/4kT)$. This equation is a good approximation for $\kappa H > 1$. In our case this condition is fullfilled for KNO_3 around a concentration of 5 mmoles/l; however, for $Ca(NO_3)_2$ at 0.5 mmoles/l and $La(NO_3)_3$ at 0.05 mmoles/l κH is 0.7 and 0.35, respectively, at distances around 50 Å. Thus eq. (6–3) is not applicable in these cases. This fact is also demonstrated in fig. 6–1, where for the three salts mentioned at some concentrations V_R is plotted against H according to the exact tables (full lines) and eq. (6–3) (broken lines). In the calculations all the salts have been considered as symmetrical electrolytes with ions of the same valency as that of the cation. At low concentrations of electrolytes con-

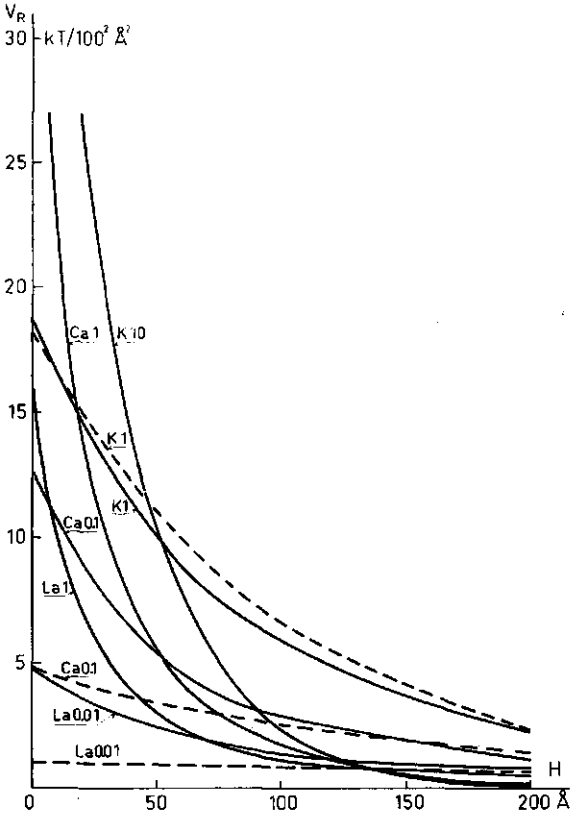

FIG. 6–1. The double layer repulsion free energy as a function of the interparticle distance for flat plates in the presence of some concentrations of KNO_3 (ψ_d = –90 mV), $Ca(NO_3)_2$ (ψ_d = –75 mV) and $La(NO_3)_3$ (ψ_d = –60 mV).
Full lines: exact numerical values according to the tables of VERWEY and OVERBEEK; broken lines: approximated according to eq. (6–3). The cation and the salt concentration (mmoles/l) are given for each curve.

taining multivalent ions the difference between the exact and the approximate values for V_R is as much as a factor of 3 for small distances. Therefore in all further calculations the exact numerical values for V_R were used.

From fig. 6–1 it can be seen that the repulsion curves for different salt concentrations cross each other. In other words, with increasing salt concentration the repulsion decreases at large distances, whereas at small distances the repulsion is enhanced. This effect has been noted and explained by VERWEY and OVERBEEK.

As mentioned the VERWEY-OVERBEEK theory has been derived with the assumption of constant potential. This assumption has been investigated by FRENS (1968). From his work it follows that for $\kappa H > 0.3$ it is irrelevant whether the potential or the charge is assumed to be constant; for lower distances the constant potential assumption leads to an underestimation of V_R. This means that in the present case only at very small distances and low salt concentrations the repulsion as given in fig. 6–1 is too low.

Although for all the calculations the flat geometry is used we shall occasionally in the forthcoming discussion refer to the repulsion energy for spherical particles. An approximative formula given by VERWEY and OVERBEEK reads:

$$V'_R = \frac{64\,\pi\, n_s RkT}{\kappa^2}\,\gamma_d^2\,\mathrm{e}^{-\kappa H} \tag{6-4}$$

where V'_R is the repulsion free energy between two spheres of radius R. Throughout this chapter a prime will be used to denote the interaction free energy between two spherical particles.

6.4. THE ADSORPTION ATTRACTION

The problem here is to estimate the gain in free energy with decreasing separation, as more and more segments of the loops adsorbed on one particle become attached to a second particle. In this process two effects can be distinguished. Firstly, when a segment adsorbs the free energy of the particle pair is lowered by an amount equal to the segmental adsorption free energy. Moreover, the configurational entropy of the polymer chain will be diminished. In this section only the first effect will be considered; it is assumed to be independent of the configurational entropy term, which is discussed in 6.5.

As a first approximation it is assumed that the adsorption attraction free energy per unit area, V_{Aa}, is proportional to the number of segments adsorbed in the first layer on the second particle per unit area, A_a. A_a will increase with

decreasing interparticle distance. The proportionality constant will be equal to the segmental adsorption free energy, ε_a, i.e.

$$V_{Aa} = -\varepsilon_a A_a \tag{6-5}$$

ε_a is assumed to be independent of the coverage of the second surface. Its value is taken to be 1 kT as discussed in 3.3.4.

The next problem is to find A_a as a function of H. On the mutual approach of an uncovered particle and a covered one the outermost segments adsorb first. For large separations the simplest approximation that can be made is, that all the segments, which would be beyond H in the undisturbed distribution, attach to the second surface (see fig. 6–2). If the number of segments, in the undisturbed distribution, beyond H per unit area is denoted by A_H, then $A_a = A_H$.

A_H can be written as:

$$A_H = \int_H^\infty \rho\,(x)\,\mathrm{d}x \tag{6-6}$$

Up to p_a values of about 1 mg/m^2 the HOEVE distribution applies so that, in this range of p_a, $\rho(x)$ is given by eq. (4–25). With the help of eqs. (4–24) and (4–26) and the relation $A_0 = \rho_0\delta$ eq. (6–6) now becomes:

$$A_H = (A_t - A_0)\,\mathrm{e}^{-p_H(H-\delta)} \tag{6-7}$$

A_t–A_0 is the number of segments per unit area in the exponential part of the

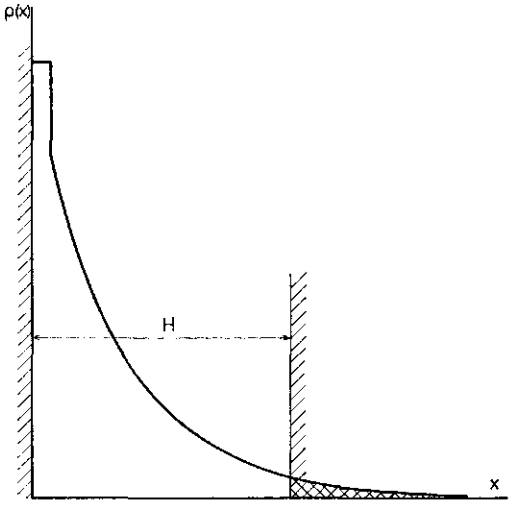

FIG. 6–2. Schematic representation of the approach of a second (uncovered) particle to a covered one.
It is assumed that, at large interparticle distance H, the number of segments which adsorbs on the (originally) bare particle per unit area is equal to the number of segments per unit area which would lie beyond H if the second particle were to be absent (shaded area).

undisturbed adsorbed layer and p_H is given by eq. (4–26); δ is the thickness of the first layer.

Thus, if the assumption $A_a = A_H$ is valid V_{Aa} is an exponential function of H. At large distances the coverage of the second surface is still very small, and it seems probable that the outermost segments can adsorb consecutively; then only trains are formed on the second surface and the approximation $A_a = A_H$ seems reasonable. However, with decreasing distances the second surface becomes more highly covered; thus for steric reasons some segments will remain unattached to the second surface and A_a will increase more slowly with decreasing H than does A_H. In addition, small loops will appear on the second surface.

At very short distances A_a would reach a maximum value corresponding to the maximum coverage in the first layer on the second surface (A_0'). It would seem likely that this maximum coverage is lower than that on the first surface, A_0, because segments of polymer molecules arriving from solution have more possibility of finding a free surface site than the segments of a loop attached to another particle. Some values for A_0' are suggested below.

Thus there are two limiting values for A_a: at low coverage on the second surface (large H) $A_a = A_H$, whereas at small values of H, A_a should approach A_0'. It is very difficult to find the physically most realistic expression to relate A_a and A_H. Therefore a simple trial formula will be chosen that satisfies both the boundary conditions. We adopted the following simple relation:

$$\frac{A_a}{A_0'} = \frac{A_H}{A_0' + A_H} \tag{6-8}$$

Combining eq. (6–8) with eq. (6–5) then gives the expression for V_{Aa}:

$$V_{Aa} = -\frac{\varepsilon_a A_H}{1 + A_H/A_0'} \tag{6-9}$$

where A_H is given by eq. (6–7).

The adsorption attraction free energy can now be obtained with the help of the distribution parameters given in 4.5.2. Under optimal flocculation conditions the polymer dosage in the first portion of sol, p_1, amounts to about 2.5 mg PVA/mmole of AgI (Ch. 5.). This corresponds roughly with $p_a = 0.9$ mg/m^2 for the first surface. Using the same parameter values as given in 4.5.2. ($K_H = 0.8$, $A_0 = 0.028$ Å^{-2}, $\delta = 4$ Å and A_t (Å^{-2}) $= 0.1345\ p_a$ (mg/m^2)) V_{Aa} can be calculated provided that a value for A_0' is assumed. As mentioned, it may be expected that $A_0' < A_0$. In fig. 6–3 V_{Aa} is plotted as a function of H for $A_0' = 0.007$ Å^{-2}, 0.010 Å^{-2} and 0.014 Å^{-2}. These values correspond to ratios of A_0' to A_0 of 0.25, 0.36 and 0.50, respectively.

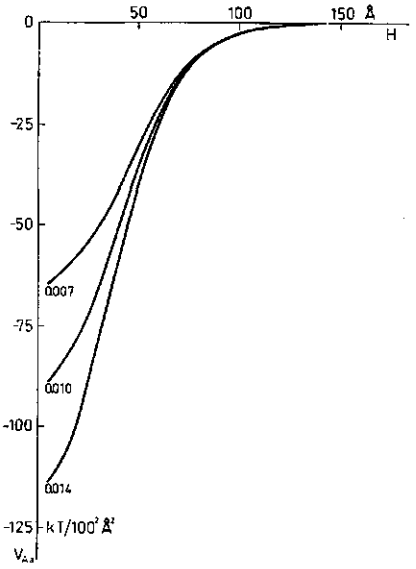

FIG. 6–3. The adsorption attraction free energy as a function of the interparticle distance for $p_a = 0.9$ mg PVA/m². The value for the coverage in the first layer on the second particle (A_0' in Å^{-2}) is given for each curve. The adsorption free energy per segment, ε_a, was taken to be 1 kT.

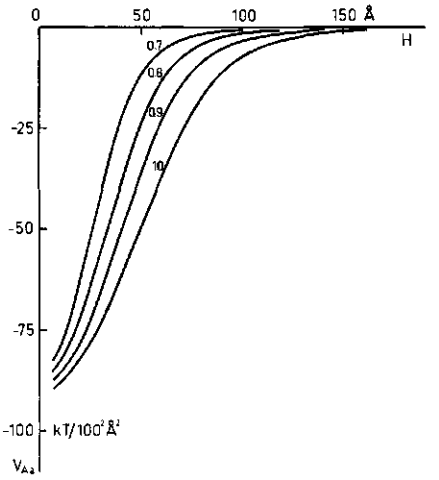

FIG. 6–4. The adsorption attraction free energy as a function of the interparticle distance for four values of the amount adsorbed (p_a in mg/m²).
The coverage in the first layer on the second particle, A_0', was assumed to be 0.010 Å^{-2}; the segmental adsorption free energy, ε_a, was taken as 1 kT.

It can be seen from fig. 6–3 that for $H > 75$ Å V_{Aa} does not depend on A_0'. In this range of H all segments which would be beyond H in the undisturbed distribution do adsorb and, consequently, the adsorption attraction term is exponential. Only at rather small distances does the value attributed to A_0' influence V_{Aa}. At small distances the validity of the derivation given is more doubtful due to the high coverage on the second surface and also due to the possible occurrence of small loops on that surface.

For the forthcoming calculations a value for A_0' of 0.010 Å^{-2} will be taken. In fig. 6–4 V_{Aa} is given for various amounts adsorbed. The adsorption attraction increases with p_a because of the thicker layer. At very small distances the differences between the curves for different p_a values become smaller because the seconds urface is then filled up and the maximum value of A_a, and thus of V_{Aa}, is attained.

6.5. THE CONFIGURATIONAL REPULSION DUE TO BRIDGING

On adsorption of a loop on the second surface there will be, in addition to the decrease in free energy due to the adsorption of segments, an increase in free energy due to the loss of configurational entropy. At large distances this entropy loss will be caused mainly by fixation of the ends of each loop; with decreasing distance effects due to the shortening of the bridges formed will also play a role. The entropy loss depends on the size of the loops. Therefore the problem will be considered in two steps. Firstly the configurational entropy loss of one loop will be estimated, and subsequently this effect will be integrated over all loop sizes with the help of the HOEVE distribution (eq. (4–20)) to give the repulsion free energy due to bridging.

6.5.1. *The configurational entropy loss of a single loop*

The process by which a loop of i statistical chain elements adsorbs on a second surface is illustrated schematically in fig. 6–5. At large interparticle distances a loop is completely free and its configuration is not affected by the second surface (fig. 6–5a). After adsorption of the first element the loop divides into two bridges. If it is assumed that the element which is at the largest distance from the covered surface (this will be, on average, the middle element of the loop) is adsorbed first on the second surface, two bridges of $i/2$ elements are

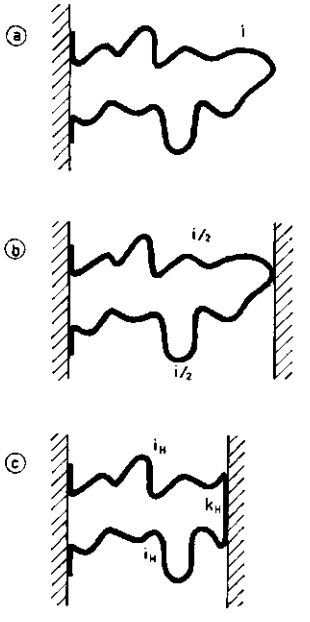

FIG. 6–5. Schematic representation of the bridging process.
a. At large interparticle distances a loop of i elements has its undisturbed configuration
b. After adsorption of the first element two bridges of $i/2$ elements each are formed
c. At shorter distances two bridges of i_H elements are present and a train of k_H elements has been adsorbed on the second surface.

formed (fig. 6–5b). With decreasing distance more elements are attached to form a train of k_H elements; the two bridges consist, with this approximation, of i_H elements each. i_H and k_H are related through:

$$k_H = i - 2\, i_H \tag{6-10}$$

In order to estimate the configurational entropy as a function of H the dependence of k_H on H must be known. To find this relationship the same assumption as was used for the calculation of V_{Aa} (eq. (6–6)) was used: k_H was taken to be equal to the number of elements which, in the undisturbed configuration (fig. 6–5a), is beyond H. Thus:

$$k_H/i = \int_H^\infty \rho_l\,(x)\,\mathrm{d}x \tag{6-11}$$

where $\rho_l(x)$ is the undisturbed distribution of elements in a loop, normalised to unity. $\rho_l(x)$ is given by eq. (4–19). Substitution of this equation into eq. (6–11) gives:

$$k_H = i\,\mathrm{e}^{-6H^2/il_s^2} \tag{6-12}$$

From eq. (6–12) k_H can be calculated for any H. i_H follows then from eq. (6–10).

In principle the configurational free energy difference between the situations represented by fig. 6–5c and 6–5a can now be calculated. We shall give the derivation and the results first, and discuss the approximations made and their consequences afterwards.

If the configurational free energy of a bridge of i elements at an interparticle distance H is denoted by $g_b(i, H)$ and that of a loop by $g_l(i, H)$ the configurational repulsion free energy at a distance H due to a loop of i elements, $\upsilon_{Rb}(i, H)$ can be written as:

$$\upsilon_{Rb}\,(i, H) = 2\, g_b\,(i_H, H) - g_l\,(i, \infty) \tag{6-13}$$

HESSELINK (1971a) has calculated the free energy difference between a bridge of i elements and a free loop of the same number of elements, $\Delta g_b\,(i, H)$ (Δf_b in his notation). Using this quantity eq. (6–13) can now be transformed as follows:

$$\upsilon_{Rb}\,(i, H) = 2\,\Delta g_b\,(i_H, H) + \left[2\, g_l\,(i_H, \infty) - g_l\,(i, \infty)\right] \tag{6-14}$$

The term between brackets can be calculated from the partition function of a free loop (HOEVE 1965, HESSELINK 1971a). The configurational free energy of a free loop, in three dimensions, is given by:

$$g_l(i, \infty)/kT = \ln (6\pi)^{1/2} + 3/2 \ln i - i \ln 6 \qquad (6\text{-}15)$$

Substituting this result in eq. (6–14) the configuration repulsion free energy due to one loop is obtained.

$$v_{Rb}(i, H) = 2\,\Delta g_b(i_H, H) + 3/2\,kT \ln [(6\pi)^{1/3} i_H^2/i] + k_H kT \ln 6 \qquad (6\text{-}16)$$

For any H, k_H and i_H can be calculated from eqs. (6–12) and (6–10). Δg_b (i_H, H) can be taken from HESSELINK's work. In fig. 6–6 v_{Rb} and its components are plotted against H for loops consisting of 10, 20 and 30 elements. These numbers are chosen to be much higher than the average number of elements per loop in the adsorbed layer (for $p_a = 0.9$ mg/m^2, $\bar{i} = 3.4$; see 4.5.2.), for it may be expected that mainly the largest loops will take part in the bridging process. The data of fig. 6–6 were calculated with $l_s = 16.9$ Å.

The second term of the right-hand side of eq. (6–16) accounts for the configurational entropy loss due to the 'fixation' of the middle elements of the original loop on the second surface. As can be expected this term is the most important one at large distances (see fig. 6–6): the entropy loss on adsorption of the first elements is relatively large. With decreasing distance this fixation term decreases, probably due to the co-operative nature of the adsorption process: after adsorp-

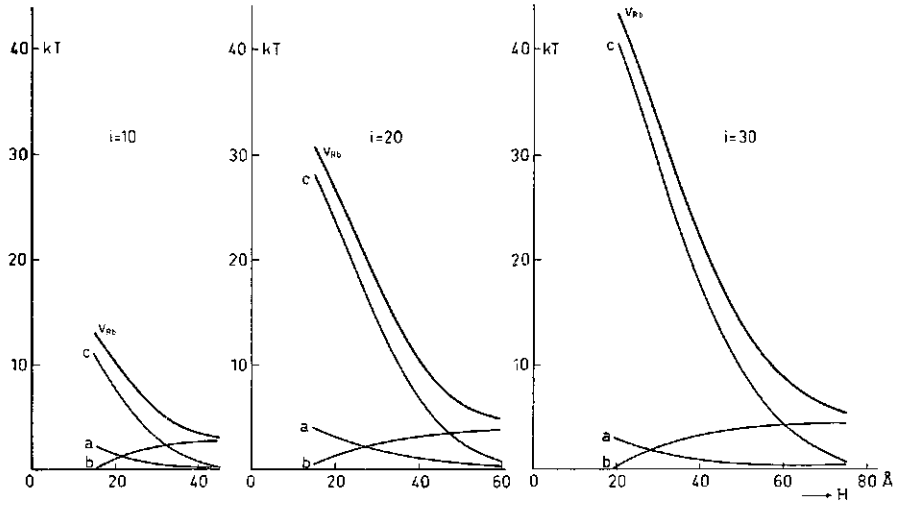

FIG. 6–6. The configurational repulsion free energy v_{Rb} and its components (a, b and c) as a function of the interparticle distance for one single loop of 10, 20 or 30 statistical chain element elements, respectively, calculated according to eq. (6–16).
a. $2\Delta g_b(i_H,H)$ b. $3/2\,kT \ln [(6\pi)^{1/3}(i_H^2/i)]$ c. $k_H kT \ln 6$
The length of a statistical chain element, l_s, was taken to be 16.9 Å.

tion of the first elements progressive adsorption of other elements becomes more easy.

The last term of eq. (6–16) represents the configurational entropy loss of the adsorbed elements. Its magnitude depends on the coordination number (see below), in this case taken to be 6. It should be possible to incorporate this term in the segmental adsorption free energy ε_a, which was assumed to be 1 kT (see 3.3.4. and 6.4.). However, it is not necessary to do so; the contribution of the configurational entropy loss to ε_a is only $(kT \ln 6)/6.65 = 0.27\ kT$ (6.65 is the number of segments per statistical element, see table 2–3). In view of the uncertainty in the exact value of ε_a, the value of 1 kT for the calculation of V_{Aa} is maintained and eq. (6–16) will be used as stated, including the last term. In effect this corresponds with a value of 0.73 kT for the segmental adsorption free energy, including the configurational entropy loss for an adsorbed segment. Then it can be seen from fig. 6–6 that the configurational repulsion energy for one loop at small interparticle distances is determined largely by the term $k_H kT \ln 6$.

The first term of eq. (6–16), $2\Delta g_b\,(i_H, H)$ is also shown in fig. 6–6. It was calculated with the assumption that the free energy of a bridge depends only on $H/\sqrt{il_s^2}$ as is the case for the free energy change due to the volume restriction of a loop and of a tail (HESSELINK 1971a). This term is a correction for the difference in configurational entropy of a long bridge at large distances and a shorter bridge at smaller distances. Its value is relatively small. The reason is, that in our approximation Δg_b is determined by the quantity $H/\sqrt{il_s^2}$, which decreases only slightly with decreasing H because i_H depends strongly on H (see eqs. (6–10) and (6–12) and fig. 6–5).

In addition to the points mentioned in the above discussion on the meaning of the different terms in eq. (6–16), there are several other uncertainties and assumptions in the derivation of this equation, with the result that this equation cannot be better than a very crude first approximation. Some of these uncertainties are summarised briefly.

In eq.(6–15) a coordination number of 6 was chosen; this applies to a six-choice cubic lattice. If it is assumed that an element in a chain cannot occupy the position of the preceding one, a five-choice lattice should be used. However, as indicated above this would mainly affect the effective value of ε_a and in view of the uncertainty in this quantity it does not seem worth-while to correct for it.

Another point is that by using the formulae given by HESSELINK it is assumed that only the first element of a loop and of a bridge is fixed; the other ends should be able to move freely along the surface. As was deduced earlier the adsorption of segments is reversible. However, it seems likely that the mobility of the end points decreases with increasing surface coverage due to the long

trains formed. Thus for longer distances the treatment given could apply, while for shorter distances $v_{Rb}(i, H)$ is probably larger than given by eq. (6–16) due to the restricted mobility of the adsorbed elements.

A further assumption made is that the two bridges formed from one loop are equally long. This is certainly not correct; presumably a distribution of bridge lengths occurs. Due to this approximation $v_{Rb}(i, H)$ is probably overestimated, thus partly compensating the underestimation due to the restricted surface mobility of the ends.

Subsequently, the approximation was made that the elements adsorb in a flat orientation on the second surface. In 6.4. it was supposed that at shorter distances not all of the elements, which in the undisturbed distribution would lie beyond H, adsorb. Then probably small loops would occur on the second surface. It is difficult to predict what the influence of these loops on v_{Rb} will be: the term $k_H \ln 6$ will be lower but on the other hand a kind of volume restriction repulsion is introduced.

Finally, especially at small distances the number of elements in the bridges becomes very small; then the applicability of statistical methods is rather doubtful.

In conclusion, it may be stated that several objections may be raised against the use of eq. (6–16), the majority of which, however, become less serious at relatively large distances. Also there might be some internal compensation of errors. For lack of a better theory this equation will nevertheless be adopted as a working hypothesis, in the hope that for shorter distances the trends at least are properly described.

6.5.2. *The configurational repulsion free energy due to the whole adsorbed layer*

An adsorbed layer consists of loops of different sizes, and the total configurational repulsion can be found by summation of the contributions of each loop length. The configurational repulsion free energy per unit area is given by:

$$V_{Rb}(H) = \int_{i=0}^{\infty} v_{Rb}(i, H)\, n_i \, \mathrm{d}i \qquad (6\text{-}17)$$

where n_i is the number of loops of size i per unit area.

Although relatively few long loops are present in the adsorbed layer these long loops contribute substantially to V_{Rb} because v_{Rb} increases strongly with increasing loop size (see fig. 6–6). As discussed in 4.5.2. the HOEVE distribution of loops may be considered to apply for PVA on AgI at amounts adsorbed between 0.5 and 1.0 mg/m^2. It will be assumed that this distribution of loops on the first surface is essentially unaltered in the presence of the second surface (see also 6.6.2.).

Furthermore, the assumption is made that the polymer layer on the first particle has reached its equilibrium state. This is probably not entirely true but the error introduced is not very large. In Ch. 5. it was shown that the critical flocculation concentration does not depend very strongly on t_1, the time of contact between polymer and sol particles, for t_1 more than 15 minutes (cf. tables 5–2 and 5–3). Moreover, no expression is available for the loop size distribution of a non-equilibrium polymer layer. Thus the equilibrium formulae will be used.

With these assumptions n_i is given by:

$$n_i = \frac{n}{\sqrt{\pi}} i^{-3/2} q \, e^{-q^2 i} \tag{4-20}$$

n is the total number of elements in the loops per unit area, and can, for PVA 98.5, be written as

$$n = (A_t - A_0)/6.65 \tag{6-18}$$

As A_t and A_0 refer to the number of segments, A_t–A_0 has to be divided by the number of segments per statistical element, 6.65, to obtain the number of elements per unit area. The parameter q in eq. (4–20) equals $l_s p_H/2\sqrt{6}$ (eqs. (4–21) and (4–27)) and can be found from the amount adsorbed by applying eqs. (4–24) and (4–26).

After substitution of eq. (4–20), eq. (6–17) can only be integrated numerically. To do this it is easier to have an analytical expression for v_{Rb}. This can be obtained from eq. (6–16) by simply dropping $\Delta g_b\,(i_H, H)$; as is shown in fig. 6–6 this term is only small and in view of the approximative character of eq. (6–16) this inaccuracy is not serious. So V_{Rb} was calculated using:

$$v_{Rb}\,(i, H)/kT = 3/2 \ln [(6\pi)^{1/3} i_H^2/i] + k_H \ln 6 \tag{6-19}$$

One other problem arises. For very large distances k_H approaches zero, and according to eq. (6–10) i_H then equals $i/2$, thus giving a constant, non-zero value for $v_{Rb}\,(i, \infty)$. This is physically unacceptable. A correction was applied by putting $v_{Rb}\,(i, \infty)$ equal to zero beyond that distance at which the first segment is just adsorbed, i.e. that distance at which $k_H = 1/6.65$.

With these conditions V_{Rb} was calculated from eqs. (6–10), (6–12), (6–17) to (6–19) and (4–20) with the help of a WANG 700 B electronic calculator.

Results are given in fig. 6–7 for four values of the amount adsorbed (p_a in mg/m^2). V_{Rb} increases strongly with increasing p_a. This is to be expected because at higher p_a more and longer loops occur and the repulsion ranges over larger distances. At very short distances the repulsion levels off. It is questionable

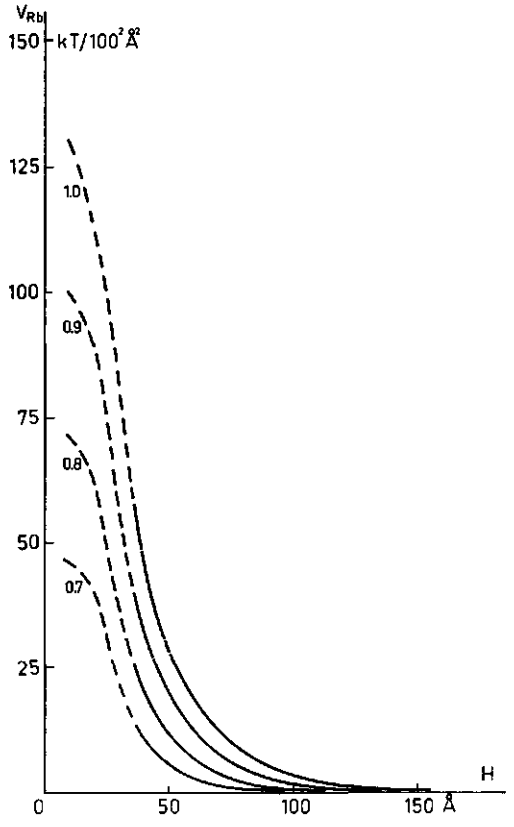

FIG. 6–7. The configurational repulsion free energy due to the adsorbed polymer layer as a function of the interparticle distance for four values of the amount adsorbed (p_a in mg/m²). l_s = 16.9 Å.

to what extent this is significant in view of the inaccuracy of v_{Rb} for one loop at short distances. Moreover, more and more very short loops contribute to V_{Rb} at short distances, and for a small number of elements per loop the statistical treatment given does not apply. Therefore not much importance should be attached to the calculated configurational repulsion free energy at very small distances.

Further implications of these results will be considered in 6.6.

6.5.3. *The osmotic repulsion between a covered and an uncovered surface*

In the preceding discussion only configurational statistics have been considered. Another mechanism which possibly could occur is an osmotic repulsion due to the increase in segment concentration between the two surfaces. For a situation in which the polymer is not able to form bridges this effect has been treated quantitatively by MEIER (1967) and HESSELINK (1971). In our case this effect will probably be very small. There are two reasons for this. Firstly, on account of the proposed adsorption mechanism the increase in segment con-

centration is only small: the segments which would be beyond H in the undisturbed situation are supposed to be adsorbed on the second surface. Consequently, these segments would not contribute to any osmotic repulsion.

Secondly, in so far as an accumulation of segments does occur its effect on the free energy of the system will only be small, because water is not a very good solvent for PVA. MEIER and HESSELINK showed that the osmotic repulsion is proportional to α^2-1 where α is the linear expansion factor. For a PVA molecule α does not differ very much from unity (see table 2–4). For an adsorbed loop having far fewer segments than a polymer molecule α is probably even smaller, so that the contribution of the osmotic term to the total free energy of interaction will be very small. Hence it will be neglected.

6.6. THE TOTAL CONTRIBUTION OF THE ADSORBED POLYMER TO THE INTERACTION FREE ENERGY

6.6.1. *The magnitude of the polymer contribution*

With the results obtained in the preceding sections the polymer contribution to the free energy of interaction between a covered and an uncovered particle can now be calculated.

In fig. 6–8 V_{pol} $(= V_{Aa} + V_{Rb})$ is plotted as a function of the interparticle distance for various values of the amount of adsorbed polymer. At very large distances V_{Aa} and V_{Rb} cancel out. In this region the fixation term of V_{Rb} is relatively important and the repulsion compensates the attractive V_{Aa}. With decreasing H a region is found where the attraction dominates because the relative contribution of the fixation term to V_{Rb} becomes smaller due to the disappearance of the longest loops; smaller loops enter in the bridging process and the entropy loss of these loops is relatively small (see also fig. 6–6). At distances around 40 Å a minimum occurs. With still smaller H the free energy rises sharply due to the very unfavourable configuration of the polymer. For very short interparticle distances anomalies seem to be present, indicated by the dashed parts of the curves (fig. 6–8). They are caused by the flattening of V_{Rb}, which is probably not significant as has already been indicated in 6.5.

The curves of fig. 6–8 have been calculated with $A_0' = 0.010$ Å^{-2}, which corresponds to a maximum coverage in the first layer on the second particle of about 36% of that on a surface after adsorption of a free polymer molecule. This value was chosen more or less arbitrarily. However, for $H > 75$ Å this assumption does not influence the shape of the curves; in that region the calculated free energy contribution due to the polymer may be expected to be reasonably reliable. Only at smaller distances does the value attributed to A_0' affect the magnitude of V_{pol}. Since it may be presumed, on physical grounds, that the particles

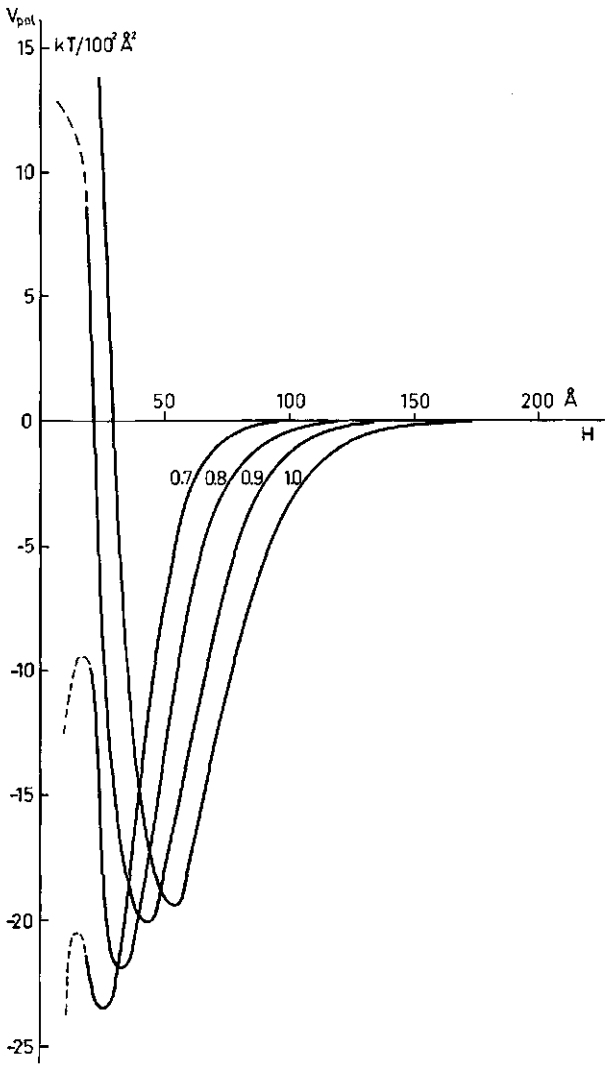

FIG. 6–8. The polymer contribution to the total free energy of interaction between a covered and an uncovered particle as a function of the interparticle distance.
The value of the amount of adsorbed polymer (mg/m²) is given for each curve. $A_0' = 0.010$ Å^{-2}, $\varepsilon_a = 1$ kT, $l = 16.9$ Å.

cannot approach each other very closely due to the adsorbed layer, the value chosen for A_0' has to be of that order of magnitude so as to give a steep rise in V_{pol} at short distances. In that respect $A_0' = 0.010$ Å^{-2} seems satisfactory. The exact value of V_{pol} for short distances remains uncertain.

From the curves given in fig. 6–8 it can be seen that flocculation by adsorbed polymer only will occur provided the double layer repulsion vanishes at large distances. The minimum around 40 Å is probably deep enough to cause irreversible flocculation even if at those distances double layer repulsion is present. This will be discussed further in 6.7.

The influence of p_a, the amount adsorbed, is in accordance with expectation. With increasing p_a the curves shift outwards due to the thicker layer: the net attraction starts at larger distances and the distance corresponding to the minimum becomes larger.

From a comparison of fig. 6–8 with the viscosimetric thickness as a function of p_a (fig. 4–4) it can be seen that at interparticle distances of about twice the viscosimetric thickness the attraction due to the polymer already amounts to approximately 1 $kT/100^2$ Å^2 (i.e. several kT per pair of particles, cf. 6.1.). This is caused by the few very long loops. Thus it follows that the effective range of V_{pol} is much more than the viscosimetric thickness.

Summarising, the polymer contribution to the free energy of interaction between a covered and an uncovered particle as given in fig. 6–8 can presumably give a reasonable explanation of the flocculation, although the exact value of this contribution, especially for short interparticle distances, is not unambiguous.

Before the total interaction free energy will be discussed (6.7.) some considerations will be made about the time-scale of the particle approach and its consequences for V_{pol}.

6.6.2. *The time-scale of the approach of two particles*

In the foregoing discussion it was tacitly assumed that the process of adsorption on the second particle and reconfiguration of the non-adsorbed parts of the polymer can take place within the time-scale of the Brownian encounter of two particles. The validity of this assumption needs to be examined. A analogous problem is the assumption of constant potential in the DLVO theory. FRENS (1968) showed that the desorption of ions, necessary to maintain a constant potential, takes more time than the collision process, so that the assumption of constant surface charge would be better (see also 6.3.2.).

For a situation in which the polymer does not adsorb on the second particle HESSELINK (1971a) concluded that the reconfiguration of loops is sufficiently fast to occur within the time of approach of two particles. The same will probably apply for the reconfiguration of bridges, so that for the configurational part of the free energy of interaction the assumption mentioned above is valid.

The rearrangement of polymer on a surface, which involves adsorption and desorption of segments, is a much slower process, as was shown also in 3.3. It may be expected that this rearrangement cannot take place within the collision time. HESSELINK concluded for the volume restriction that the loop size distribution on the approaching particles, covered by polymer, remains essentially unaltered during the time of Brownian encounter.

For flocculation rearrangements necessarily take place, since adsorption must occur for bridging. Although the rearrangements are slow it its probable that

the first segments adsorb very quickly. Since it is observed that flocculation does occur it must be concluded that indeed this first adsorption process is very fast and can occur within the time of encounter. Thus again it can be concluded that for large distances the treatment suggested does apply. As more segments become adsorbed, the diffusion process is no longer the controlling influence because the particles are now held in a potential energy well. This should allow sufficient time for any rearrangements. Such effects could perhaps show up in ageing effects of sol-polymer flocs.

However, in 6.5.2. only rearrangements occurring on the second surface have been considered, including mainly the adsorption of runs of segments on an essentially uncovered surface, at least for not too short separations. It seems likely that this adsorption is faster than the change of the loop size distribution on the first surface, so that in the early stages of the flocculation process only a slight rearrangement on the first surface will take place. After some time certainly a redistribution of polymer over the two particles, and perhaps over other particles constituting the floc will occur. However, this redistribution will not play a role in the initial stages of flocculation.

In conclusion, it may be stated that for the initial flocculation the free energy of interaction due to the polymer can be described with the equations given in 6.4. and 6.5. and the curves of fig. 6–8. This approximate treatment will fit better at larger distances than at smaller distances; in the latter case the suggested dependence of V_{pol} on the interparticle distance may be expected to be correct only in broad outline.

6.7. The total free energy of interaction between a covered and an uncovered particle

In the preceding sections the components of the free energy of interaction have been evaluated. By adding these components the total interaction free energy is obtained. In this section these results will be given and compared with the experimental observations of the flocculation.

6.7.1. *The relative magnitudes of the various interaction energy components*

In fig. 6–9 the components of the interaction free energy are plotted as a function of the interparticle distance. The units used for these components are, as in the previous figures of this chapter, kT per 100^2 Å^2.

The van der Waals attraction free energy was calculated with $A_{12} = 2.5 \cdot 10^{-13}$ ergs (6.2.). The electrostatic double layer repulsion free energy is given for the three salts used in most of the flocculation experiments at concentrations corresponding roughly to the critical flocculation concentrations measured for

a flocculation time of 1 hour (see fig. 5–8). The curves given are interpolated from the tables of VERWEY and OVERBEEK (6.3.2.) with STERN potentials of –90, –75 and –60 mV for KNO_3, $Ca(NO_3)_2$ and $La(NO_3)_3$, respectively (6.3.1.). Finally, the polymer contribution to the interaction free energy was taken from fig. 6–8, for $p_a = 0.9$ mg/m^2. This value of p_a (i.e. the adsorbed amount in mg PVA/m^2 of AgI) corresponds roughly to the optimal value for p_1, 2.5 mg/mmole (i.e. the added amount of polymer). It should be remembered that 1 mmole of AgI corresponds to an area of 2.58 m^2 (3.3.1.).

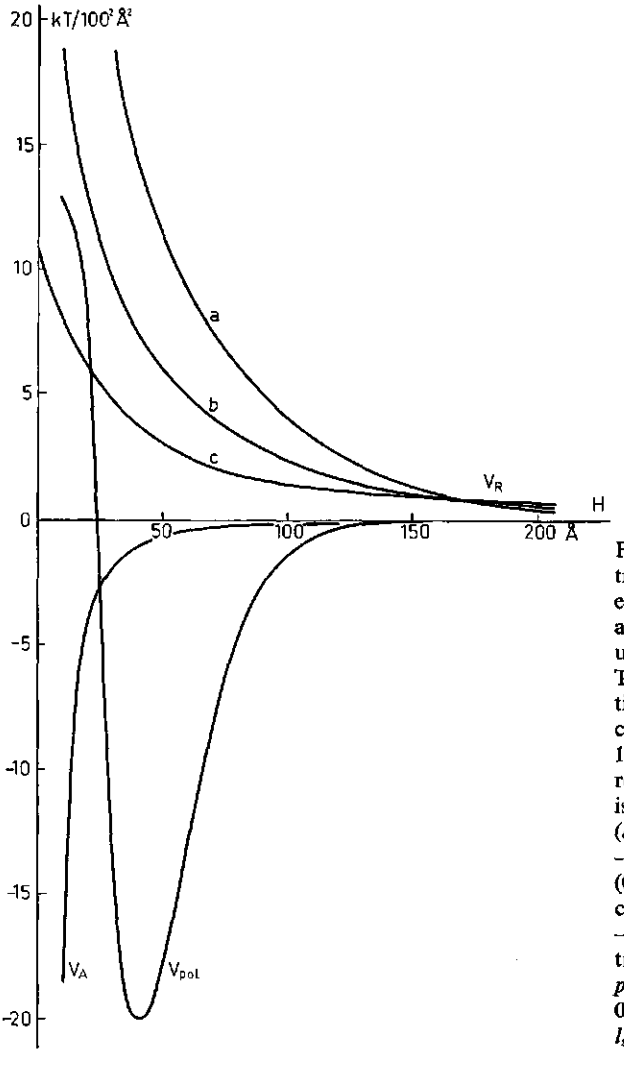

FIG. 6–9. The various contributions to the total free energy of interaction between a polymer covered and an uncovered particle.
The VAN DER WAALS interaction free energy (V_A) was calculated with $A_{12} = 2.5 \cdot 10^{-13}$ ergs. The double layer repulsion free energy (V_R) is presented for a. KNO_3 ($c_s = 5$ mmoles/l, $\psi_d = -90$ mV), b. $Ca(NO_3)_2$ (0.5 mmole/l, –75 mV) and c. $La(NO_3)_3$ (0.05 mmole/l, –60 mV). The polymer contribution (V_{pol}) is given for $p_a = 0.9$ mg/m^2, $A'_0 = 0.010$ Å^{-2}, $\varepsilon_a = 1\ kT$ and $l_s = 16.9$ Å.

It can be seen from fig. 6–9 that, over the whole range of H, V_A is small in comparison to the other contributions. Even at very small distances, where V_A becomes strongly negative, V_A is dominated by the combined action of V_R and V_{pol} so the primary minimum of the DLVO theory no longer exists. This was already predicted in 5.1.4.

In contradistinction to V_A, V_R still plays a significant role in flocculation by polymers. For small H, V_R and V_{pol} co-operate in the repulsion, at larger distances the attraction term of V_{pol} predominates to give a deep minimum, and for distances larger than about twice the layer thickness (see 6.6.1.) the total interaction free energy is determined only by the double layer repulsion. Hence, the salt concentration remains a very important parameter because only when the repulsion at very large distances has disappeared, i.e. at relatively high salt concentrations, can the polymer layer exert any influence. Thus indeed the function of the salt is to reduce the distance of closest approach to about twice the layer thickness; only then is the polymer able to bridge the two particles and to bring about flocculation of the sol. This will be further discussed in 6.7.2.

In this connection is may also be expected that the amounts of electrolytes with ions of different valencies, that are needed for flocculation, are such as to give a similar repulsion free energy at large distances. This point will be considered in 6.7.3.

6.7.2. *The total interaction free energy as a function of the salt concentration*

The total free energy of interaction for several concentrations of KNO_3 ($\psi_d = -90$ mV) is presented in fig. 6–10. The shape of the curves follows from the discussion in 6.7.1.

At low salt concentrations there is an appreciable repulsion at large distances, prohibiting flocculation. With increasing salt concentration this repulsion decreases until the maximum in V_t at large H vanishes; then fast flocculation can take place. The KNO_3 concentration at which this occurs is about 15 mmoles/l. This can also be read from fig. 6–12. In this figure the height of the maximum is plotted as a function of c_s for KNO_3, $Ca(NO_3)_2$ and $La(NO_3)_3$. We shall return to this figure in 6.7.3.

The concentration at which the maximum disappears agrees well with the salt concentration at which the initial rate of flocculation attains its maximum (fig. 5–14). This is an indication that the theory given is essentially correct.

The minimum (fig. 6–10) is sufficiently deep for irreversible flocculation. Although some incertainty exists about the exact value of V_{pol} at distances smaller than 75 Å, the minimum may be expected to be of the order 10 kT/100^2 Å^2 deep; this would correspond with several tens of kT per pair of particles. The separation between two neighbouring particles in a floc is initially about 50 Å; this could be changed, however, if after some time rearrangements

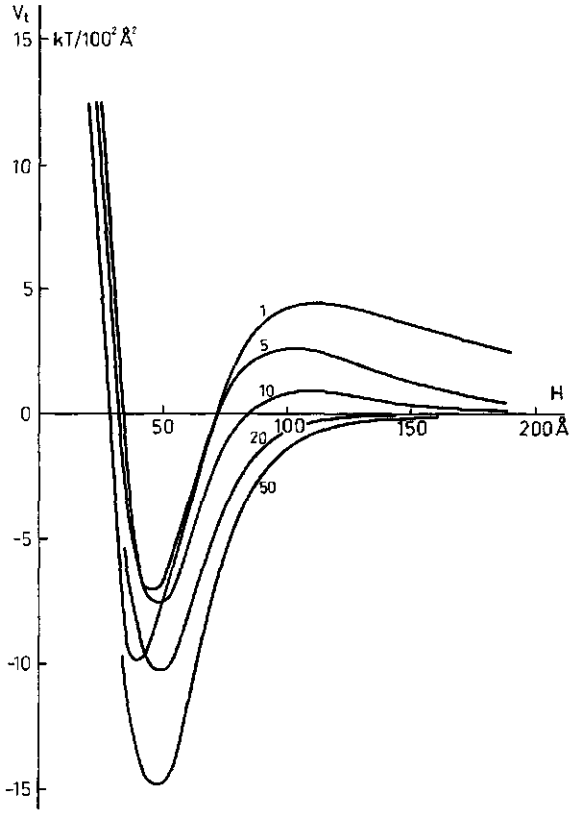

FIG. 6–10. The total free energy of interaction between a covered and an uncovered particle in the presence of several concentrations of KNO_3 (mmoles/1). $\psi_d = -90$ mV, $p_a = 0.9$ mg/m², $A'_0 = 0.010$ Å^{-2}, $\varepsilon_a = 1\ kT$ and $l_s = 16.9$ Å.

of the polymer on the first surface occur (6.6.2.).

With increasing salt concentration the depth of the minimum first decreases, passes through a minimum at about 5 mmoles of KNO_3/l and increases again with still higher c_s. This anomaly is a consequence of the way in which V_R depends on the salt concentration: with increasing c_s the repulsion increases at short distances but decreases at larger distances (see fig. 6–1). If the minimum in V_t is situated in the range of distances where V_R increases with c_s, as is the case for low salt concentrations, this minimum becomes less deep with increasing c_s. The repulsion decreases with higher values of c_s at distances around the minimum in V_t and then the depth of the minimum increases with salt concentration. However, these irregularities are of no consequence in the explanation of flocculation: in all the cases the minimum is deep enough for irreversible flocculation. Moreover, these anomalies occur only if the flat geometry is adopted: from eq. (6–4) it follows that the repulsion free energy for spheres decreases with increasing salt concentration at any distance.

Summarising, the free energy of interaction between a covered and an uncover-

ed particle, obtained by addition of V_A, V_R and V_{pol} gives an adequate description of the flocculation. Without causing any change in the general trends the VAN DER WAALS contribution, V_A, could well be left out. The stability of a colloidal system against flocculation is determined mainly by the double layer repulsion at large distances.

6.7.3. *The effect of the valency of the counterions on the interaction free energy*

In fig. 6–11 the interaction free energy is given in the presence of KNO_3, $Ca(NO_3)_2$ and $La(NO_3)_3$ at concentrations of 5, 0.5 and 0.05 mmoles/l, respectively. These concentrations correspond roughly with the critical flocculation concentrations measured after a flocculation time of 1 hour (fig. 5–8).

The shape of the curves is essentially the same for all valencies. The depth of the minimum increases with increasing valency of the counterions, suggesting somewhat stronger flocs in the presence of high-valent ions. The height of the maximum is greatest when KNO_3 is the added electrolyte; in the presence of $La(NO_3)_3$ the maximum is much lower.

As the concentrations chosen for the curves in fig. 6–11 apply to conditions

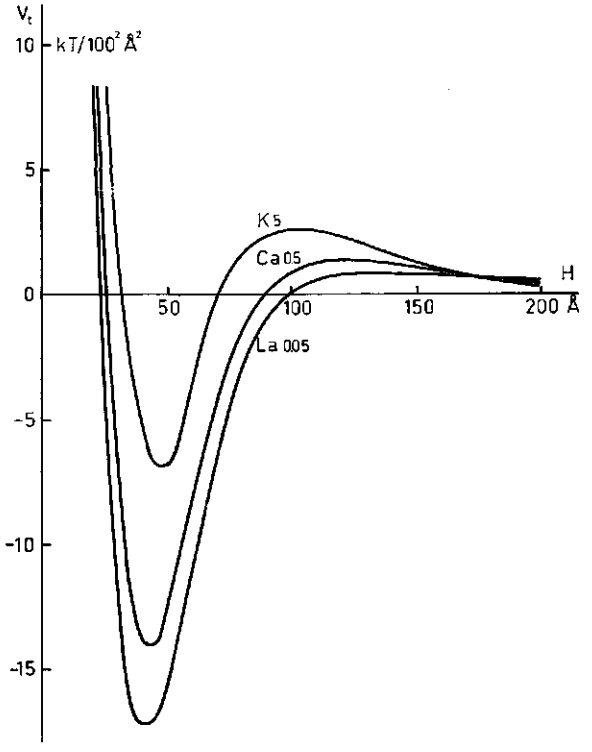

FIG. 6–11. The total free energy of interaction in the presence of three salts. The salt concentrations are given in mmoles/1. The values of ψ_d are taken as –90, –75 and –60 mV in the presence of KNO_3, $Ca(NO_3)_2$ and $La(NO_3)_3$, respectively. $p_a = 0.9$ mg/m², $A'_0 = 0.010$ Å^{-2}, $\varepsilon_a = 1\ kT$ and $l_s = 16.9$ Å.

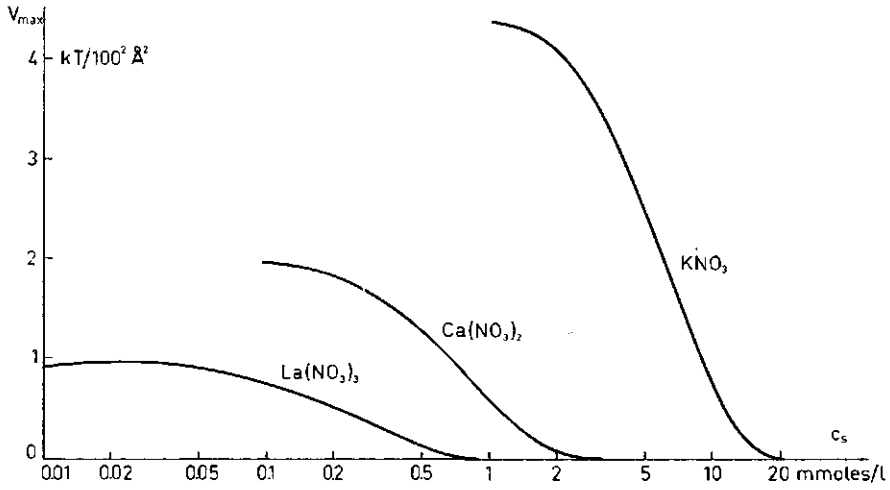

FIG. 6–12. The height of the maximum on the free energy of interaction curve as a function of the salt concentration. $\psi_d = -90$, -75 and -60 mV for KNO_3, $Ca(NO_3)_2$ and $La(NO_3)_3$, respectively; $p_a = 0.9$ mg/m².

under which an equal extent of flocculation is reached ($A_{rel} = 0.5$ at $t_2 = 1$ h) it would be expected that the maxima would be of comparable height. This appears not to be the case. Moreover, the maximum for KNO_3 (2.5 $kT/100^2$ Å^2 or at least 10 kT per pair of particles) seems to be rather high; it is hardly imaginable that after one hour half of the material is flocculated when the 'activation free energy' is so high. The possible reasons for this will be discussed below.

In fig. 6–12 the height of the maximum (V_{max}) is given as a function of c_s. As is to be expected V_{max} decreases with increasing c_s until, for high c_s, the maximum vanishes. The nearly horizontal parts at the left of the curves in fig. 6–12 are again due to the irregularities of V_R at low c_s, as discussed in 6.7.2. At salt concentrations corresponding to the steeper parts of the curves, V_R decreases with c_s at distances around 100 Å. At lower c_s, V_R increases, resulting in a maximum in V_{max} as a function of the salt concentration (see also fig. 6–1).

The salt concentrations at which the maximum disappears (fig. 6–12) agree, within the rather large experimental error, with those at which the maximum initial flocculation rate is attained (fig. 5–14) for KNO_3 and $Ca(NO_3)_2$. These are the salts for which a reasonable estimate for ψ_d is possible (see 6.3.1.). Agreement for $La(NO_3)_3$ could be obtained if a somewhat lower value for the STERN potential were taken than the arbitrarily assumed value of -60 mV. This would be quite reasonable in view of the strong specific adsorption of trivalent ions. Thus it can be concluded that the theoretical interaction free energy curves

are satisfactory in predicting the salt concentration at which the maximum flocculation rate is obtained for ions of different valencies.

However, as pointed out above, the magnitudes of the maxima differ markedly for the different salts at concentrations significantly less than those corresponding to fast flocculation. This can be seen also very clearly from fig. 6–12: the value for V_{max} in the presence of KNO_3 is much higher than that for the other salts. The question arises why, at equal experimental flocculation rates, the value of V_{max} is so different for the three valencies. Choosing other values for ψ_d would not improve the situation, because lower STERN potentials for AgI in the presence of $Ca(NO_3)_2$ and $La(NO_3)_3$ would only enhance the differences. Higher values for these STERN potentials are, on a physical basis, not reasonable. Moreover, even if the same value were to be assigned to all three STERN potentials, differences in V_{max} would remain.

In the preceding discussion it was supposed that only the value of V_{max} determines the flocculation rate. This is not necessarily the case.

For the coagulation of spherical particles FUCHS (1934) derived that the stability ratio W is given by:

$$W = 2R \int_{2R}^{\infty} e^{V_t'/kT} \frac{dH}{(H + 2R)^2} \tag{6-20}$$

where H is again the interparticle distance and V_t' the total free energy of interaction between two spherical particles of radius R.

From this equation it can be inferred that the rate of flocculation, which is determined by W, depends on the complete $V_t'(H)$ interaction free energy curve. If $V_{max}' >> kT$ and if the maximum is sharp, only the region in the neighbourhood of the maximum need be considered. By approximating this part of the exponential curve to a Gaussian curve with the same height and the same curvature in the maximum, REERINK and OVERBEEK (1954) derived that the stability ratio W, and thus the rate of coagulation is determined only by V_{max}'.

It is questionable to what extent this strategem is applicable to the flocculation by polymers. In the first place eq. (6–20) applies only if the flocculation process is completely reversible. Let us assume that this is the case for large distances. When only a small number of segments is adsorbed on the second particle complete desorption from this second surface may be possible within the time of encounter because of the reversibility of the individual segment adsorption.

Then an equation analogous to eq. (6–20) would be valid for two approaching flat plates. The approximation made by REERINK and OVERBEEK would be less justified in our case because of the small value of V_{max} and the very diffuse maximum, especially for $Ca(NO_3)_2$ and $La(NO_3)_3$ (see fig. 6–11). In the latter

cases also values of V_t far from the maximum would contribute to the integral of eq. (6–20), suggesting a more retarded flocculation in the presence of high-valent ions than predicted by the value of V_{max} alone. Thus, considering the complete curves instead of only the value of V_{max}, it is possible that the differences in the rates of flocculation for the three cases given in fig. 6–11 are less than appears at first sight. However, it still seems unlikely that the rates of flocculation predicted on these grounds from the total interaction free energy become equal, as is observed experimentally.

A more probable explanation for these discrepancies is found by considering the differences in the expression for the repulsion free energy for two plates, V_R, and that for two spheres, V_R'. From the approximate equations (6–3) and (6–4) it follows that the ratio between the repulsion free energy for two spheres of radius R, V_R', and that for two flat plates of area O, $V_R . O$, is given by:

$$V_R'/V_R O = R/\kappa O \tag{6-21}$$

This ratio depends on the salt concentration and valency through the reciprocal DEBIJE-length, κ. If this ratio between the repulsion free energies in the presence of $La(NO_3)_3$ is set equal to y, then it follows, assuming again that the formulae for symmetrical electrolytes may be applied:

$$(V_R'/V_R O)_{z=3} = y \tag{6-22a}$$

$$(V_R'/V_R O)_{z=2} = y \,.\, \kappa(z=3)/\kappa(z=2) = 0.47\, y \tag{6-22b}$$

$$(V_R'/V_R O)_{z=1} = y \,.\, \kappa(z=3)/\kappa(z=1) = 0.30\, y \tag{6-22c}$$

These figures have been calculated for a ratio of 100 : 10 : 1 between the concentrations of univalent, bivalent and trivalent ions, respectively. For 0.05 mmoles/l of $La(NO_3)_3$ y would be unity if the 'equivalent flat area' of a sphere of 500 Å radius were 270^2 Å^2. For this value of O all the values given for the free energy of interaction hitherto in the figures of this chapter ($kT/100^2$ Å^2) should be multiplied by 7.3 to give the free energy of two particles (if the same 'equivalent flat area' were to apply for any type of interaction).

From the data given in eq. (6–22) it would seem that, if the spherical geometry were chosen, the values of V_{max}' would become roughly equal, because the other contributions to V_t' (V_A' and V_{pol}') are independent of the salt concentration and because the shape of the $V_t'(H)$ curve will be essentially the same as that of the $V_t(H)$ curve. This would agree with the observed equal flocculation rates. The agreement would become even better if the STERN potential for AgI in the presence of $La(NO_3)_3$ were to be taken to be somewhat lower, as discussed above. Moreover, the relatively high value of the maximum in the interaction

energy in the presence of KNO_3 presumably would be lowered to a more reasonable value, agreeing better with the rather high flocculation rate observed. Finally, as the repulsion for spherical particles decreases more strongly with c_s than that for flat plates (compare eqs. (6–3) and (6–4)), the application of the theory for spherical particles would be more in accordance with the observed very steep increase of the extent of flocculation with increasing c_s around the critical flocculation concentration (see fig. 5–8).

This change-over to the spherical geometry will also effect the concentrations at which the maximum in V_t vanishes and where fast flocculation sets in. In view of the rather large experimental error in these concentrations (see fig. 5–14) the predictions from a treatment for spherical particles will probably be consistent with experiment as well.

Thus it would appear that the dependence of the flocculation behaviour on the valency of the electrolyte could be well explained by using the formulae for spherical particles. Regrettedly this is not possible as yet, because the expressions for V'_{Rb} and V'_{Aa} for spheres are not known.

In conclusion, the theory given for the flocculation by a combined action of the polymer contribution and the double layer repulsion is satisfactory in explaining the effect of electrolytes with respect to the value of the critical flocculation concentration for ions of different valencies. The salt concentrations at which the flocculation rate attains its maximum value are predicted reasonably well; experimental observations in slowly flocculating systems are more in line with the results to be expected for spherical particles than with those obtained for flat plates. Unfortunately, a detailed knowledge of the polymer contribution in the former case is not available as yet.

6.7.4. *The effect of the amount of polymer adsorbed on the first particle*

In Ch. 5. measurements on the amount of salt needed for flocculation as a function of the polymer dosage to the first portion of sol were presented (see fig. 5–10). These experimental results can be compared with the theoretical predictions from the interaction energy curves for different values of p_a.

In fig. 6–13 these curves are plotted for a salt concentration of 10 mmoles/l of KNO_3. It can be seen that with increasing p_a the value of V_{max} decreases and the distance at which this maximum occurs increases. This is due to the fact that, as the loops become longer, the double layer repulsion at larger distances is compensated more effectively by V_{pol}. At constant salt concentration the flocculation efficiency increases with increasing amount of adsorbed polymer, in agreement with the experimental observations. Consequently, less salt is needed to get the same extent of flocculation when the polymer layer becomes thicker. From a comparison of fig. 6–13 with fig. 4–4 it follows that the maximum is situated at an interparticle distance which is roughly twice the viscosimetric

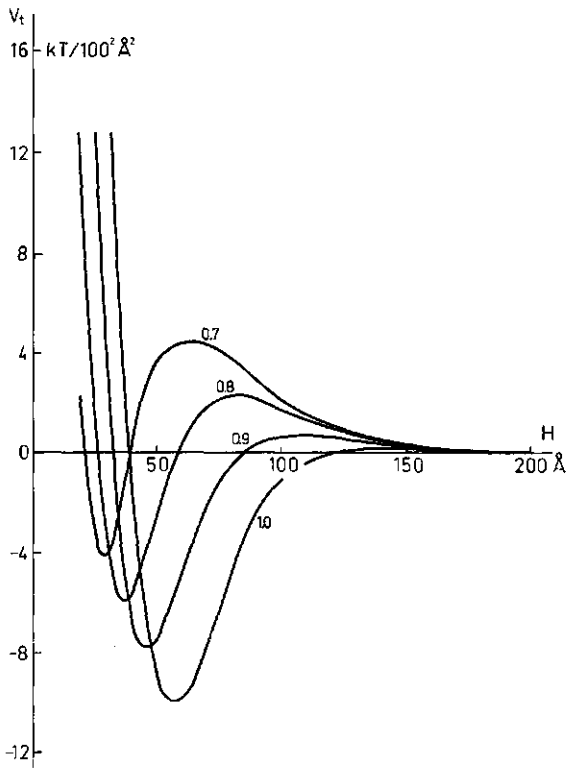

FIG. 6–13. The total interaction free energy at several amounts of adsorbed polymer(p_a in mg/m^2). KNO_3, $c_s = 10$ mmoles/l, $\psi_d = -90$ mV; $A'_0 = 0.010$ Å^{-2}, $\varepsilon_a = 1\ kT$ and $l_s = 16.9$ Å.

layer thickness. Thus again it follows that the salt concentration and valency must be high enough as to eliminate the double layer repulsion at distances of about twice the layer thickness.

As is to be expected the minimum at short distances becomes deeper with increasing p_a because more segments adsorb on the second surface, resulting in a higher adsorption attraction. As the configurational repulsion at short distances increases when more polymer is present the minimum shifts outwards.

It should be noted that the curve for $p_a = 1.0$ mg/m^2 does not apply to the PVA-AgI system. At this value of p_a too much polymer is left in solution and the second surface is partly covered before bridging can take place; this is not accounted for in the theory given. Therefore, only the curves for $p_a \leqslant 0.9$ mg/m^2 can be used for a comparison with the experiments.

In fig. 6–14, V_{max} is plotted as a function of the salt concentration for the same values of p_a as in fig. 6–13. In principle, it is possible to obtain from fig. 6–14 theoretically expected values for the critical concentration, $c_{\frac{1}{2}}$, if it is assumed that only the value of V_{max} determines the rate of flocculation. However, as pointed out in 6.7.3. the maxima for KNO_3 are too high as a

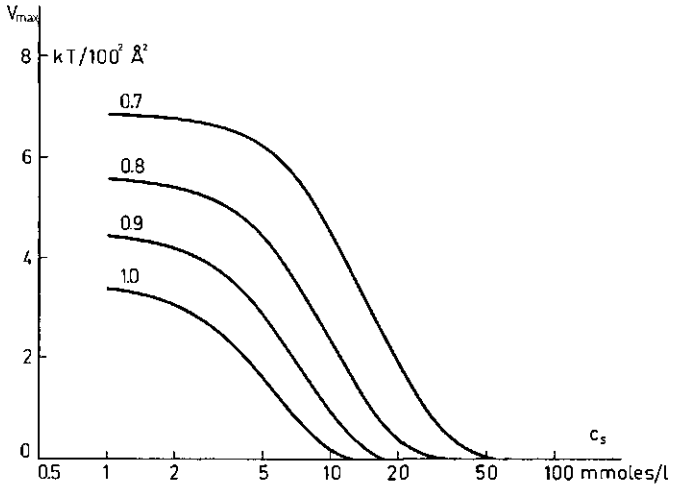

FIG. 6–14. The height of the maximum in the free energy of interaction curve as a function of the concentration of KNO_3 ($\psi_d = -90$ mV) at several amounts adsorbed (p_a in mg/m²).

consequence of the use of the flat geometry, so the theoretical values for $c_{\frac{1}{2}}$ would be also rather doubtful. For spherical particles the repulsion free energy decreases more strongly with c_s than for flat plates, so the slopes of the curves of fig. 6–14 would be greater for the spherical geometry.

For these reasons not much importance should be attached to the quantitative calculation of $c_{\frac{1}{2}}$ based on the approach for flat particles. Again it would appear that a theory applicable to spherical particles would give better agreement with the experimental findings than the one for flat plates.

It may be stated, however, that the theoretical interaction free energy curves can explain qualitatively the experimental observations with respect to the influence of the amount of adsorbed polymer on the flocculation. A thicker layer is more efficient in the flocculation because the double layer repulsion can be overcome at larger distances, thus diminishing the distance of closest approach.

6.7.5. *The influence of the molecular weight and hydrophobicity of the polymer*

As discussed already in Ch. 4., the model used for the segment density distribution in the adsorbed layer is too crude to account for the influence of molecular weight. It was assumed that the segment density distribution depends only on the amount adsorbed; thus at equal p_a the layer thickness was supposed to be independent of M. This is of course an approximation. From the flocculation experiments it appears that the extent of flocculation at a given salt con-

centration, and also the critical flocculation concentration depend only slightly on the molecular weight. From the protection measurements (4.1.) the differences between the various molecular weights seemed to be somewhat more pronounced. Unfortunately, no direct measurements of the layer thickness as a function of molecular weight are available as yet.

Whatever the dependence, it is unlikely that the model used for the segment distribution in the adsorbed layer and, consequently, the interaction free energy reflect differences between samples of different molecular weight at a given amount adsorbed. Of course, the theory as given *does* incorporate differences due to the higher adsorption levels for larger molecules.

Nevertheless, from the general form of the interaction energy curves it may be deduced that, if a segment density distribution accounting for differences in molecular weight at given amount adsorbed were to be used, these differences would also show up in the interaction energy. If the layer thickness at given p_a were to increase with M because of the possibility of longer loops in the adsorbed layer, it might be expected that the polymer contribution to the free energy of interaction would range over larger distances and thus the flocculation would be improved. In this way the resulting increase in flocculation with higher molecular weight is, at least qualitatively, in agreement with the picture presented. More quantitative predictions could be made only with a more refined segment density distribution.

With respect to the hydrophobicity of the polymer, somewhat greater experimental differences have been found. However, in this case the experimental information is too scarce to evaluate the segment density distribution. In the method discussed the experimental thickness is used to evaluate the HOEVE parameter K_H (4.5.2.). This thickness is not available for PVA 88. As K_H decreases with decreasing flexibility of the chain (HOEVE 1965, 1970) a lower value for K_H might be expected for PVA 88 than for PVA 98.5, resulting in a larger layer thickness. According to the theory given in this chapter this would lead to both better protecting and flocculating power, as is observed experimentally.

Thus we may conclude that the effects of molecular weight and hydrophobicity of the polymer are qualitatively in accord with the theoretical expectations. A more detailed consideration is not yet possible, partly due to the approximate character of the theoretical model used, and partly because the experimental information is too scanty.

6.8. CONCLUSIONS

The free energy of interaction between a covered and an uncovered particle has been considered, assuming the surfaces to be flat. The classical free energy

contributions, viz. the VAN DER WAALS attraction free energy, V_A, and the double layer repulsion free energy, V_R, could be evaluated for the PVA-AgI system by making reasonable estimations for the HAMAKER constant and the STERN potential. In addition, an extra contribution due to the adsorbed polymer, V_{pol}, occurs. This contribution was split up in two terms, the adsorption attraction free energy, V_{Aa}, and the configurational repulsion free energy due to the bridging, V_{Rb}. It was shown that an osmotic contribution to the free energy of interaction which may occur is negligible for the PVA-AgI system.

V_{Aa} was considered to be proportional to the number of segments adsorbed on the second (originally uncovered) particle. For large distances this number of adsorbed segments as a function of the interparticle distance H was assumed to be equal to the number of segments which would be beyond H in the undisturbed distribution, in the absence of the second particle. For shorter distances V_{Aa} is overestimated on the basis of this assumption because the second surface becomes more and more covered; this has been corrected for using a semi-empirical formula.

The configurational repulsion arises from the smaller number of possible configurations of a bridge in comparison to that of a free loop. For any interparticle distance the number of elements in the two bridges and in the train, formed from one loop, was estimated and by applying the theory of HESSELINK (1971a) the configurational repulsion due to one loop was obtained. By summing up the contributions from all loop sizes, with the help of the HOEVE loop size distribution, V_{Rb} was obtained.

Addition of V_{Aa} and V_{Rb} gives the polymer contribution, V_{pol}. Although, especially for short distances, the values of V_{pol} are not unambiguous, on account of the large number of assumptions and approximations made, the polymer contribution obtained in this way does explain satisfactorily the flocculation phenomena. At interparticle distances as large as twice the viscosimetric layer thickness there is, due to bridging, an appreciable attraction which increases with decreasing distance until at shorter distances a minimum occurs, followed by a repulsion at still shorter distances. This repulsion is caused by the very unfavourable configurational restrictions on the polymer.

The total energy of interaction between a covered and an uncovered particle, V_t, was obtained by addition of V_A, V_R and V_{pol}. The VAN DER WAALS attraction turned out to be of minor importance in comparison to the other terms. At large distances V_t is determined in the main by the double layer repulsion; at smaller distances V_{pol} dominates and a minimum in the free energy of interaction occurs, which is sufficiently deep for irreversible flocculation to occur. The function of the salt is to reduce the double layer repulsion at distances of about twice the viscosimetric thickness. At shorter distances any electrostatic repulsion is then dominated by the polymer contribution. Thus, in order to obtain effective

flocculation a partial compression of the double layer is sufficient, so that much less salt is needed for flocculation than for coagulation.

The salt concentrations at which flocculation occurs, and the relative amounts needed of electrolytes with ions of different valencies could be explained satisfactorily. The influence of the polymer dosage to the first portion of sol is also in accord with the theory given. In both cases it appeared that it would be worthwhile to extend the theory to spherical particles. With such a theory the experimental results would presumably agree even better with the theoretical predictions.

As stated already in Ch. 4. the model used for the segment density distribution in the adsorbed layer is too approximative to be able to distinguish between differences in the adsorbed layer for different molecular weights at a given amount adsorbed. With respect to the effect of the hydrophobicity of the polymer the experimental data are too scarce for an evaluation of the segment density distribution. However, qualitatively the experimental observations in these cases agree with the theory given for flocculation.

In conclusion, a picture has been developed for flocculation by polymers that is, at least semi-quantitatively, entirely satisfactory and that may serve as a basis for futher developments.

SUMMARY

The purpose of this study was to gain insight in the factors determining the stability of hydrophobic sols in the presence of polymers, with the emphasis on the destabilisation of sols by polymers and the role played by salts therein.

In chapter 1. the practical importance of polymer stabilisation and destabilisation is shown by several examples, a.o. in industrial applications, in water purification and soil structure improvement. Thereafter the choice of the PVA-AgI system as a model for this study was explained. PVA has a simple structure and is uncharged and its concentration in solution may be readily determined. This is important for adsorption measurements. AgI provides a good model for the dispersed phase: the properties of the electrical double layer on AgI in the presence of salts and low molecular weight organic substances have been investigated extensively and the specific surface area can be determined easily. Moreover, with a combination of PVA and AgI, one has the advantage of being able to acquire information on the properties of the first layer on the surface by a comparison with known data on the butanol-AgI and ethylene glycol-AgI systems.

The characterisation of the materials used is described in chapter 2. The specific surface area of AgI was determined by three independent methods. The results of these methods agreed well with each other. The average radius of the AgI particles turned out to be about 500 Å. From viscosimetric measurements on PVA solutions the molecular weights and configurational parameters of PVA, such as the radii of gyration, the length of a statistical chain element and the linear expansion factors were determined. In addition, it was shown that the PVA used is essentially uncharged.

In chapter 3. the measurement of the amount of PVA adsorbed per m^2 is treated. The adsorption isotherm shows a pronounced high affinity character. The maximum amount adsorbed is 1–1.5 mg/m^2, depending on the molecular weight and the degree of hydrolysis of the PVA. The maximum adsorption increases somewhat with increasing molecular weight; for PVA with 12% of acetate groups it is distinctly higher than for PVA which is nearly completely hydrolysed. At maximum adsorption one fourth of the segments at most can be in contact with the surface; the remaining parts of the molecule protrude into the solution in the form of loops and tails. From measurements of the adsorption as a function of time and from 'two-step' adsorption experiments it could be deduced that the adsorption of segments is reversible. However, desorption of whole polymer molecules is not measurable.

In chapter 4. measurements are described to obtain the layer thickness and

the coverage in the first layer on the surface by PVA. From protection measurements qualitative information was obtained about the layer thickness. The protective power appeared to be slightly dependent on the molecular weight and to depend somewhat more strongly on the degree of hydrolysis of the PVA. The thickness of the adsorbed layer was viscosimetrically determined as a function of the amount adsorbed. The maximum layer thickness is about 100 Å. By measuring the electrophoretic mobility of polymer covered particles the layer thickness was likewise estimated. These results are in good agreement with the viscosimetric results.

The coverage in the first layer on the surface was estimated from the shift of the point of zero charge and from the change in the surface charge on adsorption of polymer, in comparison with the same properties of AgI in the presence of butanol and ethylene glycol. A reasonable estimation for the percentage of the surface which is occupied by PVA turned out to be 70% for amounts adsorbed of more than half the maximum.

With the help of these data the distribution of segments in the adsorbed layer could be obtained. For amounts adsorbed between 0.5 and 1.0 mg/m^2 a HOEVE distribution applies. In the first layer on the surface the polymer volume fraction is about 70%. At a distance equal to the thickness of the first layer a discontinuity occurs, the volume fraction dropping to 56%, and in the remaining part of the adsorbed layer the segment distribution is exponential. If more than 1 mg/m^2 is adsorbed possible end effects occur: due to the presence of long tails at the ends of a polymer molecule the thickness increases more strongly with the amount adsorbed than predicted from the HOEVE distribution.

The model for the segment distribution is somewhat oversimplified: it appeared to be impossible to account for the differences between different molecular weights at a given amount adsorbed.

Results with respect to the flocculation of AgI by PVA have been given in chapter 5. Flocculation was found to be optimal if a special method is used for the mixing of PVA and AgI. Most efficient flocculation is obtained if a given volume of sol with uncovered particles is added to an equal volume of a sol with nearly completely covered particles. This phenomenon could be easily explained on the bridging model: flocculation occurs because loops of the adsorbed layer of one particle attach to the other. In this way a network of AgI particles interconnected by polymer bridges is formed. For the explanation of the efficiency of the way of mixing irreversibility of the adsorption of the polymer molecules is essential.

Another important condition for efficient flocculation is the presence of a small amount of electrolyte. On these grounds the flocculation should be referred to as sensitisation. The minimum salt concentrations which are needed for

flocculation are in the ratio of about 100 :10 :1 for salts with univalent, bivalent and trivalent counterions, respectively. Critical flocculation concentrations measured after a fixed time of flocculation were found to depend on the sol concentration. From measurements of the initial rate of flocculation, and from experiments in which the flocculation time was adjusted to the sol concentration, it was shown that this dependence on the salt concentration has a kinetic origin. The flocculation by bridging was found to be a bimolecular process.

The critical flocculation concentrations were found to depend only slightly on the molecular weight of the PVA. For a PVA with a higher acetate content the amount of electrolyte needed was found to be significantly lower.

In chapter 6. an attempt has been made to interpret the flocculation theoretically. To that order the free energy of interaction between a covered and an uncovered particle has been calculated. On account of the complicated nature of the problem only an approach for flat surfaces has been considered.

In addition to the VAN DER WAALS attraction and the double layer repulsion the contribution to the free energy of interaction due to the adsorbed polymer has to be calculated. This contribution was formally split up in two terms, the first being the adsorption attraction due to the gain in free energy on account of the adsorption of segments on the second particle. The second term is the configurational repulsion which is caused by the entropy loss if a loop becomes two bridges by the adsorption of the middle segments of the loop. The fundamental assumption used to evaluate these two terms is that the number of segments which, at a given interparticle separation H, adsorbs on the second particle equals the number of segments which, in the absence of the second particle, would lie beyond a distance H from the surface. Using the theories of HOEVE and HESSELINK and the distribution of segments derived in chapter 4. these two polymer contributions to the free energy of interaction could be obtained.

It was found that the VAN DER WAALS attraction is negligibly small in comparison to the other terms. The total free energy of interaction has the following characteristics. At small salt concentrations a maximum occurs at large distances due to the double layer repulsion, whilst at distances of some tens of Ångströms a minimum is present, sufficiently deep for irreversible flocculation. The function of salt is to suppress the maximum at large distances by partial compression of the double layer, so that the particles can approach each other to a distance corresponding to the minimum in the free energy. The system will then flocculate.

Although the magnitude of the polymer contribution, especially at small distances, is somewhat doubtful on account of various approximations made, the theory does give a good explanation for the amount of salt, with ions of different valencies, which is needed for flocculation. The theoretical predictions

with respect to the effect of the amount of adsorbed polymer agree also with the experimental observations. From this it follows that the theory is essentially correct. Indications were obtained that a theory which is applicable to spherical particles would agree even better with the experiments. The development of such a theory would be a promising next step.

In conclusion, this study firmly establishes the bridging model for flocculation by polymer. It appeared possible to interpret several aspects quantitatively. Especially the function of indifferent electrolytes emerged clearly.

ACKNOWLEDGEMENTS

This work was carried out in the laboratory for Physical and Colloid Chemistry of the Agricultural University, Wageningen. Many people have made valuable contributions in this study.

Mrs. W. de Kok-Bats assisted by making careful measurements in the adsorption and flocculation experiments.

Several parts of the work have been carried out by students. The author wishes to express in particular his thanks to Ir. A. Klapwijk for his help in evaluating the way of mixing in the flocculation studies, to Ir. J. T. C. Böhm for the measurements of the viscosimetric layer thickness and to Ir. B. J. M. Verduin for the viscosimetric experiments on polyvinyl alcohol solutions.

The kindness of Ir. L. K. Koopal for permission to use his data on the electrophoretic and double layer measurements is gratefully acknowledged.

The author is deeply indebted to Prof. Dr. J. Lyklema for the way in which his leadership and guidance in the laboratory creates such a pleasant and friendly atmosphere. Moreover, his stimulating interest in this work has been of great profit.

Many thanks are also due to all those working in the laboratory for their friendship and helpfulness.

The discussions with Dr. F. Th. Hesselink about the free energy of interaction between a covered and an uncovered particle are gratefully mentioned.

Dr. B. Vincent was kind enough to correct the English text of this thesis.

SAMENVATTING

Het doel van dit onderzoek was een inzicht te krijgen in de stabiliteit van hydrofobe solen in aanwezigheid van polymeren. De nadruk werd hierbij gelegd op de destabilisatie van solen met polymeren en de rol die hierbij gespeeld wordt door toegevoegde zouten.

In hoofdstuk 1. wordt aan de hand van enkele voorbeelden aangetoond hoe groot het praktische belang is van stabilisatie en destabilisatie van solen en suspensies door polymeren, o.a. in industriële toepassingen, bij de waterzuivering en bij de grondverbetering. Daarna wordt toegelicht waarom het PVA-AgI systeem als model voor dit onderzoek werd gekozen. PVA is een eenvoudig en ongeladen polymeer dat betrekkelijk gemakkelijk kwantitatief in oplossing te bepalen is. Dit laatste is van belang voor goede adsorptiemetingen. Het AgI-sol is ook een goed model : de eigenschappen van de electrische dubbellaag op AgI in aanwezigheid van zouten en laag-molekulaire organische stoffen zijn uitvoerig onderzocht en het specifiek oppervlak is goed te bepalen. Bovendien heeft de combinatie PVA-AgI het voordeel, dat door vergelijking met gegevens van de systemen butanol-AgI en ethyleenglycol-AgI informatie kan worden verkregen over de eigenschappen van de eerste polymeerlaag op het oppervlak.

De karakterisering van de gebruikte materialen wordt beschreven in hoofdstuk 2. Het specifiek oppervlak van AgI werd bepaald volgens drie onafhankelijke methoden. De uitkomsten hiervan stemden goed overeen. De gemiddelde straal van de AgI deeltjes bleek ongeveer 500 Å te bedragen. Via viscositeitsmetingen aan PVA oplossingen werden het molekuulgewicht en configuratieparameters van PVA, zoals de gyratiestraal, de lengte van een statistisch ketenelement en de lineaire expansiefactor bepaald. Bovendien werd aangetoond dat het gebruikte PVA vrijwel ongeladen is.

Hoofdstuk 3. behandelt de meting van de geadsorbeerde hoeveelheid PVA per m^2 AgI. De adsorptieisotherm vertoont een uitgesproken 'high-affinity' karakter. De maximaal te adsorberen hoeveelheid bedraagt, afhankelijk van het molekuulgewicht en de hydrolysegraad van het gebruikte PVA, 1–1,5 mg/m^2. De maximale adsorptie neemt enigszins toe met toenemend molekuulgewicht en is voor PVA met 12% acetaat-groepen duidelijk groter dan voor bijna volledig gehydrolyseerd PVA. Bij de maximale adsorptie kan hoogstens een kwart van de segmenten in contact zijn met het oppervlak; de rest steekt in de vorm van lussen de oplossing in. Uit adsorptiemetingen als functie van de tijd en uit 'twee-traps'-adsorptie kan afgeleid worden dat de adsorptie van segmenten reversibel is; er treedt echter geen meetbare desorptie van hele polymeermolekulen op.

In hoofdstuk 4. worden metingen beschreven om de laagdikte en de oppervlaktebezetting van PVA op AgI te bepalen. Kwalitatieve informatie met betrekking tot de laagdikte werd verkregen uit meting van de beschermende werking. De protectie is enigzins afhankelijk van het molekuulgewicht en iets sterker van de hydrolysegraad van PVA. Uit de viscositeitstoename van een sol waaraan PVA was toegevoegd werd de dikte van de geadsorbeerde laag als functie van de geadsorbeerde hoeveelheid bepaald. De maximale laagdikte bedraagt ongeveer 100 Å. Via metingen van de elektroforesesnelheid van met polymeer bedekte deeltjes werd eveneens een schatting gemaakt van de laagdikte. Deze resultaten zijn in goede overeenstemming met die uit de viscosimetrie.

De bezetting van de eerste laag op het oppervlak werd geschat uit de verschuiving van het ladingsnulpunt en uit de verandering van de oppervlaktelading door het geadsorbeerde polymeer in vergelijking met dezelfde eigenschappen van een AgI oppervlak in aanwezigheid van butanol en ethyleenglycol. Een redelijke schatting van het percentage bedekt oppervlak bleek 70% te zijn voor geadsorbeerde hoeveelheden groter dan de helft van de maximale waarde.

Met behulp van deze gegevens kon de distributie van segmenten in de geadsorbeerde laag verkregen worden. Voor geadsorbeerde hoeveelheden tussen 0,5 and 1,0 mg/m^2 geldt een HOEVE distributie. In de eerste laag op het oppervlak is de volumefractie aan polymeer ongeveer 70%. Op een afstand gelijk aan de dikte van de eerste laag treedt een discontinue verlaging op tot 56%, en in de rest van de geadsorbeerde laag daalt de volumefractie exponentieel als functie van de afstand tot het oppervlak. Als meer dan 1 mg/m^2 is geadsorbeerd treden mogelijk eindeffecten op: door de aanwezigheid van lange staarten aan de einden van een polymeermolekuul neemt de dikte sterker toe met de geadsorbeerde hoeveelheid dan volgens een HOEVE distributie mogelijk zou zijn.

Het model voor de segment distributie is enigszins ongenuanceerd: het bleek niet mogelijk om verschillen tussen verschillende molekuulgewichten bij gelijke geadsorbeerde hoeveelheden in de distributie te verdisconteren.

Resultaten met betrekking tot de vlokking van AgI met PVA worden gegeven in hoofdstuk 5. Het bleek dat de vlokking optimaal is indien een speciale methode van menging van PVA en AgI wordt gebruikt. De vlokking is het meest efficiënt wanneer gelijke volumina van sol met onbedekte deeltjes en sol met bijna volledig bedekte deeltjes worden gemengd. Dit verschijnsel kan verklaard worden uit het brugvormingsmechanisme: vlokking treedt op doordat perifere segmenten uit lussen van de geadsorbeerde laag van het ene deeltje adsorberen op het andere deeltje. Op deze wijze wordt een netwerk van AgI deeltjes, verbonden door polymeerbruggen, gevormd. Voor de verklaring van de mengmethode is de irreversibiliteit van de adsorptie van polymeermolekulen essentieel.

Een andere belangrijke voorwaarde voor efficiënte vlokking is de aanwezig-

heid van een geringe hoeveelheid elektrolyt. Op grond hiervan kan deze vlokking aangemerkt worden als sensibilisatie. De minimaal benodigde zout concentraties voor de vlokking verhouden zich ongeveer als 100:10:1 voor zouten met één-, twee- en driewaardige tegenionen. Kritische vlokkingsconcentraties, gemeten bij een constante beoordelingstijd, bleken afhankelijk te zijn van de solconcentratie. Via metingen van de initiële vloksnelheid en uit proeven met een aan de solconcentratie aangepaste beoordelingstijd kon aangetoond worden dat deze afhankelijkheid van de solconcentratie een kinetische oorzaak heeft. De vlokking door brugvorming is een bimolekulair proces.

De gemeten kritische vlokkingsconcentratie bleek slechts weinig af te hangen van het molekuulgewicht; bij PVA met een hoger acetaatgehalte bleek de benodigde hoeveelheid elektrolyt duidelijk lager te zijn.

In hoofdstuk 6. wordt een poging tot theoretische interpretatie gedaan. Daartoe werd de vrije energie van de interactie tussen een bedekt en een onbedekt deeltje berekend. In verband met de ingewikkeldheid van deze materie werd de procedure vooralsnog beperkt tot vlakke oppervlakken. Naast de VAN DER WAALS-attractie en de dubbellaagrepulsie moet daartoe de bijdrage tengevolge van het geadsorbeerde polymeer berekend worden. Deze bijdrage werd formeel opgesplitst in twee termen, nl. de adsorptie-attractie ten gevolge van de vrije energiewinst door adsorptie van segmenten op het tweede deeltje, en de configuratie-repulsie, veroorzaakt door het entropieverlies als een lus, door adsorptie van de middelste segmenten, overgaat in twee bruggen. De fundamentele aanname was, dat het aantal segmenten, dat adsorbeert op het tweede deeltje bij een zekere deeltjesafstand H, gelijk is aan het aantal segmenten dat bij afwezigheid van het tweede deeltje zich zou bevinden buiten de afstand H. Door gebruik te maken van theorieën van HOEVE en HESSELINK en van de segmentdistributie, berekend in hoofdstuk 4., kon de polymeerbijdrage tot de wisselwerkings vrije energie verkregen worden.

Het blijkt dat de VAN DER WAALS-attractie verwaarloosbaar klein is in vergelijking met de andere termen. De totale interactie-energie wordt gekenmerkt door het volgende verloop: bij kleine zoutconcentraties is op grote onderlinge afstand van de deeltjes een maximum aanwezig tengevolge van de dubbellaagrepulsie, terwijl zich op afstanden van enkele tientallen Å een minimum bevindt, dat voldoende diep is voor irreversibele vlokking. De functie van zout bij de vlokking is de verlaging van het maximum op grote afstand door gedeeltelijk indrukken van de dubbellaag, zodat de deeltjes elkaar kunnen naderen tot de afstand die overeenkomt met de minimale vrije energie. Dan is het systeem gevlokt.

Hoewel door diverse benaderingen de precieze grootte van de polymeerbijdrage tot de vrije energie enigszins onzeker is, vooral voor kleine deeltjesafstanden, geeft de theorie een goede verklaring voor de hoeveelheden zout met

ionen van verschillende valentie, die nodig zijn voor de vlokking. Ook de theoretische voorspellingen met betrekking tot het effect van de geadsorbeerde hoeveelheid polymeer komen goed overeen met de experimentele waarnemingen. Hieruit volgt, dat de theorie in principe correct moet zijn. Er zijn aanwijzingen dat een theorie die toepasbaar is voor bolvormige deeltjes een nog betere aansluiting met de experimenten zou geven. Uitbreiding van de theorie in dit opzicht lijkt daarom zinvol.

Als conclusie kan gesteld worden, dat uit dit onderzoek het mechanisme van de vlokking door polymeren, en met name het brugvormingsmodel en de functie van zout duidelijk naar voren gekomen zijn. De ontwikkelde theorie verklaart, zeker in grote lijnen, deze verschijnselen ook kwantitatief.

REFERENCES

ANONYMOUS (1969) Anal. Chem. **41**, 2139

AUDSLEY, A. (1965) Mineral Processing Information Note no 5 (Warren Spring Laboratory, Stevenage, Herts, G.B.)

BASF-brochure (1967) Klären von Trüben, Badische Anilin und Soda-Fabrik, Ludwigshafen, Germany

BERESFORD, J. (1967) J. Oil Colour Chem. Ass. **50**, 594

BERESNIEWICS, A. (1959) J. Polym. Sci. **39**, 63

BIANCHI, E., CONIO, G. and CIFFERI, A. (1967) J. Phys. Chem. **71**, 4563

BOOTH, F. (1950) Proc. Roy. Soc. A **203**, 514

BOER, J. H. DE (1936) Trans. Faraday Soc. **32**, 21

BRANDRUP, J. and IMMERGUT, E. H. (1965) Polymer Handbook, Interscience Publ., New York

BRUYN, H. DE (1942) Rec. Trav. Chim. **61**, 5, 12

BIJSTERBOSCH, B. H. (1965) Thesis, State University Utrecht, Netherlands

BIJSTERBOSCH, B. H. and LYKLEMA, J. (1965) J. Colloid Sci. **20**, 665

CHENE, M., MARTIN-BORRET, O. and CLERY, M. (1966) La Papeterie **3**, 273

CLAYFIELD, E. J. and LUMB, E. C. (1966) J. Colloid Interface Sci. **22**, 269

CLAYFIELD, E. J. and LUMB, E. C. (1968) Macromolecules **1**, 133

CONWAY, B. E. and DOBRY-DUCLAUX, A. (1960) in: Rheology, Theory and Application, F. R. Eirich Ed. Vol. 3, Ch. 3, Academic Press, New York

DAMASKIN, B. B., SURVILA, A. A. and RYBALKA, L. E. (1967) Elektrokhimya **3**, 146

DERYAGIN, B. V. and LANDAU, L. D. (1941) Acta Physico Chim. U.R.S.S. **14**, 633

DEVEREUX, O. F. and DE BRUYN, P. L. (1963) Interaction of Plane-Parallel Double Layers, MIT-press, Cambridge

DIEU, H. A. (1954) J. Polym. Sci. **12**, 497

DOROSZKOWSKI, A. and LAMBOURNE, R. (1968) J. Colloid Interface Sci. **26**, 214

EINSTEIN, A. (1906) Ann. Physik **19**, 289

FINCH, C. A. (1968) Properties and Applications of Polyvinyl Alcohol, S.C.I. Monograph no **30**, Soc. Chem. Ind., London

FISCHER, E. W. (1958) Kolloid-Z. **160**, 120

FLASCHKA, H. (1953) Microchemie **40**, 21

FLASCHKA, H. and HUDITZ, F. (1952/1953) Z. Anal. Chem. **137**, 104

FLEER, G. J. and LYKLEMA, J. (1968) Vth Intern. Congr. Surface Activity, Barcelona; Proceedings Vol. 2, 247 (1969)

FLEER, G. J. and LYKLEMA, J. (1969) J. Colloid Interface Sci. **29**, 171

FLORY, P. J. and FOX, T. G. (1951) J. Am. Chem. Soc. **73**, 1904

FLORY, P. J. (1953) Principles of Polymer Chemistry, Cornell University Press, Ithaca

FONTANA, B. J. and THOMAS, J. R. (1961) J. Phys. Chem. **65**, 408

FRENS, G. (1968) Thesis, State University Utrecht, Netherlands

FRISCH, H. L. and SIMHA, R. (1954) J. Phys. Chem. **58**, 507

FRISCH, H. L. (1955) J. Phys. Chem. **59**, 633

FRISCH, H. L. and SIMHA, R. (1956) in: Rheology, Theory and Application, F. R. Eirich Ed. Vol. 1, Ch. 14, Academic Press, New York

FRISCH, H. L. and SIMHA, R. (1957) J. Chem. Phys. **27**, 702

FRUMKIN, A. (1926) Z. Physik **35**, 792

FUCHS, N. (1934) Z. Physik **89**, 736

FUNGAROLI, A. A. and PRAGER, S. R. (1969) Ind. Eng. Chem., Prod. Res. Dev. **8**, 450

GALGÓCZI, B. (1964) IVth Intern. Congr. Surface Activity, Brussels; Proceedings Vol. 3, 913 (1967)

GREGORY, J. (1969) Trans. Faraday Soc. **65**, 2260
GREGORY, J. (1970) personal communication
HAAN, F. A. M. DE (1964) J. Phys. Chem. **68**, 2970
HACKEL, E. (1968) in: Properties and Applications of Polyvinyl Alcohol, S.C.I. Monograph no **30**, Soc. Chem. Ind., London
HARMSEN, G. J., SCHOOTEN, J. VAN and OVERBEEK, J. TH. G. (1953) J. Colloid Sci. **8**, 64, 72
HEALY, T. W. and LA MER, V. K. (1962) J. Phys. Chem. **66**, 1835
HESSELINK, F. TH. (1969) J. Phys. Chem. **73**, 3488
HESSELINK, F. TH. (1970) personal communication
HESSELINK, F. TH. (1971a) J. Phys. Chem. **75**, 65
HESSELINK, F. TH., VRIJ, A. and OVERBEEK, J. TH. G. (1971b) J. Phys. Chem. **75**, 2094
HOEVE, C. A. J. (1965) J. Chem. Phys. **43**, 3007
HOEVE, C. A. J., DIMARZIO, E. A. and PEYSER, P. (1965) J. Chem. Phys. **42**, 2558
HOEVE, C. A. J. (1966) J. Chem. Phys. **44**, 1505
HOEVE, C. A. J. (1970) J. Polym. Sci. C **30**, 361
HOFFMAN, R. F. and FORSMAN, F. C. (1970) J. Polym. Sci. A–2 **8**, 1847
HOGG, R., HEALY, T. W. and FUERSTENAU, D. W. (1966) Trans. Faraday Soc. **62**, 1638
HONIG, E. P., ROEBERSEN, G. J. and WIERSEMA, P. H. (1971) J. Colloid Interface Sci. **36**, 97
HORACEK, J. (1962) Chem. Prumysl. **12**, 385; C.A. **58**, 10305 f
HUGGINS, M. L. (1958) Physical Chemistry of High Polymers, Wiley, New York
HUL, H. J. VAN DEN (1966) Thesis, State University Utrecht, Netherlands
HUL, H. J. VAN DEN and LYKLEMA, J. (1967) J. Colloid Interface Sci. **23**, 500
HUQUE, M. M., FISHMAN, M. and GORING, D. A. J. (1959) J. Phys. Chem. **63**, 766
IMAI, S. (1969) Proc. Roy. Soc. A **308**, 497
JENKEL, E. and RUMBACH, B. (1951) Z. Elektrochem. **55**, 612
JONES, M. H. and MANLEY, T. R. (1967) Anal. Chim. Acta **38**, 143
KERKER, M. (1969) The Scattering of Light and Other Electromagnetic Radiation, Academic Press, New York
KILLMANN, E. and WIEGAND, H. G. (1970) Makromol. Chem. **132**, 239
KIPLING, J. J. (1965) Adsorption from Solution of Non-Electrolytes, Academic Press, London
KITCHENER, J. A. and MUSSELWHITE, P. R. (1968) in: Emulsion Science, P. Sherman Ed., Academic Press, London
KOOPAL, L. K. (1970) personal communication
KREVELEN, D. W. VAN and HOFTIJZER, P. J. (1967) J. Appl. Polym. Sci. **11**, 1409
KRUYT, H. R. and KLOMPÉ, M. A. M. (1942) Kolloid-Beih. **54**, 484
KUHN, W. (1934) Kolloid-Z. **68**, 2
KURATA, M. and STOCKMAYER, W. H. (1963) Fortschr. Hochpolym. Forsch. **3**, 196
KUZ'KIN, S. K. and NEBERA, V. P. (1963) Synthetic Flocculants in De-watering Processes, Moscow (Trans. Nat. Lending Library, Boston, G.B., 1966).
KUNE, J. W. (1967) Soil Sci. Am. Proc. **31**, 8
LA MER, V. K. and HEALY, T. W. (1963) Rev. Pure Appl. Chem. **13**, 112
LA MER, V. K. (1966) Discussions Faraday Soc. **42**, 248
LANKVELD, J. M. G. (1970) Thesis, Agricultural University, Wageningen, Netherlands; Meded. Landbouwhogeschool Wageningen 70–21 (1970)
LEVI, S. M. and STEPANOVA, T. K. (1965) Colloid J. USSR **27**, 42
LINDE, A. J. VAN DER (1971) unpublished results
LINKE, W. F. and BOOTH, R. B. (1960) Trans. A.I.M.E. **217**, 364
LIPS, H. J. M. (1968) Flocculation Aids, Course Coagulation and Sedimentation, Technical University, Delft, Netherlands
LYKLEMA, J. and OVERBEEK, J. TH. G. (1961) J. Colloid Sci. **16**, 595
LYKLEMA, J. (1963) Trans. Faraday Soc. **59**, 418
LYKLEMA, J. (1966) III Intern. Vortragung über grenzflächenaktiven Stoffe, Berlin; Abhandlungen p. 542 (1967)
LYKLEMA, J. (1968) Adv. Colloid Interface Sci. **2**, 65

MACKOR, E. L. (1951) Rec. Trav. Chim. **70**, 747
MAEDA, H., KAWAI, T. and SEKII, S. (1959) J. Polym. Sci. **35**, 288
MATSUO, T. and INAGAKI, H. (1968) Makromol. Chem. **53**, 130
MEIER, D. J. (1967) J. Phys. Chem. **71**, 1861
MICHAELS, A. S. and LAMBE, T. W. (1953) J. Agr. Food Chem. **1**, 835
MICHAELS, A. S. (1954) Ind. Eng. Chem. **46**, 1485
MONTE-BOVI, A. J. (1969) J. Ass. Offic. Anal. Chem. **52**, 891
MOORE, W. R. A. D., EPSTEIN, J. A., BROWN, A. M. and TIDSWELL, B. M. (1957) J. Polym. Sci. **23**, 23
MOORE, W. R. A. D. and O'DOWD, M. (1968) in: Properties and Applications of Polyvinyl Alcohol, S.C.I. Monograph no **30**, Soc. Chem. Ind., London
MORAWETZ, H. (1965) Macromolecules in Solution, Interscience Publ., New York
MOTOMURA, K. and MATUURA, R. (1968) Mem. Fac. Sci. Kyushu Univ. **6**, 97
MOTOMURA, K. and MATUURA, R. (1969) J. Chem. Phys. **50**, 1281
NEMETH, R. and MATIJEVIČ, E. (1968) Kolloid Z. Z. Polymere **225**, 155
ÖHRN, O. E. (1955) J. Polym. Sci. **17**, 137
OTTEWILL, R. H. and SHAW, J. N. (1968) J. Colloid Interface Sci. **26**, 110
OVERBEEK, J. TH. G. (1952) in: Colloid Science, H. R. Kruyt Ed., Elsevier, Amsterdam
PATAT, F., KILLMANN, E. and SCHLIEBENER, C. (1964) Fortschr. Hochpolym. Forsch. **3**, 332
PRITCHARD, J. G. (1970) Polyvinyl Alcohol, Basic Properties and Uses, Polymer Monographs Vol. 4, Gordon and Breach, London
REERINK, H. and OVERBEEK, J. TH. G. (1954) Discussions Faraday Soc. **18**, 74
ROE, R. J. (1965a) Proc. Nat. Acad. Sci. U.S. **53**, 50
ROE, R. J. (1965b) J. Chem. Phys. **43**, 1591
ROE, R. J. (1966) J. Chem. Phys. **44**, 4264
ROTHSTEIN, F. C. (1964) Offic. Digest Paint Manuf. **36**, 1448
ROWLAND, F., BULAS, R., ROTHSTEIN, E. and EIRICH, F. R. (1965) Ind. Eng. Chem. **57**, 46
RUBIN, R. J. (1965) J. Chem. Phys. **43**, 2392
RUEHRWEIN, R. A. and WARD, D. W. (1952) Soil Sci. **73**, 485
SAITO, SH. (1969) J. Polym. Sci. A–1 **7**, 1789
SAKAI, TS. (1968) J. Polym. Sci. A–2 **6**, 1659
SAKAI, TS. (1970) Macromolecules **3**, 96
SAKURADA, I., NAKAJIMA, A. and FUJIWARA, H. (1959) J. Polym. Sci. **35**, 497
SCHENKEL, J. H. and KITCHENER, J. A. (1960) Trans. Faraday Soc. **56**, 161
SILBERBERG, A. (1962a) J. Phys. Chem. **66**, 1872
SILBERBERG, A. (1962b) J. Phys. Chem. **66**, 1884
SILBERBERG, A. (1967) J. Chem. Phys. **46**, 1105
SILBERBERG, A. (1968) J. Chem. Phys. **48**, 2835
SLATER, R. W. and KITCHENER, J. A. (1966) Discussions Faraday Soc. **42**, 267
SMOLUCHOWSKI, M. VON (1916) Physik. Z. **17**, 557, 585
SMOLUCHOWSKI, M. VON (1917) Z. Physik. Chem. **92**, 129
SOMMERAUER, A., SUSSMAN, D. L. and STUMM, W. (1968) Kolloid Z. Z. Polym. **225**, 147
SONNTAG, H. (1968) Tenside **5**, 188
SPIELMAN, L. A. (1970) J. Colloid Interface Sci. **33**, 562
STACEY, K. A. (1956) Light-scattering in Physical Chemistry, Butterworths, London
STOCKMAYER, W. H. (1955) J. Polym. Sci. **15**, 595
STONE-MASUI, J. and WATILLON, A. (1968) J. Colloid Interface Sci. **28**, 187
STROMBERG, R. R., PASSAGLIA, E. and TUTAS, D. J. (1963) J. Res. Nat. Bur. Stand. **67A**, 431
STROMBERG, R. R. (1967) in: Treatise on Adhesion and Adhesives, R. Patrick Ed., Dekker, New York
SUGIURA, M. and YABE, A. (1970) Kogyo Kagaku Zasshi **73**, 243
TAJOMA, S. (1957) Technol. Reports Kyushu Univ. **30**, 2
TAKEDA, M. and ENDO, R. (1956) J. Phys. Chem. **60**, 1202
TANFORD, CH. (1961) Physical Chemistry of Macromolecules, Wiley, New York

THIES, C., PEYSER, P. and ULLMAN, R. (1964) IVth Intern. Congr. Surface Activity, Brussels; Proceedings Vol. 2, 1041 (1967)
TOJOSHIMA, K. (1968) in: Properties and Applications of Polyvinyl Alcohol, S.C.I. Monograph no **30**, Soc. Chem. Ind., London
TROELSTRA, S. A. (1941) Thesis, State University Utrecht, Netherlands; H. R. KRUYT and S. A. TROELSTRA (1943) Kolloidchem. Beihefte **54**, 225
VERWEY, E. J. W. and OVERBEEK, J. TH. G. (1948) Theory of the Stability of Lyophobic Colloids, Elsevier, Amsterdam
VINCENT, B., BIJSTERBOSCH, B. H. and LYKLEMA, J. (1971) J. Colloid Interface Sci. **37**, 171
VOLD, M. J. (1961) J. Colloid Sci. **16**, 1
WIERSEMA, P. H., LOEB, A. L. and OVERBEEK, J. TH. G. (1966) J. Colloid Interface Sci. **22**, 78
WILLIAMS, B. G., GREENLAND, R. J. and QUIRK, J. P. (1968) Austr. J. Soil Res. **6**, 59
WIT, J. N. DE (1971) personal communication
WOLFRAM, E. and NAGY, M. (1968) Kolloid Z. Z. Polym. **227**, 86
ZWICK, M. M. (1965) J. Appl. Polym. Sci. **9**, 2393
ZWICK, M. M. (1966) J. Polym. Sci. A–1, **4**, 1642

SOME DEFINITIONS USED IN THIS STUDY

coagulation	destabilisation of a sol by electrolytes only
flocculation	destabilisation of a sol by polymer (possibly with the help of small amounts of salts)
segment	monomer unit (for PVA: CH_2-CHOH)
element	statistical chain element (for PVA about 7 segments)

LIST OF SYMBOLS

BuOH	n-butanol
EG	ethylene glycol
PVA	polyvinyl alcohol
PVAc	polyvinyl acetate
a	exponent in the MARK-HOUWINK equation (eq. 2–3)
A	absorbance (formerly *extinction*; see 3.2.2.)
A_a	number of segments adsorbed per unit area on the second particle
A_H	number of segments per unit area which in the undisturbed distribution are beyond the distance H
A_{rel}	relative absorbance
A_t	total number of segments adsorbed per unit area
A_0	number of segments per unit area in the first layer on the surface
A_0'	*ibid.* on the second particle
A_{12}	HAMAKER constant of particles 1 in medium 2
b	numerical constant in eq. (4–21)
c_c	critical coagulation concentration
c_p	polymer concentration
c_s	salt concentration
c_{sol}	sol concentration
$c_{\frac{1}{2}}$	critical flocculation concentration, measured at $A_{rel} = 0.5$
$c_{\frac{1}{2}}'$	*ibid.*, measured from the rate of initial flocculation
C_M	constant, defined in eq. (2–15)
d	density of the solid
e	elementary charge
f	φ^*/φ
$g_b\,(i, H)$	configurational free energy of a bridge of i elements at an interparticle distance H
$g_l\,(i, H)$	*ibid.* of a loop
$\Delta g_b\,(i, H)$	$g_b\,(i, H) - g_l\,(i, H)$
$(\overline{h^2})^{1/2}$	root-mean-square distance between the endpoints of a chain
$(\overline{h_0^2})^{1/2}$	*ibid.* under Θ-conditions
$(\overline{h_{0F}^2})^{1/2}$	*ibid.* if no steric hindrance is present
H	interparticle distance
H_{max}	interparticle distance at the maximum in V_t or V_t'
i	number of statistical chain elements in a loop or tail
$\bar{i}$	average number of elements per loop

i_H	number of elements in a bridge at an interparticle distance H
iep	isoelectric point
j	number of primary particles in a floc
j_{cr}	highest j in the supernatant after centrifugation
k	BOLTZMANN constant
k_H	number of elements in a train adsorbed on the second particle
k'	HUGGINS constant (eqs. (2–4), (2–5) and (4–1))
k_1	constant in the MARK-HOUWINK equation (eq. 2–3)
K	polymer constant defined in eq. (2–14)
K_E	EINSTEIN coefficient (eq. 4–1)
K_H	constant in the HOEVE segment density distribution (eq. 4–23b)
K_b^{max}	maximal integral double layer capacity per unit area in the presence of butanol
K_p^{max}	*ibid.* in the presence of PVA
l	length of a C-C bond
l_s	length of a statistical chain element
L	contour length of a polymer chain (eq. 2–11)
m	number of skeletal carbon atoms in a molecule
M	molecular weight
n	total number of elements in the loops per unit area
n_a	number of small molecules adsorbed per unit area
n_i	number of loops of i elements per unit area
n_j	number of particles in fraction j
n_p	number of segments adsorbed in the first layer on the surface per unit area
n_p^{max}	ibid. at $\theta_p = 1$
n_s	number of counterions per unit volume
N	number of primary particles
N_{Av}	AVOGADRO's number
N_j	number of j-fold particles
O	area; 'equivalent flat area' of a spherical particle (eq. 6–21)
p_a	amount of polymer adsorbed per unit area (mg/m^2)
pAg	negative logarithm of the Ag^+ concentration
p_H	$(K_H/\delta)(v/1-v)$
pI	negative logarithm of the I^- concentration
p_t	$18/7\overline{h^2}$
p_1	amount of polymer added to the first portion of sol (mg/mmole)
pzc	point of zero charge
Δpzc	shift of the pzc
Δpzc^{max}	shift of the pzc if the first layer on the surface is fully occupied
q	$b/\bar{l}$

r	distance from the centre of gravity
R	particle radius
R_h	hydrodynamic radius
$\overline{R}_{32}$	volume-surface averaged particle radius
$(\overline{s^2})^{1/2}$	radius of gyration
$(\overline{s_0^2})^{1/2}$	radius of gyration under Θ-conditions
S	specific surface area
t_1	time of contact between PVA and the first portion of sol
t_2	flocculation time
$t_{\frac{1}{2}}$	time in which the number of primary particles is just halved
T	absolute temperature
u	electrophoretic mobility
$\bar{v}$	partial specific volume of polymer
v_1	volume of the first portion of sol
v_2	volume of the second portion of sol
v_{Rb}	configurational repulsion free energy due to one loop
V	volume of a primary particle
V_A	VAN DER WAALS attraction free energy for two flat plates (ergs/cm^2)
V_{Aa}	adsorption attraction free energy for two flat plates (ergs/cm^2)
V_{Rb}	configurational repulsion free energy for two flat plates due to the adsorbed layer (ergs/cm^2)
V_j	volume of a j-fold particle
V_{max}	value of V_t in its maximum (ergs/cm^2)
V_{pol}	polymer contribution to the interaction free energy for two flat plates (ergs/cm^2)
V_R	double layer repulsion free energy for two flat plates (ergs/cm^2)
V_t	total free energy of interaction between a covered and an uncovered flat plate (ergs/cm^2)
V_A'	VAN DER WAALS attraction free energy for two spheres (ergs)
V_{max}'	value of V_t' in its maximum (ergs)
V_{pol}'	polymer contribution to the interaction free energy for two spheres (ergs)
V_R'	double layer repulsion free energy for two spheres (ergs)
V_t'	total free energy of interaction between a covered and an uncovered spherical particle (ergs)
V_1	molar volume of the solvent
w_j	weight of fraction j
W	stability ratio
x	distance from the surface
$X(\kappa R)$	HENRY function (eq. 2–23)

y	$V_R/V_R'O$ for $La(NO_3)_3$ (eq. 6–22)
z	valency of an ion
Z	number of charged sites on a polymer molecule
α	linear expansion factor
β	fraction of the total number of segments which is present in the tails
γ_d	$\tanh(ze\psi_d/4kT)$
γ_1	$2\Delta pzc(CH_2)^{max}/\Delta pzc(BuOH)^{max}$
γ_2	$2\Delta pzc(CHOH)^{max}/\Delta pzc(BuOH)^{max}$
γ_3	$\sigma_p^{max}/\sigma_b^{max}$
δ	thickness of the STERN layer; thickness of the first polymer layer on the surface
δ_b^{max}	thickness of the STERN layer on a surface fully covered by butanol
δ_p^{max}	*ibid.* by PVA
Δ	experimental thickness of the polymer layer
ε	dielectric constant
ε_a	adsorption free energy per segment
ε_b^{max}	dielectric constant of the STERN layer on a surface fully covered by butanol
ε_p^{max}	*ibid.* by PVA
ζ	electrokinetic potential
η	viscosity
$[\eta]$	intrinsic viscosity
η_{re}	viscosity ratio excess (= viscosity ratio minus one)
η_{re}^*	viscosity ratio excess of a sol in which the particles are covered by PVA
θ	valence angle
θ_p	fraction of the surface which is occupied by PVA
Θ	theta temperature; theta conditions
κ	reciprocal DEBIJE-length
ν	fraction of the number of segments which is in contact with the surface
ξ	$R_h/(\overline{s^2})^{1/2}$
ρ	polymer density (number of segments/Å^3)
ρ_0	*ibid.* in the first layer on the surface
ρ_c	*ibid.* of a Gaussian coil in solution
ρ_{eff}	*ibid.* at the boundary of mobile and immobile water in the adsorbed layer
ρ_h	polymer density of an adsorbed homopolymer (Å^{-1})
ρ_l	*ibid.* of an adsorbed loop
ρ_t	*ibid.* of an adsorbed tail

σ	steric factor (eq. 2–9)
σ_0	surface charge per unit area of an uncovered surface
σ_d	charge in the diffuse layer per unit area
σ_p	surface charge per unit area of a polymer covered surface
σ_p^{max}	*ibid.* of a surface fully covered by polymer
σ_b^{max}	*ibid.* of a surface fully covered by butanol
τ	transmittance
φ	volume fraction of solid in a sol
φ^*	effective volume fraction of polymer covered particles in a sol
φ_1	$v_1/(v_1+v_2)$
φ_2	$v_2/(v_1+v_2)$
Φ	FLORY constant (eqs. (2–14) and (2–16))
χ	FLORY-HUGGINS polymer-solvent interaction parameter
ψ	potential with respect to the bulk of the solution
ψ_0	surface potential
ψ_d	STERN potential

ENKELE PERSOONLIJKE GEGEVENS:

Mijn middelbare schoolopleiding kreeg ik aan het Carmellyceum te Oldenzaal, afdeling Gymnasium β. Na het eindexamen aan deze school begon ik in 1960 de chemische studie aan de Rijksuniversiteit te Utrecht. Het kandidaatsexamen (letter e) werd afgelegd in maart 1964, en het doctoraalexamen (kolloidchemie met theoretische natuurkunde) volgde in juli 1966.

Sinds augustus 1966 ben ik werkzaam als wetenschappelijk medewerker aan het laboratorium voor Fysische en Kolloidchemie van de Landbouwhogeschool te Wageningen.